

UNIVERSITY OF CAPE COAST

EVALUATION OF PATIENT ORGAN AND EFFECTIVE DOSES FROM  
SELECTED INTERVENTIONAL RADIOLOGY PROCEDURES: THE  
RADIATION PROTECTION POINT OF VIEW

BY

CYNTHIA KAIKOR ENGMANN

Thesis submitted to the Department of Physics, School of Physical Sciences,  
College of Agriculture and Natural Sciences, University of Cape Coast, in  
partial fulfillment of the requirements for the award of Doctor of Philosophy  
degree in Physics

NOBIS

CALL No.	
ACCESSION No.	
7107	
CAT. CHECKED	FINAL CHECKED

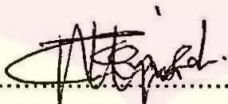
SEPTEMBER 2021

**SAM JONAH LIBRARY**  
UNIVERSITY OF CAPE COAST  
CAPE COAST

## DECLARATION

### Candidate's Declaration

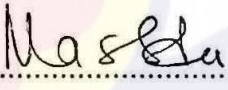
I hereby declare that this thesis is the result of my own original research and that no part of it has been presented for another degree in this university or elsewhere.

Candidate's Signature:  Date: 10-08-2021

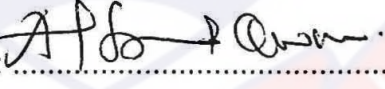
Name: Cynthia Kaikor Engmann

### Supervisors' Declaration

We hereby declare that the preparation and presentation of the thesis were supervised in accordance with the guidelines on supervision of thesis laid down by the University of Cape Coast.

Principal Supervisor's Signature:  Date: 10-08-2021

Name: Prof. Mary Boadu

Co-Supervisor's Signature:  Date: 10-08-2021

Name: Dr. Alfred Owusu

## ABSTRACT

The objective of this study was to assess patient organ and effective doses from the selected interventional radiology procedures and propose effective dose prediction strategies. This objective was achieved by surveying dose area product and peak skin doses for three interventional radiology procedures (endovascular aortic aneurysm repair, stenting of femoropopliteal and transarterial chemoembolization). Organ and effective doses were assessed and a mathematical relation for predicting effective dose from dose-area-product has been established for each of the three interventional radiology procedures. Also, percentage differences between two dose assessment protocols (ICRP 60 and ICRP 103) was estimated. The study was undertaken by performing Monte Carlo (PCXMC version 2) simulations of dose data of ninety-nine (99) patients who underwent the interventional procedures. The dose data was analyzed with ICRP 60 and ICRP 103 dose assessment protocols. The study revealed that mean effective doses for endovascular aneurysm repair, stenting of femoropopliteal and transarterial chemoembolization were 28.495, 1.969 and 20.278 mSv; 23.985, 1.429 and 17.644 mSv; respectively for ICRP 60 and ICRP 103 protocols. This means that percentage difference between the ICRP 60 and ICRP 103 protocols were respectively 15.8, 27.4 and 13.0%. From outcome of the study, it is recommended that the derived mathematical equations from this study could be adopted and used as predictor tool to estimate effective doses of patients before the interventional radiology procedure is undertaken. Also, in the assessment of radiation doses in interventional radiology procedures, ICRP 103 protocol should be used instead of ICRP 60 protocol.

## KEY WORDS

Angiography;

Anthropomorphic phantom;

Effective dose;

Endovascular Aortic aneurysm;

Femoropopliteal;

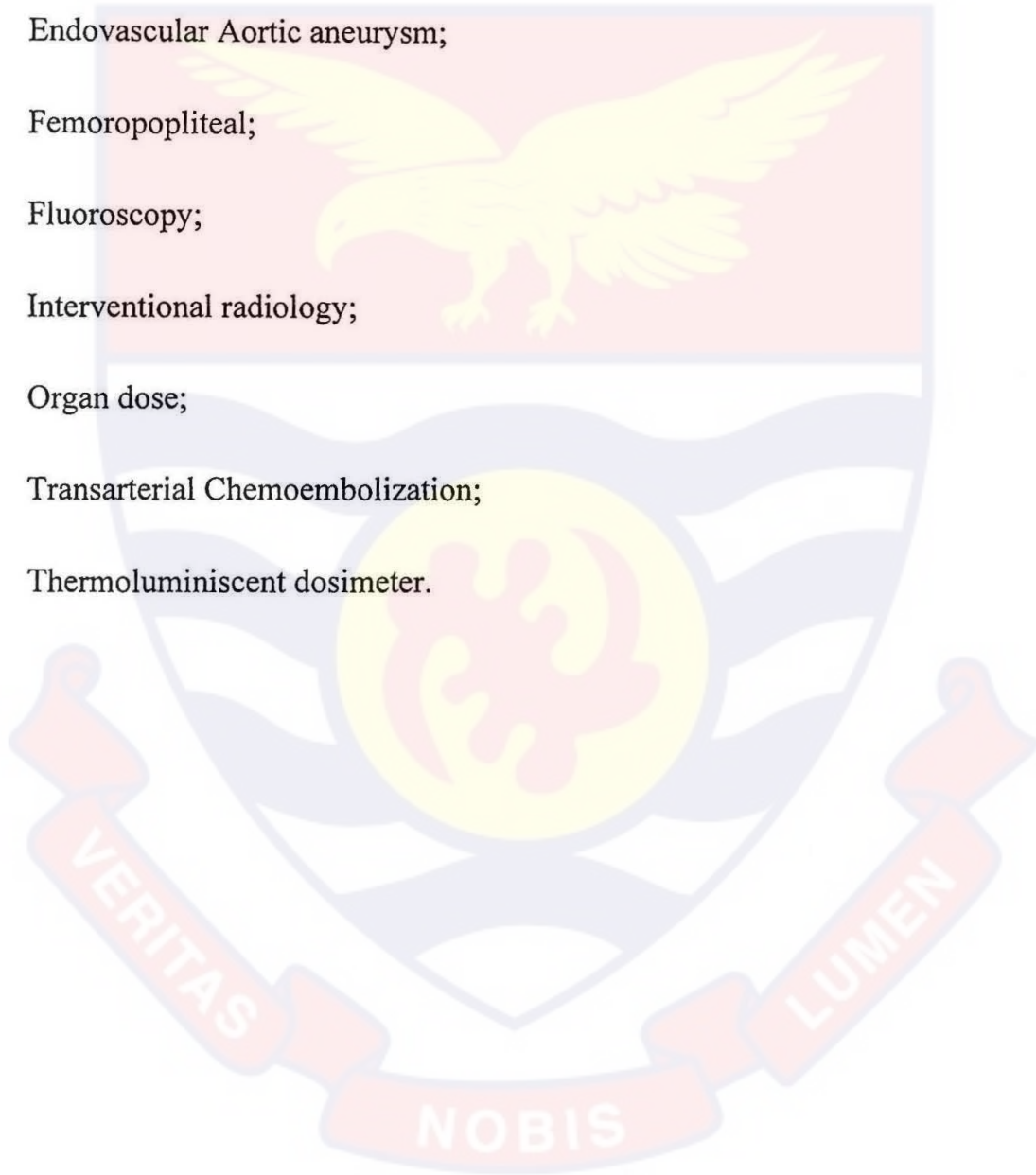
Fluoroscopy;

Interventional radiology;

Organ dose;

Transarterial Chemoembolization;

Thermoluminescent dosimeter.



## ACKNOWLEDGEMENTS

I thank the International Atomic Energy Agency and the Ghana Atomic Energy Commission for the scholarship awarded me to carry out my research work at the University hospital of Crete, Greece. For the immense support of the Nuclear Regulatory Authority to accept and grant me permission to study abroad.

I appreciate the guidance, right coaching from my thesis supervisors, Prof. Mary Boadu (Ghana Atomic Energy Commission), Dr. Alfred Owusu (University of Cape Coast). I also appreciate the guidance of Prof. John Damilakis (University of Crete) and his team for their assistance throughout my fellowship study and stay in Greece. Am grateful for the clinical technical knowledge I obtained from the interventional radiologists (Doctors Adam Hadzadakis and Illias Tsetis), the Radiation technologist (Mr Nikos Filippakis) at the angiography suit where I performed all of my practical studies.

I am grateful for the selfless assistance offered me by the staff of the Toxicology laboratory especially, Manolis Dolapsakis, Athanasios Alegakis and Evi Kortsidaki (International relations officer). All at the University of Crete.

To my ever-loving husband, sons, parents, siblings, my in-laws, friends and colleagues who encouraged me through it all, am grateful.

## DEDICATION

This work is dedicated to my family.



## TABLE OF CONTENTS

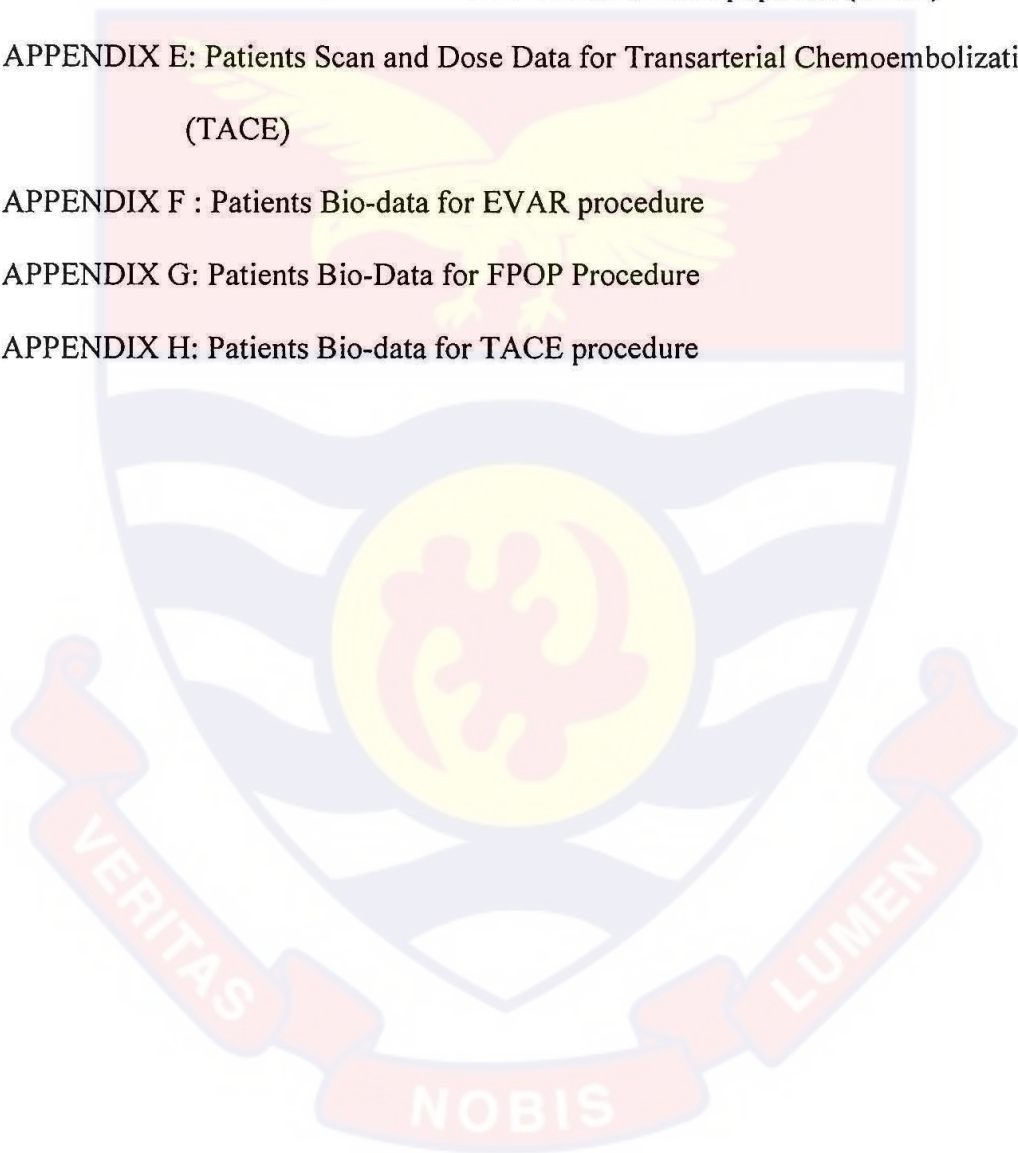
	Page
DECLARATION	ii
ABSTRACT	iii
KEY WORDS	iv
ACKNOWLEDGEMENTS	v
DEDICATION	vi
LIST OF TABLES	xii
LIST OF FIGURES	xiv
LIST OF ABBREVIATIONS	xv
CHAPTER ONE	
INTRODUCTION	1
Background to the Study	1
Problem Statement	4
Purpose of the Study	5
Significance of Study	6
Organization of Study	7
Summary: Chapter One	7
CHAPTER TWO: LITERATURE REVIEW	
Introduction	9
Ionizing Radiation	9
Energy Transferred from Radiation	10
Dosimetric Quantities and Units	11
Exposure (X)	12
Kerma (K)	12
Kerma Rate ( $\dot{K}$ )	13

Absorbed Dose (D)	13
Absorbed Dose Rate ( $\dot{D}$ )	13
Difference between Kerma and Absorbed Dose	14
Incident Air Kerma ( $K_{a,i}$ )	15
Incident Air Kerma Rate ( $\dot{K}_{a,i}$ )	15
X-ray Tube Output	16
Entrance-Surface Air Kerma and Entrance-Surface Air Kerma Rate	16
Fluoroscopy System	17
Fluoroscopy device for interventional procedures	19
Endovascular Aneurysm Repair (EVAR)	25
Patient Dose during Image Guided Procedures	27
Dose Measurements Techniques	27
Measurement of ESD in Interventional Radiology	27
Measurement of ESD from DAP Measurements	28
Measurement of ESD from Tube Output Measurements	30
Estimation of ESD from TLD Measurements	30
Estimation of ESD using Slow Films	31
Radiochromic Media	31
Measurement of Effective Dose (E) in Interventional Radiology	32
Radiation Risk during Image-Guided Procedures	33
Radiation Risk Estimates	34
Quality Assurance (QA) and Quality Control (QC)	34
Summary: Chapter Two	35
CHAPTER THREE: METHODOLOGY	
Quality Control	36
Siemens Axiom Artis FA Angiography Unit	36
Calibration of Radcal Model 3035	37

Leeds Test Objects	38
Calibration of TLD Chips	39
Set up for calibration	39
Annealing and irradiation of dosimeters	40
Calculation of Calibration coefficient	41
Anthropomorphic Phantom Measurements	42
Placement of TLDs in phantom	43
Dose measurement with TLDs in physical phantom	43
Patient Data Collection	44
Sample Size	44
Data Retrieval from Database	44
Inclusion and Exclusion Criteria	45
Ethical Clearance for Data Acquisition	46
Dose Calculation with PCXMC	46
Corroboration of Organ Doses Calculated with PCXMC	49
Dose Evaluation	50
Statistical Analysis of Data	51
Summary: Chapter Three	51
CHAPTER FOUR: RESULT AND DISCUSSION	
Introduction	53
Endovascular Aortic Aneurysm Repair (EVAR)	53
Type I endoleak	54
Type II endoleak	56
Type III endoleak	56
Type IV endoleak	59
Summarized Dose Data for EVAR Procedures	60
Stenting of Femoropopliteal (FPOP)	64

Type I Popliteal aneurysm (single aneurysm with local pain and pulsating mass)	66
Type I Popliteal aneurysm (multiple aneurysm with local pain and pulsating mass)	68
Type I Popliteal aneurysm (multiple aneurysm with acute thrombosis)	68
Type II Popliteal aneurysm (multiple aneurysm with acute thrombosis)	71
Type II Popliteal aneurysm (multiple aneurysm with peripheral embolization)	71
Type II Popliteal aneurysm (multiple aneurysms with acute thrombosis and limb-threatening ischemia)	74
Summarized Dose Data for FPOP Procedures	76
Transarterial Chemoembolization (TACE)	80
Stage II Hepatic Cancer	81
Stage III-A Hepatic Cancer	82
Stage III--B Hepatic Cancer	84
Stage IV-A Hepatic Cancer	86
Stage IV-B Hepatic Cancer	87
Summarized Dose Data for TACE Procedures	89
Relationships between Dose Area Product (DAP) and Effective Dose (ED)	93
Endovascular Aortic Aneurysm Repair	93
Stenting of Femoropopliteal	94
Transarterial Chemoembolization	95
Comparison of ICRP 60 and ICRP 103 Estimated Effective Doses	96
Summary: Chapter Four	97
CHAPTER FIVE: SUMMARY, CONCLUSIONS AND RECOMMENDATIONS	
Summary	99
Conclusions	102
Recommendations	103
Limitations	104
REFERENCES	105

APPENDICES	116
APPENDIX A: Ethical clearance obtained from University of Crete	116
APPENDIX B: Ethical approval obtained from University of Cape Coast	117
APPENDIX C: Patients Scan and Dose Data for Endovascular Aortic Aneurysm Repair (EVAR)	118
APPENDIX D: Patients Scan and Dose Data for Femoropopliteal (FPOP)	134
APPENDIX E: Patients Scan and Dose Data for Transarterial Chemoembolization (TACE)	156
APPENDIX F : Patients Bio-data for EVAR procedure	166
APPENDIX G: Patients Bio-Data for FPOP Procedure	167
APPENDIX H: Patients Bio-data for TACE procedure	169



LIST OF TABLES

	Page
1 Weighting factors for the different organs	24
2 Data from image-guided procedures from literature	24
3 Dose data for patients with Type I endoleak undergoing EVAR procedures	55
4 Dose data for patients with Type II endoleak undergoing EVAR procedures	57
5 Dose data for patients with Type III endoleak undergoing EVAR procedures	58
6 Dose data for patients with Type IV endoleak undergoing EVAR procedures	59
7 Summary of simulated organ doses (mGy) from EVAR Procedures	61
8 Dose data for patients undergoing FPOP procedures with Type I single aneurysm and pulsating mass	67
9 Dose data for patients undergoing FPOP procedures with Type I multiple aneurysm and pulsating mass	69
10 Dose data for patients undergoing FPOP procedures with Type I multiple aneurysm and acute thrombosis	70
11 Dose data for patients undergoing FPOP procedures with Type II multiple aneurysm and acute thrombosis	72
12 Dose data for patients undergoing FPOP procedures with	

	Type II multiple aneurysm peripheral embolization	73
13	Dose data for patients undergoing FPOP procedures with multiple aneurysm, acute thrombosis and limb-threatening ischemia	75
14	Summary of simulated organ doses (mGy) from FPOP procedures	77
15	Dose data for patients undergoing TACE procedures with stage II hepatic cancer	81
16	Dose data for patients undergoing TACE procedures with stage III-A hepatic cancer	83
17	Dose data for patients undergoing TACE procedures with stage III-B hepatic cancer	85
18	Dose data for patients undergoing TACE procedures with stage IV-A hepatic cancer	86
19	Dose data for patients undergoing TACE procedures with stage IV-B hepatic cancer	88
20	Summary of simulated organ doses (mGy) from TACE procedures	90
21	Percentage differences between ICRP60 and ICRP103 effective doses	97

## LIST OF FIGURES

	Page
1	Schematic diagram for measurement of dosimetric quantities. 14
2	Schematic diagram of a fluoroscopy system (Radiology Key, 2020) 18
3	C-arm commonly used for image-guided procedures label major parts (Reference: image from this study's field work). 20
4	Fixed C-arm angiography unit: Siemens Axiom Artis FA 37
5	a. Radcal Model 3035 Ionization Chamber; b. sensitive area of the Radcal Model 3035. 38
6	The Leeds test object for radiography 39
7	Photos of a) Victoreen annealing oven b) Handling tools i) tong for handling hot brass plate in and out of annealing oven ii) and iv) tong for handling TLD chips iii) scissors c) Harshaw 3500 reader d) Brass plate with some TLD chips. 41
8	Definition file window (top) with DICOM image (bottom) 47 - 48
9	PCXMC image simulation window 48
10	Dose calculation window 49
11	a. Physical anthropomorphic phantom (RANDO, Alderson research labs); b. a section of phantom slice; c. TLD chip cooling and organizing tray. 50
12	Box plot for simulated organ doses (mGy) from EVAR procedures 62
13	Box plot for average and effective doses from EVAR procedures 63
14	Box plot of simulated organ doses (mGy) from FPOP procedures 78
15	Box plot for average and effective doses from FPOP procedures 79
16	Box plot of simulated organ doses (mGy) from TACE procedures 91
17	Box plot for average and effective doses from TACE procedures 92
18	Relationship between DAP and ED for EVAR procedure 94
19	Relationship between DAP and ED for FPOP procedure 95
20	Relationship between DAP and ED for TACE procedure 96

## LIST OF ABBREVIATIONS

3D	3-dimensional
AAA	Abdominal aortic aneurysm
ABC	Automatic Brightness Control
AEC	Automatic exposure control
ALARA	As low as reasonably achievable
BEIR	Biological Effects of Ionizing Radiation
CAU	Caudal
CD	Cumulative dose
CRA	Cranial
CT	Computed tomography
<i>D</i>	Absorbed dose
$\dot{D}$	Absorbed dose rate
DAP	Dose area product
DICOM	Digital communication
DSA	Digital subtraction angiography
E	Effective dose
EM	electromagnetic
ESAK	Entrance-surface air kerma
ESD	Entrance skin dose
EVAR	Endovascular aortic aneurysm repair
FDA	Food and Drugs Authority
FID	Focus to image distance
FPOP	Femoropopliteal
FSD	Focus to skin distance

Gy	Gray
HCC	Hepatocellular carcinoma
HVL	Half value layer
IAEA	International Atomic Energy Agency
IAK	Incident air kerma
ICRP	International Commission on Radiation Protection
ICRU	International Commission on Radiation Units and Measurements
IEC	International Electrotechnical Commission
IR	Interventional radiology
K	Kerma
LAO	Left anterior oblique
LAR	Lifetime attributable risk
MeV	Mega electronvolt
mGy	milli Gray
NRPB	National Radiation Protection Board
PSD	Peak skin dose
$Q$	electric charge
QA	Quality assurance
QC	Quality control
RAO	Right anterior oblique
Sv	Sievert
TAA	Thoracic aortic aneurysm
TACE	Transarterial chemoembolization
TEVAR	Thoracic endovascular aortic aneurysm repair

TLD	Thermoluminiscent dosimeter
UCC	University of Cape Coast
UOC	University of Crete, Greece
UV	Ultraviolet
X	Exposure



## CHAPTER ONE

### INTRODUCTION

#### Background to the Study

Interventional radiology (IR) is a medical specialty which utilizes minimally-invasive image-guided procedures to diagnose and treat diseases in several organ systems ([https://en.wikipedia.org/wiki/Interventional\\_radiology](https://en.wikipedia.org/wiki/Interventional_radiology), 2018). Diseases of the vascular system (artery, vein or lymphatic vessel i.e. circulatory system) are diagnosed and treated by Vascular Surgeons. Vascular Interventional Radiology is the diagnosis and treatment of diseases of all parts of the vascular system (except the heart and the brain) by small incisions through the skin in conjunction with image guidance techniques (John Hopkins Medicine, 2018; MUSC, 2018). An example of diagnostic IR procedure is angiography which is a fluoroscopic technique that employs the administration of a radiopaque substance into the blood vessels to make the organs visible. Example of therapeutic IR procedure is trans-arterial chemoembolization (TACE) which is performed to curb the blood supply to a tumor. This is achieved through the introduction of a combination of chemotherapy drug with blockage-causing pieces of materials (Wah, 2017). Angiography is performed in dedicated suits, furnished with mobile or fixed C-arm fluoroscopy machines designed for such purposes (Foerth, 2015) while others are attempted with conventional fluoroscopy machines (Geijer, 2005).

Endovascular is a medical practice relating to a surgical procedure in the vascular system involving placement of catheters or tiny instruments with drugs (radiopaque) into the blood vessels through an incision in the skin in order to

treat a disease condition. Atherosclerosis thickening of inner lining of blood vessels leading to blockage and aneurysm is a balloon-like bulging of the blood vessels. Endovascular Aneurysm Repair (EVAR) is an IR procedure performed to manage the aneurysm with a stent through an incision in the femoral artery using guide wires and catheters to position the stent at the abnormal location with angiography. When the aneurysm occurs, in the thorax, it is referred to as Thoracic EVAR (TEVAR) and if it occurs in the abdomen, it is popularly referred to as EVAR ([https://en.wikipedia.org/wiki/Interventional\\_radiology](https://en.wikipedia.org/wiki/Interventional_radiology), 2018; Fossaceca, 2012).

EVAR is minimally-invasive, time effective, associated with fewer complications and has lower mortality rate compared to open surgery (Oliveira, 2018; Jackson, 2012). A patient is often stung in the groin when image-guided procedure is executed. A catheter is passed through stung position in the groin to the aorta. The passing of the catheter is done using fluoroscopy system which shows images of the anatomy on a monitor to guide the operators during the procedure. During the IR procedures, the fluoroscopy system provides different imaging techniques. Fluoroscopy, is a medical imaging practice which displays continuous X-ray images on a monitor. The continuous display of the images shows live image of the structures in the body. To obtain very good overview, three-dimensional rotation is used prior to each procedure. In addition, high-quality exposure is used during and after the procedures. This results in less body injury, quicker recovery time so that patients spend less time in the hospital (Locham, 2018).

In recent times, IR is used in studies such as EVAR (Oliveira, 2018; Foerth, 2015), femoropopliteal (FPOP) (Secemsky, 2018) and TACE (Jia,

2018). Image-guided techniques have become common nowadays hence, the increasing number of interventional suites to carry out the procedures. Hybrid interventional suites are the most advanced rooms with a combination of the fluoroscopy machine and a sterile operating environment. Such suites are used for difficult and dire cases where both open surgery and image guidance are required to resolve a patients condition (Miller et al, 2010; Dance et al, 2014).

Image-guided technique helps to treat ailments without a need for open surgery. Image-guided techniques apply ionizing radiation to direct the catheter through the anatomy. Basically most of the highest doses associated with X-ray imaging, are related to image-guided procedures. Though interventional procedures require patients to spend less time in the hospital to recover, daily use of such procedures have led to increase in patient and staff doses, comparative to open surgery (Miller et al, 2010; Dance et al, 2014; Duncan et al, 2011; FDA, 2014). With increase in the use of ionizing radiation globally (NRCNA, 2006 ), it has become necessary to equally increase the radiation protection for the patient and the staff.

TACE is the palliative treatment option for hepatocellular carcinoma (HCC), in the late and occasionally mid stages where surgery is not an option for the patient. The early stages can be treated by resection, percutaneous ablation and liver transplant (Horikawa 2015; Khoury, 2015). The history of TACE as recounted by Guan in 2012, specifies the advancement it has gone through right from the 1930s (Guan, 2012). There have been several reports of high curative potential and survival rates in patients who are treated with a combination of TACE and other local ablatives (Kim et al, 2011; Wang et al, 2011). Reviews of El-Serag in 2012 based on the studies by International

Agency for Research in Cancer together with those of Horikawa et al, 2015 reveals HCC as the fifth most common cancer in men (523,000 cases/y, 7.9% of all cancers), the seventh most common cancer in women (226,000 cases/y, 6.5% of all cancers) and the third leading cause of death associated with cancer worldwide. Occurrence of HCC in eastern Asia and sub-Saharan Africa is more than 2 out of every 10,000 population (El-Serag, 2012; Horikawa, 2015; Khoury, 2015). Angiography is seen as the most accurate procedure of diagnosing HCC in patients (Guan, 2012).

### **Problem Statement**

Interventional Radiology procedures require that patients are subjected to extended periods of exposure to X-rays, before, during, and after the intervention. This translates into high radiation dose delivery to the body organs of patients undergoing the procedure. This is seen as drawback for the treatment technique due to the associated radiation risk from the very long exposures. Considering the complications which may arise even many years after the procedures, the life-long follow-up often includes computed tomography (CT) imaging, a modality that requires substantial radiologic burden. Therefore, the assessment of the corresponding radiologic burden to the patient and the definition of the steps required to keep the dose as low as reasonably achievable is one of the many prerequisites for the choice of this treatment option in each facility.

With the increase of EVAR and complexity of procedures, coupled with technological advances relating to equipment and endografts, much prolonged fluoroscopy times are more frequently observed lately (Miller et al. 2003a;

Miller et al. 2003b). Concern has grown regarding substantial radiation exposure risks for both patients and operators (Klein et al, 2009; Hirshfeld et al, 2005; Stecker et al, 2009). Monitoring, recording of radiation exposure and an assessment of radiation effects are thus recommended (Administration FaD, 1995; Commission E, 1999; Protection ICoR, 2000). Radiation dose during EVAR includes the screening time, the number of angiographic acquisitions, as well as the collimation and the magnification. The automated dose reporting systems of fluoroscopy time and radiation dose are normally used to report the radiation exposure, but these indirect parameters can be inaccurate.

For TACE, both the diagnosis and treatment methods for the disease (if not in the early stages) have the potential of exposing patients and personnel to high levels of ionizing radiation (Guan, 2012; Khoury, 2015; Hidajat, 2006).

Most Centers offering the IR procedures hardly undertake dosimetric assessment to understand the risks being posed to affected patients.

### **Purpose of the Study**

Through the assessment of exposure levels, organ doses and radiation risks, radiation reduction mechanisms that achieve same treatment outcomes could be attained in IR.

The objective of this study was to assess patient organ and effective doses from the selected IR procedures and propose effective dose prediction strategies. To achieve this, focus would be on the following specific objectives:

- Survey dose area product (DAP) and peak skin doses (PSD) during EVAR, TACE and FPOP procedures.

- Assess organ doses and effective doses to patients during these procedures.
- Propose possibilities of using DAP in the prediction of effective dose (ED).
- Compare effective dose estimates using ICRP 60 and ICRP 103) protocols.

### **Significance of Study**

The IR procedure has become an important treatment process which involves the application of high amounts of radiation to deal with the medical condition in question. There has been growing concern regarding the very high radiation exposure risks associated with undergoing the procedure. Though EVAR, TACE and FPOP have been well accepted as necessary procedures for the treatment of pathology of the aorta, only few dosimetric studies are found in literature (Molyvda-Athanasopoulou, 2011; Jones et al, 2010; Mohapatra, 2013; Thakor, 2011; Fossaceca, 2012; Howells et al, 2012; Walsh et al, 2012).

This study to assess radiation exposure and doses for patients undergoing such procedures is highly relevant and a step towards ensuring radiation safety for affected patients. The study forms part of a broader target of dosimetry audit of the IR procedures. The effect of specific parameters like fluoroscopy time, angulation and exposure mode on dose descriptors (i.e. DAP, organ dose and effective dose) were addressed in the study. Survey on skin, organ and effective doses as well as DAP during the medical procedure would be performed to serve as baseline data and to guide practices of EVAR, TACE and FPOP procedures in future. The study also explored possibilities to optimize

radiation use during these procedures. This is envisaged to promote radiation protection and safety culture in the Angiography suit of radiology department.

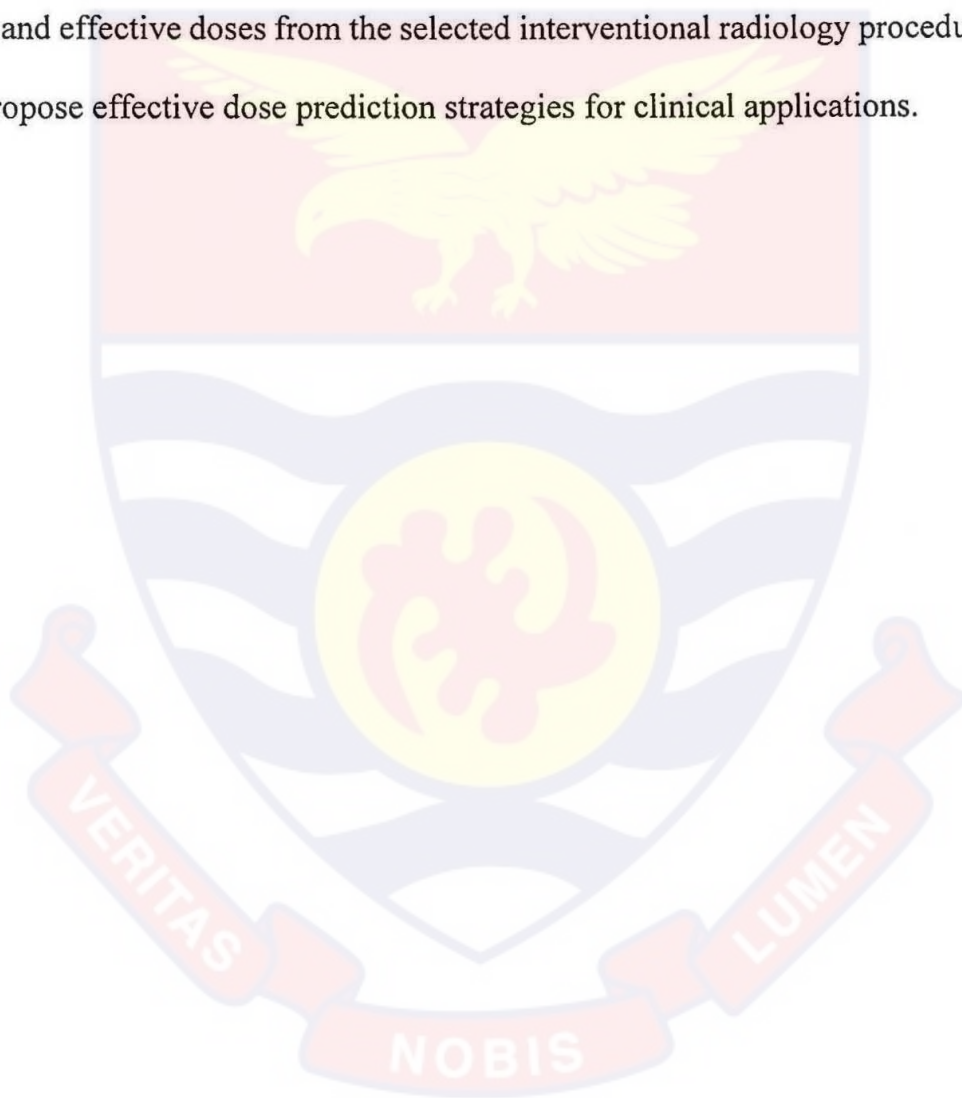
### **Organization of Study**

Chapter One of this study gives a general overview of the research topic. It highlights on background information related to dose evaluations in EVAR, TACE and FPOP procedures, the existing problems associated with the medical procedure and significance of the study. It also states clearly the objectives of the study. Chapter Two reviews literature pertinent to this study. It reviews literature on the selected procedures. Chapter Three addresses the methodology for the study. Materials for performing the X-ray imaging and the data collection have been described. Quality control (QC) tests performed on the imaging equipment, the experimental set-up and the processes of data collection have been described. Results and discussion are presented in Chapter Four and the study is concluded in Chapter Five, with relevant recommendations.

### **Summary: Chapter One**

Angiography is an interventional radiology procedure that employs the administration of radiopaque substances to visualize blood vessels under fluoroscopic imaging. The procedure is performed in dedicated suits, furnished with mobile or fixed C-arm fluoroscopy machines. Endovascular aneurysm repair, trans-arterial chemoembolization and femoropopliteal are some of the procedures performed in interventional radiology. EVAR is performed when there is indication of atherosclerosis or aneurysm in the blood vessels by making an incision in the groin; using guide wires and catheters to position stent at the abnormal location with imaging guidance. TACE is performed by combination

of chemotherapy drug with blockage-causing pieces of materials to control blood supply to the tumors in hepatocellular cancer. FPOP on the other hand, is performed as bypass to treat blocked femoral artery disease in the leg. Though the image-guided interventional radiology procedures apply ionizing radiation to treat the medical conditions, use of such procedures lead to increased patient and staff radiation doses. The study is therefore conducted to assess patient organ and effective doses from the selected interventional radiology procedures and propose effective dose prediction strategies for clinical applications.



## CHAPTER TWO

### LITERATURE REVIEW

#### Introduction

This chapter presents a review of literature on organ and effective doses in interventional radiology and discusses the need for evaluation of dose descriptors such as Kerma, absorbed dose, dose area product, entrance surface dose, etc. Differences between Kerma and absorbed dose are highlighted and the means for X-ray output measurements are presented. The chapter addresses pertinent information on energy transfer and dosimetric quantities associated with ionizing radiation. The principle of operation of fluoroscopic X-ray systems are also presented in detail. Dose measuring techniques for patients undergoing image guided procedures such as EVAR, FPOP and TACE are presented. The chapter also discusses radiation risks associated with the interventional procedures as well as quality control and quality assurance measures needed for optimal functioning of the interventional radiology imaging systems.

#### Ionizing Radiation

Ionizing radiation is made up of subatomic particles or electromagnetic (EM) waves that are energetic enough to knock off electrons from atoms or molecules, thereby causing ionization. The probability for ionization to occur depends heavily on the energy of the particles or waves, it does not depend on the number. Several particles or waves undergoing interaction will not cause ionization if they do not carry enough energy to make them ionizing (Camphausen and Lawrence, 2008). Examples of ionizing particles are alpha particles, beta particles, and neutrons. The ability for an electromagnetic

radiation to ionize atoms or molecules depends on the associated wavelength. Radiation on the short wavelength end of the EM spectrum is ionizing while radiation on the long wavelength end of the spectrum is non-ionizing. Ionizing radiation is present in the environment and comes from X-ray tubes, particle accelerators and radioactive materials (Camphausen and Lawrence, 2008; IAEA, 2007).

Acute levels of radiation exposure to tissues and organs have the potential of causing damage, resulting in skin burns and radiation sickness, otherwise called deterministic effects. At low doses of radiation exposure, stochastic effects are resulted, leading to formation of genetic damage and cancers (Camphausen and Lawrence, 2008). In the medical field, X-rays are largely used for diagnosis and treatment of medical conditions. They form part of the EM spectrum. X-rays commonly used in medical applications have wavelength in the range of 10 to 0.01 nm, corresponding to energies of 40 to 150 kV in diagnostic procedures (IAEA, 2007). They are shorter in wavelength than ultraviolet (UV) radiation and infra-red waves. X-rays are a form of ionizing radiation and as such can be dangerous if not carefully used (Camphausen and Lawrence, 2008; IAEA, 2007). They are primarily used for diagnostic radiography.

### **Energy Transferred from Radiation**

When an uncharged particle, for instance an X-ray photon, interacts with matter, part of its energy is transferred in various interaction events. In a volume,  $V$ , of material, the energy transferred ( $E_{tr}$ ) is given by the sum of all the initial kinetic energies of charged ionizing particles liberated by the uncharged particles in the volume  $V$ . For the case where photons in the diagnostic energy

range are the uncharged interacting particles,  $E_{tr}$  corresponds to the sum of the kinetic energies of electrons at the moment they are set free in an incoherent scattering or photoelectric interaction in the volume  $V$ . For photon energies above the pair production threshold of 1.022 MeV, kinetic energy may also be transferred to positrons (Dance et al, 2014).

As the liberated charged particles interact with matter, part of their initial kinetic energy can be irradiated as photons. There are two main processes responsible for the emission of photons (Dance et al, 2014):

- (i) the emission of bremsstrahlung radiation by electrons and positrons interacting with nuclei.
- (ii) the in-flight annihilation of positrons; the remaining kinetic energy of the positron at the moment of the annihilation plus the rest mass energies of the annihilated particles (1.02 MeV) being converted to photon energy.

### **Dosimetric Quantities and Units**

Dosimetric quantities used to specify the amount of dose received by patient during diagnostic or interventional radiology procedures are exposure, absorbed dose, and kerma. Measurement of the ionization produced by radiation was the first choice used to quantify the passage of radiation through matter. The quantity exposure, or, more precisely, exposure dose, as defined by the International Commission on Radiation Units and Measurements (ICRU, 1978), is related to the ability of a photon beam to ionize air. In recent years, the use of this quantity has been replaced by kerma, a more general quantity that is recommended for dosimeter calibration purposes.

This notwithstanding, absorbed dose is the quantity that better indicates the effects of radiation on human beings, and, accordingly, all the protection related quantities are based on it (Dance et al, 2014). The use of dosimetric quantities is important in many aspects of the application of radiation. In diagnostic radiology, radiation protection of staff and patients is the most important application of the dosimetric quantities.

### Exposure (X)

Radiation exposure is a measure of the ionization of air due to ionizing radiation from photons (i.e. X-rays or gamma rays). Exposure is defined as the electric charge ( $Q$ ) freed by such radiation in a specified volume of air divided by the mass ( $m$ ) of the air, as presented in equation (1). The International System of Unit (SI) unit of exposure is  $C / kg$ , which is defined by equation (1)

$$X = \frac{dQ}{dm} \quad (1)$$

### Kerma (K)

Kerma (K) is the acronym for **k**inetic **e**nergy **r**eleased per unit **m**ass. Kerma is related to the energy transferred from uncharged particles to matter. It is the quotient of  $dE_{tr}$  by  $dm$ , where  $dE_{tr}$  is the sum of the initial kinetic energies of all the charged particles liberated by uncharged particles in a mass  $dm$  of material, as expressed in equation (2). Kerma is expressed in  $J/kg$  or  $Gy$ .

$$K = \frac{dE_{tr}}{dm} \quad (2)$$

### Kerma Rate ( $\dot{K}$ )

Kerma rate is the rate of change of kerma ( $K$ ) with respect to time ( $t$ ), where  $dK$  is the increment of kerma in the time interval  $dt$ , as expressed in equation (3). Kerma rate is expressed in unit of  $(J/kg)/s$ , or  $Gy/s$ .

$$\dot{K} = \frac{dK}{dt} \quad (3)$$

### Absorbed Dose ( $D$ )

Absorbed dose ( $D$ ) is used to quantify the deposition of energy by ionizing radiation. It is a physical non-stochastic quantity and is defined as the ratio of  $d\varepsilon$  to  $dm$ , where  $d\varepsilon$  is the mean energy imparted to matter of mass  $dm$ . Absorbed dose is expressed in equation (4).

$$D = \frac{d\varepsilon}{dm} \quad (4)$$

Absorbed dose is expressed in unit of  $J/kg$  or  $Gy$ .

### Absorbed Dose Rate ( $\dot{D}$ )

Absorbed dose rate ( $\dot{D}$ ) is defined as the rate of change of dose with respect to time, where  $dD$  is the increment of absorbed dose in the time interval  $dt$ , as expressed in equation (5). The unit of absorbed dose is  $(J/kg)/s$  or  $Gy/s$ .

$$\dot{D} = \frac{dD}{dt} \quad (5)$$

The set-up for measuring dosimetric quantities in diagnostic radiology is presented in Figure 1.

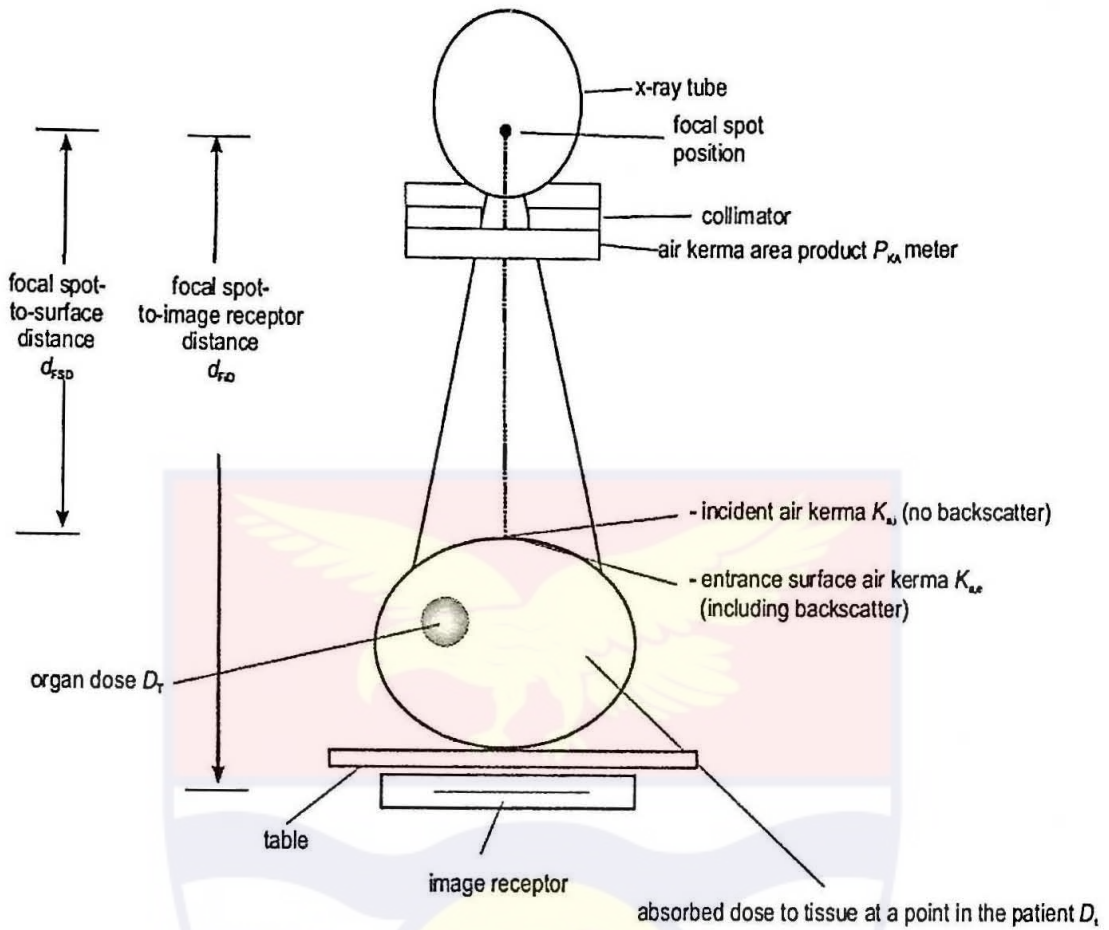


Figure 1: Schematic diagram for measurement of dosimetric quantities.

### Difference between Kerma and Absorbed Dose

Kerma and absorbed dose are expressed with the same units, and both are related to the quantification of the interaction of radiation with matter. Apart from the main fact that kerma is used to quantify a radiation field and absorbed dose is used to quantify the effects of radiation, there are some important points in their definitions that should be emphasized. One of the differences is the role of the volume of interest in these quantities; for kerma, it is the place where energy is transferred from uncharged to charged particles; for absorbed dose, the volume of interest is where the kinetic energy of charged particles is spent. For instance, for kerma, only the energy transfer due to interactions of uncharged particles within the volume is included; for absorbed dose, all the

energy deposited in the volume is included. Thus, charged particles entering the volume of interest contribute to absorbed dose, but not to kerma. Also, charged particles liberated by a photon in the volume of interest may leave it, carrying away part of their kinetic energy. This energy is included in kerma, but it does not contribute to the absorbed dose (Dance et al, 2014).

### **Incident Air Kerma ( $K_{a,i}$ )**

Incident air kerma ( $K_{a,i}$ ) is the air kerma from the incident beam on the X-ray beam's central axis at the focal spot-to-surface distance ( $d_{FSD}$ ). Only the primary radiation incident on the patient or phantom and not the backscattered radiation, is included in the determination of incident air kerma. The unit of incident air kerma is  $J/kg$  or  $Gy$ . Incident air kerma is related to  $K_a(d)$ , the air-kerma free-in-air at any other distance ( $d$ ) from the tube focal spot, by the inverse-square law, and is expressed as:

$$K_{a,i} = k_a(d) \left( \frac{d}{d_{FSD}} \right)^2 \quad (6)$$

Incident air kerma could be estimated from an X-ray tube output, given that the  $d_{FSD}$  and the tube-current exposure-time products are known for the specified radiation quality.

### **Incident Air Kerma Rate ( $\dot{K}_{a,i}$ )**

Incident air kerma rate ( $\dot{K}_{a,i}$ ) is the rate of change of incident air kerma with respect to time. The unit of incident air kerma rate is  $J/(kg/s)$  or  $Gy/s$  as expressed by equation (7).

$$\dot{K} = \frac{dk_{a,i}}{dt} \quad (7)$$

where  $dk_{a,i}$  is the increment of incident air kerma in the time interval  $dt$ .

### X-ray Tube Output

X-ray tube output,  $Y(d)$  is defined as the ratio of the air kerma at specified distant ( $d$ ) from the X-ray tube focus to the tube current-exposure time product ( $P_{It}$ ). The unit of X-ray tube output is  $J/kg.C$  or  $Gy/C$  or  $Gy/A.s$ . The tube current-exposure time product,  $P_{It}$ , is also referred to as the tube loading.

$$Y(d) = \frac{K(d)}{P_{It}} \quad (8)$$

### Entrance-Surface Air Kerma and Entrance-Surface Air Kerma Rate

Entrance-surface air kerma (ESAK) is the air kerma on the X-ray beam's central axis at the point where the X-ray beam enters the patient or phantom. Backscattered radiation's contribution is included in this. Formula for ESAK is expressed in equation 9. ESAK is related to the incident air kerma by the backscatter factor,  $B$ .

$$K_{a,e} = \dot{K}_{a,e} \times B \quad (9)$$

The backscatter factor depends on the X-ray field size, X-ray spectrum, and the thickness and composition of the patient or phantom.

Entrance-surface air-kerma rate,  $\dot{K}_{a,e}$ , is the rate of change of  $k_{a,e}$  with respect to time,  $t$ , where  $dk_{a,e}$  is the increment of entrance surface air kerma in the time interval  $dt$ . The unit of  $\dot{K}_{a,e}$  is:  $J/(kg/s)$ , or  $Gy/s$ .

$$\dot{K}_{a,e} = \frac{dk_{a,e}}{dt} \quad (10)$$

### Air Kerma–Area Product and Air Kerma–Area Product

The air kerma–area product ( $P_{KA}$ ) is the integral of the air kerma free-in-air over the area  $A$  of the X-ray beam in a plane perpendicular to the beam axis. The unit for  $P_{KA}$  is  $\text{Jm}^2/\text{kg}$ , or  $\text{Gym}^2$

$$P_{KA} = \int a.K_a(A)dA \quad (11)$$

If the air kerma free-in-air  $K_a(A)$  is constant over the beam area, which is approximately valid for small beam areas, then:

$$P_{KA} = K_a A \quad (12)$$

The PKA has the useful property of being approximately invariant with distance from the x-ray tube focal spot, as long as the plane of measurement or calculation is not so close to the patient or phantom as to receive a significant contribution from backscattered radiation. Usually, the position of the plane does not need to be specified.

### Fluoroscopy System

Fluoroscopy is an imaging technique that uses X-rays to obtain real-time moving images of the interior of an object. Design of fluoroscopy systems vary depending on their requirements and the imaging demands of various radiology examinations. As shown in Figure 2, the key components of a fluoroscopy system include an X-ray tube, spectral shaping filters, field restriction device (collimator), anti-scatter grid, image receptor, image processing computer, and display device. Ancillary but necessary components include high voltage generator, patient support device (table or couch) and hardware to allow

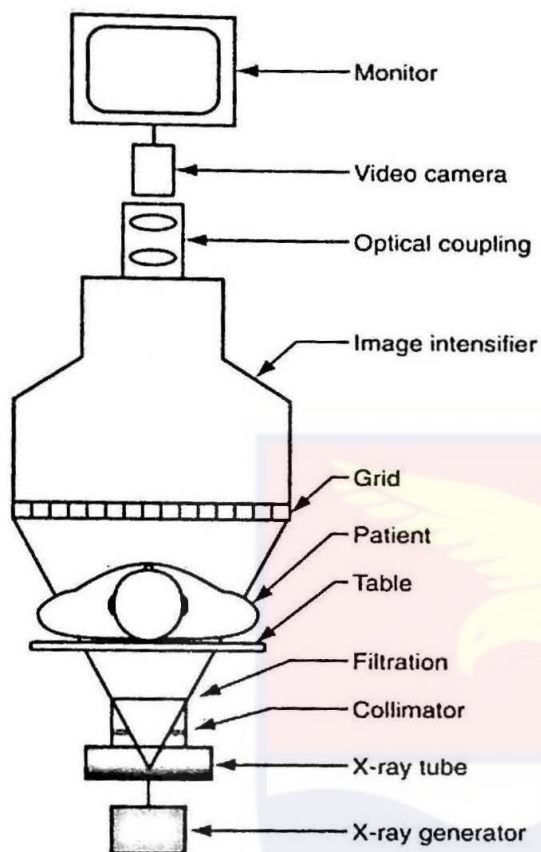


Figure 2: Schematic diagram of a fluoroscopy system (Radiology Key, 2020)

Examinations carried out with a fluoroscopy system may be complex. In addition to the image intensifier, different types of cameras following the intensifier output, as well as variety of viewing monitors are required. The performance of a fluoroscopy system, including image quality and doses delivered to patients, are dependent on the type and make of the system. Most equipment functions are subject to automatic control. For example the generator factors, the aperture between the image intensifier and TV camera, and the TV camera gain may all be automatically controlled. If creation aspects of the system performance deteriorate, then the system will automatically compensate, perhaps by increasing the image intensifier input dose or dose rate. Due to the nature of automatic fluoroscopy systems, a user may not be aware of any problem. For such reason, it is essential to evaluate dose and dose rates with image quality of conventional and digital fluoroscopy systems (Finch, 2001).

nature of automatic fluoroscopy systems, a user may not be aware of any problem. For such reason, it is essential to evaluate dose and dose rates with image quality of conventional and digital fluoroscopy systems (Finch, 2001).

Before commencing any quality assurance assessment of the fluoroscopy system, the X-ray tube generator should be checked. It is essential to first of all check the beam quality of the X-ray tube and generator. This is achieved with a non-invasive X-ray tube potential divider used to establish the calibration of the fluoroscopic setting. The purpose of such measurement is to establish the nominal tube potential settings corresponding to stated kVp energy. This is especially useful when assessing performance and dose rates according to the manufacture specifications.

Assessment of the operation of the automatic dose rate control system is the next stage. Image intensifier entrance doses as well as patient dose rates may be assessed. These measurements involve the use of phantoms to simulate patients of varying thickness. Image quality phantoms containing test piece inserts are used to assess the fluoroscopy system. First, the contrast and brightness setting on the monitor must be adjusted correctly. Once correct monitor adjustment is assured, low contrast detectability, high contrast detectability, threshold contrast detectability, limiting resolution and distortion may be checked (Finch, 2001).

### **Fluoroscopy device for interventional procedures**

C-arms are often used to perform image-guided procedures in angiographic suites. Figure 3 shows an angiographic suit for performing interventional procedures. The C-arm as the name denotes, is designed as a C with the X-ray tube on one end and the image intensifier or detector on the

right or the left shoulder of the patient respectively. Tilting the C-arm towards either the feet or head of the patient, is called caudal (CAU) or cranial (CRA) respectively (Kern, 2011).

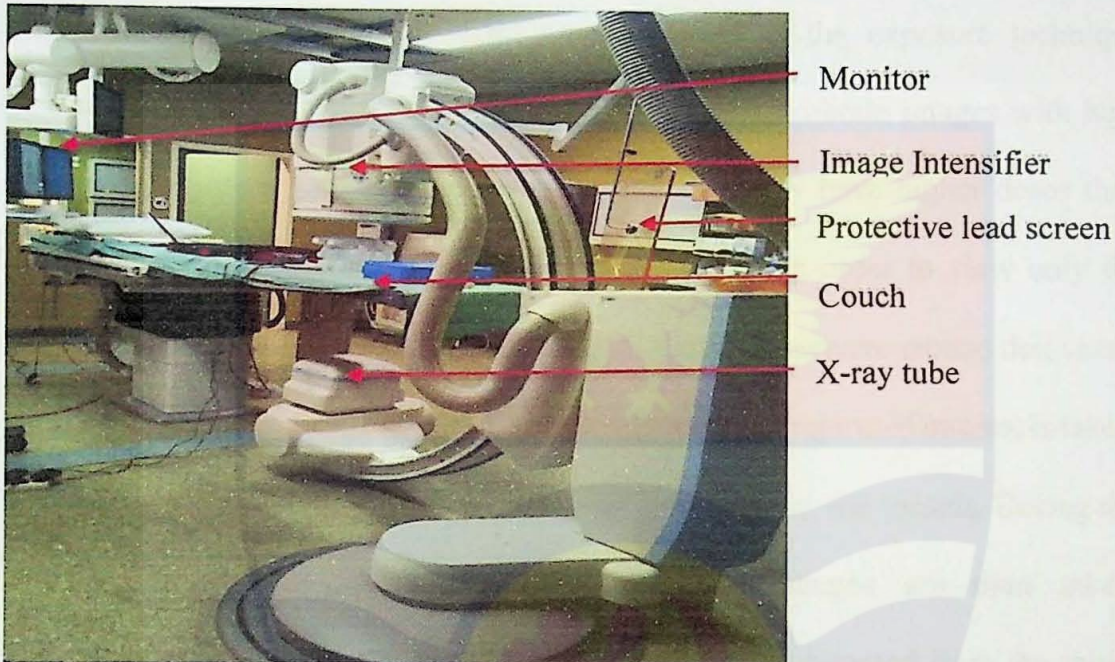


*Figure 3: C-arm commonly used for image-guided procedures label major parts (Reference: image from this study's field work).*

An operator of a fluoroscopy system mainly uses X-rays to navigate the patient's internal organs. Image quality of fluoroscopy should be highly visible to identify when the catheters reach the location of interest. Pulsed fluoroscopy can be used in different ways depending on the dose per pulse and the number of pulses used from the operator. The images with breaks between them when taken are referred to as pulsed fluoroscopy images. The break may be long or short and is dependent on the number of pulses set within a time interval. Nevertheless, these breaks have no effect on the images being viewed on the screen unless a patient moves rapidly during a procedure. An advantage of using pulsed fluoroscopy for patient procedure is that, there is much lower radiation

screen unless a patient moves rapidly during a procedure. An advantage of using pulsed fluoroscopy for patient procedure is that, there is much lower radiation dose to the patient as compared to continuous fluoroscopy (Kern, 2011; Miller et al, 2003a).

Digital Subtraction Angiography (DSA) is the exposure technique normally used in vascular procedures. The aim is to obtain images with high diagnostic quality, however, these techniques usually have higher doses than ordinary fluoroscopy. The DSA technique is used in order to view only the blood vessel in the region of interest while all other structures around that vessel are subtracted from the image. An initial image of the region of interest is taken, then followed by injection of the contrast medium into the vessels. During the injection of the contrast medium, series of images are then taken, simultaneously, all other anatomical structures are subtracted from the initial image to view the circulation of the contrast media in the blood vessels. Iodine is one of the contrast medium used for these procedures. The resulting images show only the contrast filled vessels in the region of interest (Castleman and Tobis, 1985).

There are different types of exposure modes (DSA modes) that vary in dose and image quality. These different modes are pre-programmed in the system and are selectable for the operator. When 3-dimensional imaging is performed, the C-arm is rotated automatically and takes images in different projections. The intra-operative 3D images are sometimes matched with a CT that is taken preoperatively. This is called image fusion and helps the operators before and during the procedure with stent placement (Koutouzi et al, 2015).

During the procedure a pedal is used for pulsed fluoroscopy or angiographic series (high dose images). With the help of the pedal, the operator can irradiate and have both hands free to example insert catheters into the patient's vessels. Fluoroscopy systems can be divided into two categories, depending on the detector type. The first category is image intensifier systems, which are rarely used anymore, and the second one is flat-panel detector systems. The flat-panel detector systems can be divided into two different classes. The first one is direct conversion (X-ray photons are converted to electric charge directly) and the second one is based on indirect conversion. Indirect conversion converts X-ray photons to light by the use of a phosphor material that absorbs the X-ray photons and produces light. This light interacts with a photodiode electrode and creates the electric charge that is used by the system to produce an image.

In the X-ray machine a number of programmes specifying some technique factors and image reconstruction are set and used specifically for different procedures. Parameters such as tube voltage, tube current and filtration are controlled and varied by the system's automatic exposure control (AEC). The purpose of the AEC is to deliver consistent radiation to the detector regardless of the patient thickness in different parts of the body. This is achieved by adjusting the parameters for different exposure situations mentioned above. However, the parameters cannot vary out of the programmed range. There is a pre-programmed range for all the parameters that are controlled by the AEC. Therefore these parameters are altered with the purpose to produce adequate image quality, regardless of patient thickness. Parameters that are not

automatically controlled by the system but controlled by the operator are rotation of the C-arm and fluoroscopy mode/exposure mode.

### Dose Area Product

Dose-area-product (DAP), with unit  $\text{Gycm}^2$ , is defined as the absorbed dose multiplied with the irradiated area. The DAP value provides the operator with a simple dose estimation during a procedure. DAP gives a simplified indication of stochastic risk, but the quantity that is used to estimate the stochastic risk of the patient is effective dose. Effective dose ( $E$ ) is used to estimate the stochastic risk of the patient and is determined using equation 13:

$$E = \sum D * W_T * W_R \quad (13)$$

where  $D$  is the absorbed dose in each organ;  $W_R$  is the weighting factor that depends on the different radiation types (e.g. X-ray, protons, alpha particles, etc.) and  $W_T$  is the weighting factor for specific organs.

For example, the human bone marrow has a weighting factor of 0.12 and the skin has a weighting factor of 0.01. Tissues or organs with higher sensitivities have higher value of the weighting factors than those with lesser sensitivities. The unit of effective dose is Sievert (Sv). The risk of cancer is estimated to increase with 5.5 % per Sievert. This estimation is derived from the survivors of the atom bomb dropped over Hiroshima and Nagasaki (Rehani et al, 2010). If one is to get an estimation of stochastic risk, one must convert the DAP value to  $E$  (Martin & Sutton, 2002). Table 1 illustrates the weighting factors for the different organs (ICRP, 2007).

Table 1: Weighting factors for the different organs

Organs	Weighting Factors
Bone marrow, colon, stomach, lungs, breasts	0.12
Gonads	0.08
Bladder, liver, esophagus, thyroid	0.04
Salivary gland, brain, skin, bone surface	0.01
Remainder* (all other organs not listed above)	0.12

\* Adrenals, extrathoracic region, gall bladder, heart, kidneys, lymphatic nodes, muscle, oral mucosa, pancreas, prostate, small intestines, spleen, thymus, uterus/ cervix.

X-ray as image guidance is used for many different procedures. Dose data from literature for different image-guided procedures and on different anatomical structures is presented in Table 2.

Table 2: Data from image-guided procedures from literature

Study	Procedure	Total cases	Fluoro Time (min)	DAP (Gy.cm <sup>2</sup> )	Estimated skin dose (Gy)
			Mean	Mean	Mean
Howells et. al. (2012)	TEVAR	232	10.0	194.0	0.80
Walsh et. al. (2012)	EVAR	111	18.5	85.6	0.69
Geijer et. al. (2005)	EVAR	24	28.0	72.0	0.39
Jones et. al. (2010)	EVAR	320	29.4	46.8	-

DAP: Dose Area Product; min: minutes;

In IR procedures, the benefits and risks always must be assessed. If the benefit of the procedure outweighs the risk of radiation damage, one could go ahead with the procedure. Dose restrictions for patients do not exist as it does for staff members performing the procedure. The procedure, however, should

be executed on the ALARA (as low as reasonably achievable) principle (Strauss, 2006). There is however some standardised procedures that have reference doses. For example, in Sweden the reference dose for a coronary angiography procedure is 80 Gy $\text{cm}^2$  (Swedish Radiation Safety Authority, 2016). The reason that some procedures do not have reference doses is due to the lack of standardized work.

### **Endovascular Aneurysm Repair (EVAR)**

EVAR is an endovascular procedure practiced in order to treat abdominal aortic aneurysm (AAA). The aorta is the biggest artery in the body and the main blood cell that supplies blood to abdomen, pelvis, legs and the smaller arteries. An abdominal aortic aneurysm occurs when an area of the aorta is enlarged and becomes like a balloon. If the aneurysm grows fast one might feel pain but usually the aneurysm itself does not come with any symptoms. If the aneurysm is ruptured it can cause life-threatening damage. The cause of the disease is unknown but there are some risk factors such as smoking, high blood pressure, heredity and increasing age. Patients with AAA are treated with EVAR or open surgery. Approximately ten percent of the patients with AAA require open surgery. Open surgery is – clinically recommended during acute conditions, for example when the aneurysm has ruptured or is growing fast. This is one major reason why a hybrid suite is required, for its sterility if the operators have to change to open surgery procedures (Kern, 2011; Miller et al, 2003b; Howells et al, 2012; Walsh et al, 2012; Pantos et al, 2009; Geijer et al, 2005; Jones et al, 2012).

EVAR procedures use image-guided technique and are minimally invasive. The operator cuts the patient in the groin, to get access to the femoral

artery. From the femoral artery a long tube, called a catheter, is led up via the iliac artery to the aneurysm. The operator is guided with the help of fluoroscopy up to the dysfunctional/damaged aorta. Attached to the catheter is a stent graft. A stent is a tube that is placed in the anatomy to create a passage for blood to go through vessels, in this case the aneurysm. The placement must be done with great care because of the risk of blockade of the renal arteries. When the stent is placed the pressure reduces in the abdominal aorta and reduces the risk of rupture dramatically.

The benefit of an EVAR compared to open surgery is that the patient spends less time in the hospital because there is no need for opening the chest or abdomen to execute the procedure. This decreases the risk of damaging the body's main arteries, veins and nerves. Studies have shown that the 30-day operative mortality is reduced by two-thirds when the aneurysm is repaired using EVAR instead of open surgery (Jones et al, 2010; Greenhalgh, 2004). Even though there are multiple benefits with EVAR, it is however one of the most dose-requiring procedures using image-guidance. A study by Weerakkody et al. in 2008 showed that skin damage of 2 Gy was exceeded in 29 % of the procedures performed (Weerakkody, 2008). This indicates that EVAR requires high doses. The aneurysm can occur in the thoracic aorta as well and is then called thoracic aortic aneurysm (TAA).

The treatment for TAA is called TEVAR. Usually this procedure requires more advanced methods compared to EVAR, because of the complexity of the blood circulation to the upper body and cerebral arteries, leading to the brain (Rexius, 2013). It is challenging to determine the radiation dose from EVAR and TEVAR since patients vary from each other. The lack of

standardized treatment routines makes it hard to determine dose to operator and patient. In the present study both EVAR and TEVAR were examined.

### **Patient Dose during Image Guided Procedures**

Patient doses are monitored in two ways by the X-ray equipment during image -guided procedures. The first one is an estimation of skin dose, measured as incident air kerma (IAK) and the second is the estimation of effective dose (Kern, 2011; Martin and Sutton, 2002). The skin dose can either be overestimated and underestimated, however, the interventional reference point remains constant throughout the scan. The IAK value is an indication of the dose to the skin, i.e. an indication of deterministic risk. The unit for IAK is Gray (Gy).

### **Dose Measurements Techniques**

#### **Measurement of ESD in Interventional Radiology**

Some confusion exists in the literature with regard to the definition of entrance surface dose (ESD). That is, whether the definition should refer to absorbed dose to air or absorbed dose to tissue. The consensus definition proposed by the NRPB would be adopted. Therefore, the ESD is taken as the absorbed dose to air including backscatter at the point of incidence of the beam axis with the patient entrance surface. Many different dosimetry approaches exist for the determination of ESD in IR. The following sections describe approaches to measurement of ESD from DAP, tube output, TLD measurements and slow-film dosimetry (IEC, 2000).

## Measurement of ESD from DAP Measurements

Use of DAP to estimate ESD may be desirable in many cases (Geijer et al, 2005, Jones et al, 2010, Molyvda-Athanasopoulou et al 2011) since many departments will not have easy access to TLDs, which are often used for this purpose. McParland has developed a method utilizing DAP for the estimation of ESD (entrance skin dose; i.e. dose to tissue at the intersection of the beam axis with the patient). It has been shown that this approach to the calculation of ESD from DAP measurements can contribute an uncertainty of up to  $\pm 40\%$  to the measurement of ESD. In this approach DAP measurements are used to estimate the ESD to the patient by means of estimates of the field size at the entrance surface to the patient. If the beam size is sufficiently large then the assumption may be made that the dose is approximately homogeneous across the extent of the beam area. Therefore, the dose at the centre of the beam may be estimated by dividing the DAP by the beam area at the entrance surface to the patient (McParland, 1998). This approach has been shown to be quite accurate in practice. Thus equation 14 can be used to calculate the ESD from DAP measurements:

$$ESD = \left( \frac{DAP}{A} \right) * C.F * BSF \quad (14)$$

where:

BSF is the back-scatter factor appropriate for any given beam kVp, field size, and HVL.

DAP is the Dose Area Product recorded in any given instance.

A is the beam area recorded in any given instance.

C.F. is the calibration factor for the DAP meter estimated using a standard.

This beam area may then be corrected geometrically to the entrance surface of the patient if either:

- a) It can be assumed that the tube focus to patient entrance surface distance, FSD, and tube focus to image intensifier (II) entrance surface, FID, are determinable and practically the same for each projection in a certain IR procedure, or
- b) The FSD can be determined from existing recordings of FID and patient characteristics.

The following equations may be used respectively to correct the beam area to the entrance surface with the patient in either case:

$$A(FSD) = A(FID) * \left(\frac{FSD}{FID}\right)^2 \quad (15)$$

$$A(FSD) = A(FID) * \left(\frac{FID - W}{FID}\right)^2 \quad (16)$$

where A (FSD) and A (FID) are the area of the beam at the entrance to the image intensifier and the entrance to the patient respectively, and W is the equivalent thickness of the patient. This equation may be used in situations involving fixed systems where the image intensifier is brought close to the exit surface with the patient to eliminate scatter. The Finnish Radiation Protection Authority (STUK, 2008) has developed regression models which describe the variation in weight with height, and corresponding variation in body thickness with such parameters. The regression function takes the following form:

$$y = ax + b \quad (17)$$

where x is weight of the individual in kilograms, y is the width or thickness of the region concerned, a, b are the regression parameters. This is a procedure that can be used for both mobile and fixed fluoroscopy systems (IEC, 2000).

### Measurement of ESD from Tube Output Measurements

ESD may be calculated in practice by means of knowledge of the tube output. This is useful in situations where the tube does not have a DAP facility. Tube output measurements are routinely acquired during the QC performed on X-ray equipment. In such instances, the following equation may be used:

$$ESD = \frac{O}{P} * \left(\frac{kVp}{80}\right)^2 * mAs * \left(\frac{100}{FSD}\right)^2 \quad (18)$$

where:

mAs is the tube milli-Amp-current-time which is used at any given instance. FSD is the focus to entrance surface distance used at any given instance (IEC, 2000).

$\frac{O}{P}$  is the tube output per mAs measured at a distance of 100 cm from the tube focus along the beam axis at 80 kVp.

kVp is the beam kVp recorded for any given examination (in many cases the output is measured at 80 kVp, and therefore this appears in the equation as a quotient to convert the output into an estimate of that which would be expected at the operational kVp). The value of “80” should be substituted with whatever kVp the actual output is recorded at any given instance).

### Estimation of ESD from TLD Measurements

TLDs are accepted as the best standards for estimation of entrance surface dose in practice (Stecker et al, 2009). In interventional radiology, they are commonly placed around and at the centre of the entrance surface to the patient at points where the maximum exposure is anticipated to occur. This requires knowledge of the procedure and exposure pattern that is to be employed by the clinician to be available prior to the start of the procedure. TLDs are read in the standard manner and the maximum value read is used as an estimate of

the maximum ESD received by the patient. Frequently, many TLDs are spaced around the irradiated area on both the entrance and exit site to enable the determination of the most irradiated area and maximum surface (or skin) dose. Again, there is a requirement that the location of the most irradiated area is known prior to the start of the procedure so that the number of TLDs used per patient is minimized. The advantage is that the measurement is the most accurate in-vivo estimate of skin dose available (IEC, 2000).

### **Estimation of ESD using Slow Films**

Radiotherapy slow films are used for the verification of patient doses and orientation in radiotherapy procedures. In IR procedures, the film is placed underneath the patient and exposed throughout the normal IR protocol. The films are calibrated by standard sensitometer, and read by densitometer. They have a linear range from 400 mGy to 2000 mGy for Co-60 energies, which makes them ideal for identifying whether deterministic levels for skin have been exceeded. When used in conjunction with DAP and TLD measurements of ESD, it was found that the measurements were within 5 - 20%. The films can be used to estimate total ESD, total DAP, or maximum ESD (IEC, 2000).”

### **Radiochromic Media**

Radiochromic dosimetry media (commonly referred to as “films”) can be handled in normal lighting conditions, are self-developing, respond nearly immediately to exposure to radiation, and they require no chemical processing. They are used to measure absorbed dose and to map radiation fields produced by X-ray beams in a manner similar to that of portal film. As such, radiochromic media have the same advantage of locally specific dose monitoring without

error resulting from beam reorientation or backscatter. And radiochromic film can be examined during a procedure if there is a need to obtain an estimate of skin dose. Exposure to ionizing radiation causes radiochromic film to immediately change color and darken. The degree of darkening is proportional to exposure and can be quantitatively measured with a reflectance densitometer. There does exist a gradual darkening of the film with time and darkening is usually maximum within 24 hours. However, the amount of darkening within the period immediately following the initial exposure is not large and does not interfere with the ability to use it for skin dose guidance during a procedure as long as this phenomenon is understood and taken into account (Faulkner, 2001).

### **Measurement of Effective Dose (E) in Interventional Radiology**

Effective Dose (E) has been introduced as an estimator of the potential for detriment from exposures to ionizing radiation (Dance et al, 2014). Recently many reports (Duncan et al, 2011, Foerth et al, 2015, Fossaceca et al, 2012) have been written on methods for the estimation of E in IR. Various techniques have been employed which depend on procedure type, methods of estimation of conversion coefficients, and quantity to be used as an estimator for E. In IR, coefficients for the estimation of E from DAP and ESD measurements have been developed. They have been calculated from Rando phantom measurements and Monte Carlo simulations on photon transport in mathematical phantoms. However, given that the fluoroscopy and radiography sequences may vary significantly throughout a given procedure, it is difficult to characterize an IR procedure for the purposes of calculation of E. Consequently, approaches to the calculation of E vary widely in accuracy, where some employ a single conversion coefficient for the procedure as a whole, while others calculate

conversion factors which are specific to each radiography and fluoroscopy projection throughout the procedure. Further still, automated systems which allow the calculation of E from any number of defined exposure projections and conditions have been developed. Indeed, there is a significant uncertainty in any calculation of E where deviations in exposure factors, irradiation geometry and patient characteristics (from those for which the conversion factors have been calculated) invariably exists. In many cases the size of this uncertainty is not known, but is thought to have a minimal value of a factor of 2 surrounding the estimate. Consequently, E has significance as a normalization of the detriment attributable to exposures of different individuals in IR, but the uncertainty in its calculation leads to the conclusion that DAP is a more appropriate estimator of the stochastic detriment from exposures in IR (IEC, 2000).

### **Radiation Risk during Image-Guided Procedures**

During image-guided procedures there may be a risk of tissue damage, for example skin burns and circulatory disease regarding the patient and also eye cataract for the operators if they are not properly protected (ICRP, 2001). These tissue damages are called deterministic effects and are noticed after exceeding a threshold dose. The threshold dose for circulatory disease can be as low as 0.5 Gy to the heart and brain (Rehani et al, 2010). The threshold dose for skin erythema is 2 Gy (Miller et al, 2003b). There is also a risk of stochastic effects i.e – cancer induction. For stochastic effects the risk increases with dose without any threshold. It is essential for the whole procedure that the operator, together with the staff, plans the imaging in advance as much as possible. This way the dose to the patient can be kept to a minimum. Generally, for patient protection, it is important that the operator rotates the X-ray equipment (this

way the risk of skin injury is decreased), keeps the distance between the detector and the patient as close as possible, uses the lowest dose per pulse (and only increase the dose per pulse when necessary), keeps the fluoroscopy time as low as possible and uses as few exposures as possible (Rehani et al, 2010).

### **Radiation Risk Estimates**

The lifetime attributable risk (LAR) of cancer incidence and mortality models have been derived by the Biological Effects of Ionizing Radiation (BEIR VII) committee (NRCNA, 2006). The models take into account the cancer location, gender and the age of the exposed individual. The risk models have been derived for leukemia, cancers of some organs (liver, lung, stomach, bladder and colon) and all solid cancers. Solid cancers have a latency period of 5 years and leukemia has a latency period of 2 years. These values are used in the PCXMC software to determine the LAR, which is expressed as risk of exposure-induced death (REID) (STUK, 2008).

### **Quality Assurance (QA) and Quality Control (QC)**

A QA programme, which includes quality control tests, helps to ensure that high quality diagnostic images are consistently produced while minimizing radiation exposure. The QA program covers the entire X-ray system from machine, to processor, to view box. This programme enables the facility to recognize when parameters are out of limits, which tends to result in poor quality images and can increase radiation exposure to patients. Simply performing the QC tests is not sufficient. When QC test results exceed established operating parameters, appropriate corrective actions are recommended to be taken immediately and documented. QA programme is

required to maintain high quality diagnostic or therapeutic output and reduce patient exposure in interventional procedures (Dance et al, 2014).

### **Summary: Chapter Two**

In interventional radiology procedures, the application of ionizing radiation is known to have the potential of causing acute damage (deterministic effects) or long-term genetic damage or cancer (stochastic effect). Literature on organ and effective doses in interventional radiology has been reviewed under this chapter. Dose descriptors (Kerma, absorbed dose, dose area product, entrance surface dose, etc.) have been defined and described in their application to interventional radiology procedures. Description for measurement of dosimetric quantities has been explained. Fluoroscopy has been described as an imaging technique that uses X-rays to obtain real-time moving images of the interior of an object. C-arm fluoroscopy systems are often used to perform image-guided procedures in angiographic suites. Theories behind energy transfer and dosimetric quantities associated with ionizing radiation have been explained in detail and dose measuring techniques for patients undergoing EVAR, FPOP and TACE image guided procedures also presented. The interventional radiology procedures were executed on the ALARA (as low as reasonably achievable) principle.

the unit could be varied among four preset dimensions of 14 cm, 20 cm, 28 cm and 40 cm. The maximum focus-to-detector distance (FDD) of the C-arm angiography unit is approximately 118 cm. The patient couch is movable in the directions of up-down, left-right and forward-backward, which accounts for the focus-to-skin distance (FSD) and simultaneously the DAP and cumulative dose (CD) measurements.

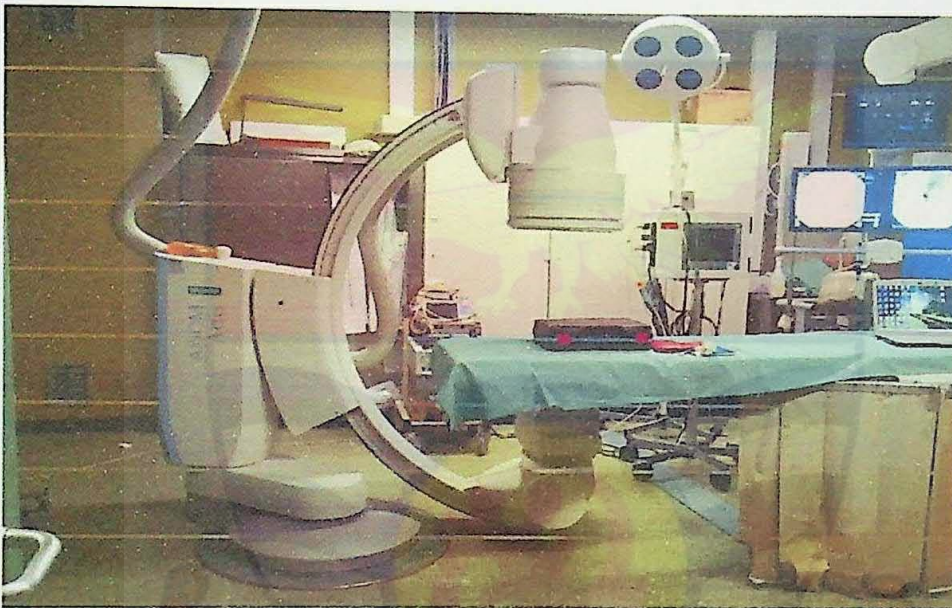


*Figure 4: Fixed C-arm angiography unit: Siemens Axiom Artis FA*

### **Calibration of Radcal Model 3035**

The Radcal model 3035 was used for measuring radiation exposure values during the irradiation of the TLD chips for calibration purposes. Figure 5 shows the Radcal model 3035. It displays measurement results of radiation exposure in mGy or rad and time in milliseconds or minutes. Typical applications include direct beam measurements for diagnostic X-ray and fluoroscopy. The function switch on the face of the control unit, toggles from 'Off' to 'Rate', to 'Pulsed', and then back to 'Off'. To use the device in any of the modes, the function switch is pressed to enter the mode required. In the 'Rate' mode, the unit of measurement is displayed as mGy/min and the device

could be exposed to continuous X-ray beam for measurement. In the ‘Pulsed’ mode, the unit of measurement is displayed to alternate between mGy and milliseconds and the chamber could be used for single exposure purposes. The chamber may be exposed through the bottom without loss of accuracy. It goes off automatically after 10 minutes of inactivity. The ‘Pulsed’ mode was used for the exposure measurements during the TLD irradiation. The dose-to-air ratio (exposure) measured by the ionization chamber was recorded.

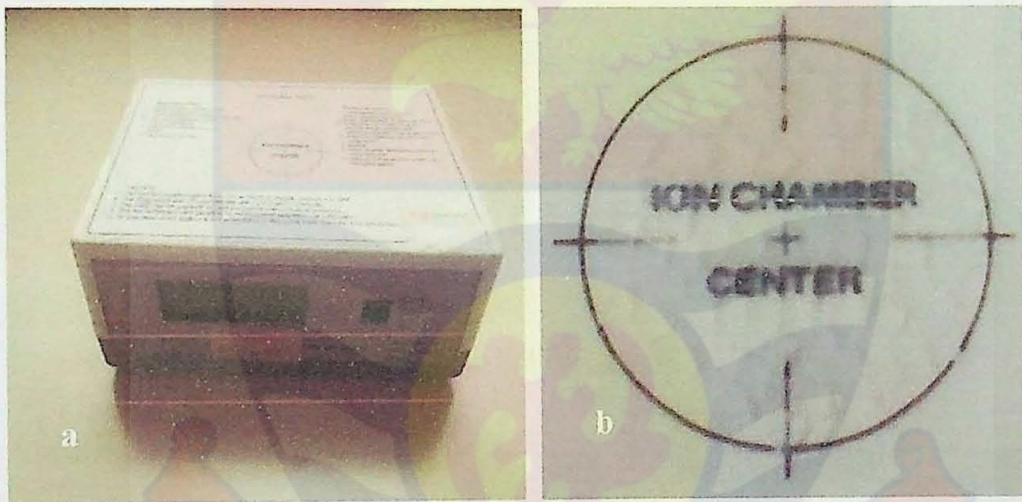
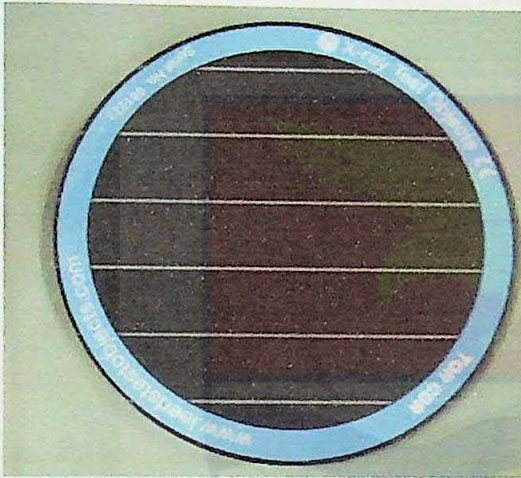


Figure 5: a. Radcal Model 3035 Ionization Chamber; b. sensitive area of the Radcal Model 3035.

### Leeds Test Objects

The Leeds test phantom, Figure 6, (Leeds test object limited, UK) is designed for routine test purposes to check image performance of the fluoroscopy machine. These tests are performed regularly, monthly or whenever there is any maintenance that could affect the image quality. The test tool could be used to check image clarity, high and low-contrast image detail detection and image resolution in units of line pairs per millimeter (LP/mm).

In performing the test, an initial image is taken, and then, the image quality is measured by counting the number of details detected and the number of bar-patterns resolved in the image. To determine any deterioration in the images from the angiographic unit, an ongoing record of these measurements is maintained and compared consistently.



*Figure 6: The Leeds test object for radiography*

### **Calibration of TLD Chips**

#### **Set up for calibration**

First the TLD chips were annealed in a special oven for that purpose at appropriate temperatures according to the manufacturer's specifications. The chips were then irradiated under an X-ray beam energy equivalent to the optimal energy range used during the procedures to be measured. The TLD reader was then used to read out the signal from each TLD chip which was recorded in order by arranging the chips on the numbered cooling plate. The cooling plate helped to identify each chip for individual marking; therefore it was easy to calculate the actual dose to a specific organ where each chip was placed based on the calibration coefficient.

## Annealing and irradiation of dosimeters

The TLD chips were annealed using a Victoreen annealing oven (Victoreen Incorporated, Ohio, USA) at 240 ° C and 360 ° C for the TLD-100H and TLD-200 respectively for 10 minutes each. Annealing clears the dosimeters of all exposure. To anneal, all 212 TLD-100H chips were arranged individually on a brass plate using tweezers. Afterwards, the chips were arranged on a cooling plate for about a minute and then packed into a light proof container and transferred onto the ionization chamber for irradiation. Same process was used for the TLD-200 chips.

The dosimeters were arranged individually in the center (most sensitive region) of the ionization chamber such that no one chip lays on top of the other, as shown in Figure 6b. This arrangement allows even irradiation of the dosimeters in the primary radiation beam. The dosimeters (TLD-100H and TLD-200) were then irradiated at 85 kV, 320 mAs in two separate groups of identical chips. At 100 cm distance from tube to couch, radiation beam was collimated to cover the chips in the sensitive part of the ionization chamber. The exposure value which is displayed on the ionization chamber screen is then recorded and used to evaluate the calibration factor.

Again the chips were arranged on the cooling plate (Figure 7d) and individually read using the TLD-reader, Harshaw 3500. Each reading was recorded against the number on the cooling plate to help identify each TLD chip.

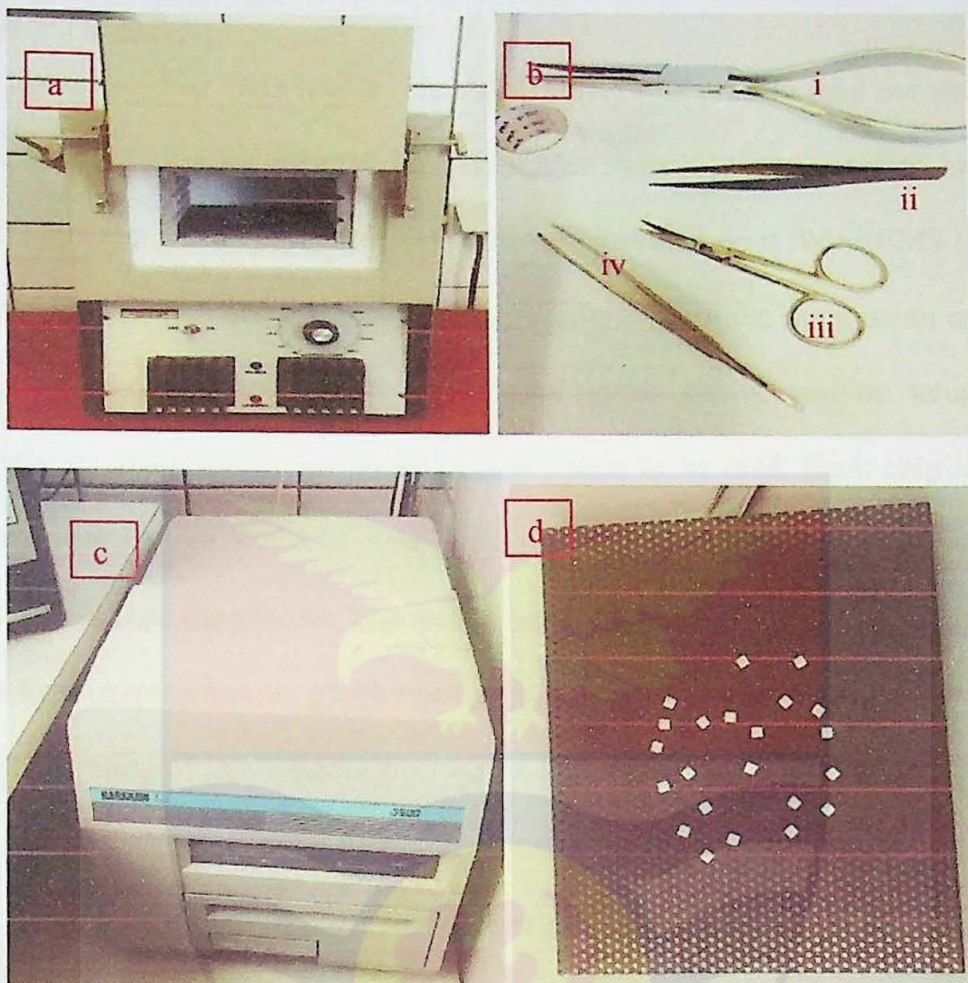


Figure 7: Photos of a) Victoreen annealing oven b) Handling tools i) tong for handling hot brass plate in and out of annealing oven ii) and iv) tong for handling TLD chips iii) scissors c) Harshaw 3500 reader d) Brass plate with some TLD chips.

### Calculation of Calibration coefficient

The calibration coefficient was calculated as the ratio of the exposure measured by the ionization chamber divided by the TLD signal recorded by the reader. The TLD chips were read individually and as a group for the TLD-100H and TLD-200.

The TLD chips were grouped into batches based on their sensitivities such that, the standard deviation of each batch was less than 3%.

### *Reading of TLD Chips*

Harshaw 3500 TLD reader (Harshaw, USA) was used to read out the irradiated TLD chips for calibration. The reader system is connected to an external computer which has WinREMS software installed on it. WinREMS is the operating software for all Harshaw TLD readers. From the main menu of the software, the appropriate time temperature profile and acquisition setup conditions are selected for the group of dosimeters to be read. Each chip is placed manually on an allocated plate in the reader and then the 'Read' button is pressed to initiate the process. The reader automatically heats the TL material using a heating-planchet. A photo multiplier measures the TL-light released during the heating of the material from room temperature to 240 °C for TLD-100H and 360 °C for TLD-200 chips. The photomultiplier tube and an integrated charge measuring system, record the information in the form of a glow curve. The area under the glow curve quantifies the total light output from the heated TL material which is recorded as the TLD chip signal in units of nano Coulombs (nC) or micro Coulombs ( $\mu\text{C}$ ).

### **Anthropomorphic Phantom Measurements**

The phantom, Figure 11, represents an adult individual who weighs 73.5 kg and has a height of 1.73 m. The phantom is constructed with tissue equivalent material and contains air cavities, lungs and skeleton.

The TLD chips were used to measure the radiation dose at 314 different points in and on the anthropomorphic phantom. The 212 TLD-100H and 102 TLD-200 chips (Hashaw, USA) were used for the organ dose measurement with the anthropomorphic phantom. The TLD materials are lithium fluoride chips,

doped with magnesium, copper and phosphorus in the case of TLD-100H (LiF: Mg, Cu, P) and magnesium and titanium in the case of TLD-200 (LiF: Mg, Ti).

### **Placement of TLDs in phantom**

To clinically set up the anthropomorphic phantom for the dose measurement, the region of interest was set from the thyroid (slice 9) to slice 33 (pelvis). An anatomical atlas was used to map the location of organ positions of interest depending on the selected procedure (EVAR, TACE, femoropopliteal). The TLD-100H chips were placed in the location which may be in the primary beam and the TLD-200 chips were placed in the locations that would be outside the direction of the primary beam.

The phantom's slice-sections 21 to 30 were chosen to represent the possible location of the abdominal aorta and therefore, the most exposed location during the EVAR procedure. Consequently, 254 chips were inserted in the organ locations in the phantom and 60 chips were distributed on the surface to sample entrance and exit skin doses.

The slice sections 9 to 20 were chosen to represent the possible location where the liver could be found as well as the veins for the contrast agent used during the TACE procedure on patients.

The Digital Imaging and Communications in Medicine (DICOM) header information summary of the patient exposure was used as a guide to perform the experimental measurements.

### **Dose measurement with TLDs in physical phantom**

TLD chips were placed in the designated holes which match the organ of interest based on the anatomical atlas. Depending on the size of the organ and

patient anthropometric data (i.e. age, weight and height), angiographic images, and X-ray field location on patient's body surface.

### **Inclusion and Exclusion Criteria**

Criteria for the data collection was complete records of DICOM structured reports which includes the exposure parameters, angulations, dose area product and total fluoroscopy time.

- a) The inclusion criteria set for the EVAR procedure were patients with aneurysm located in the abdominal part. This implies both supra-and infra-renal arteries with no concurrent aneurysm in the thoracic aorta or other arteries.
- b) For femoropopliteal (FPOP) procedures, the inclusion criteria were patients with aneurysms occurring in the femoral and popliteal arteries and with no accompanying aneurysm of other arteries.
- c) Inclusion criteria for the TACE procedures were patients with tumors (benign or malignant) and artery malformations in the liver which had been treated with no concomitant aneurysms.

The exclusions criteria were:

- i. incomplete radiographic images and DICOM datasets;
- ii. absence of one of the inclusion criteria for the procedures (EVAR, FPOP and TACE).

This was a retrospective study based on available DICOM structured reports of patients who had undergone such procedures. Organ and effective doses were estimated through MC simulations with the dataset received from the DICOM.

## Ethical Clearance for Data Acquisition

Due process was followed through to obtain ethical clearance to start the data acquisition and simulation of the examination with the MC software and finally perform the experimental setup of the patient procedures in clinical settings. The University of Crete Hospital, Greece and the University of Cape Coast, Ghana ethical review boards approved the study. Ethical clearance obtained from UOC is attached in APPENDIX A and the ethical approval obtained from UCC is attached in APPENDIX B.

## Dose Calculation with PCXMC

The dose calculations followed three algorithms. At the first window (Figure 8), the patient anthropometric data and the radiation beam geometry were input. The anatomical regions displayed on the DICOM image were replicated with PCXMC phantom to obtain a virtual image. The PCXMC phantom weight and height were adjusted to mimic the actual patient and likewise the other examination parameters from the DICOM header. Simulations were then defined for each virtual image to track 2,000,000 photons per energy level. This was saved in the software as a definition file.

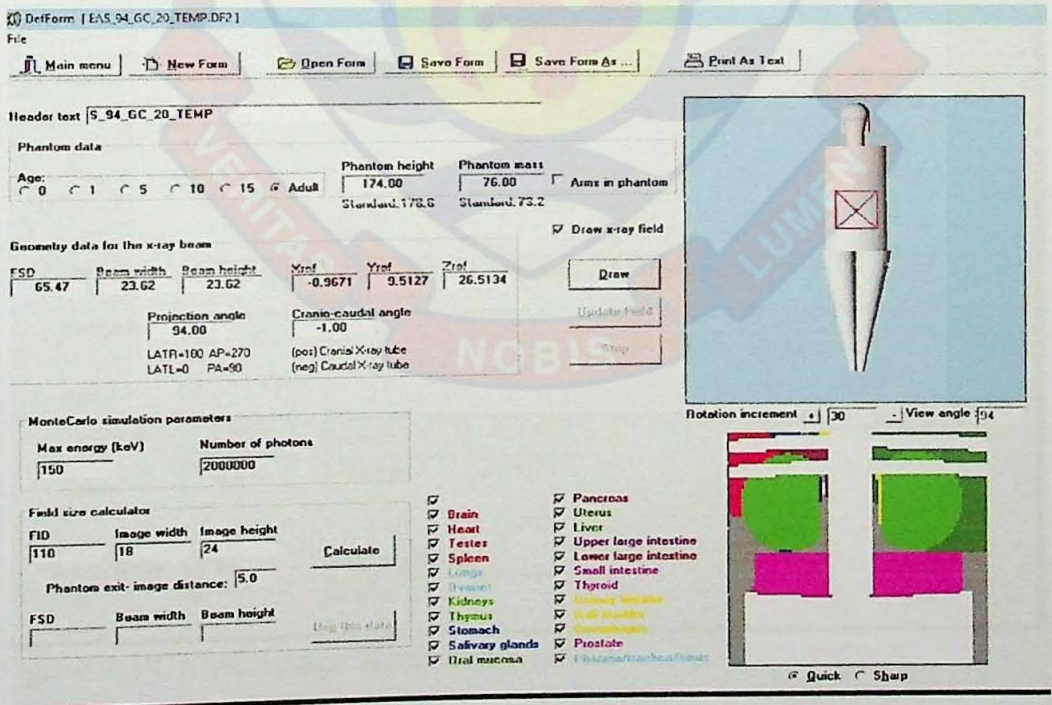
At the second window, simulations were performed for all the saved definition files. PCXMC performed ten simulations for each energy level with specified number of individual photon histories, thus  $10 \times 200,000$  photons per radiation field. These were saved as energy files, as shown in Figure 9, for the next phase.

At the third window (shown in Figure 10), information about the kV used for a specific geometry, tube anode angle, filtration material and filtration material thickness were input to generate the X-ray spectrum. The saved energy

file which corresponds to the X-ray spectrum generated and the DAP value were input to calculate the organ and effective doses. The ICRP publication 103 tissue weighting factors were considered for this study.

### PCXMC Software

The exposure data from DSA, single and fluoroscopy were used in the simulation. The PCXMC software has a user windows interface where appropriate data can be input for the Monte Carlo simulation to be effected and then the final output (dose) is then obtained through several minutes of calculations. It uses the Christy and Eckerman (Cristy & Eckerman, 1987) hermaphrodite mathematical phantom models. Some adjustments have been made in the phantoms to enable calculation of effective dose according to ICRP 60 and 103 (Agency et al., 2007) recommendation on tissue weighting factors.



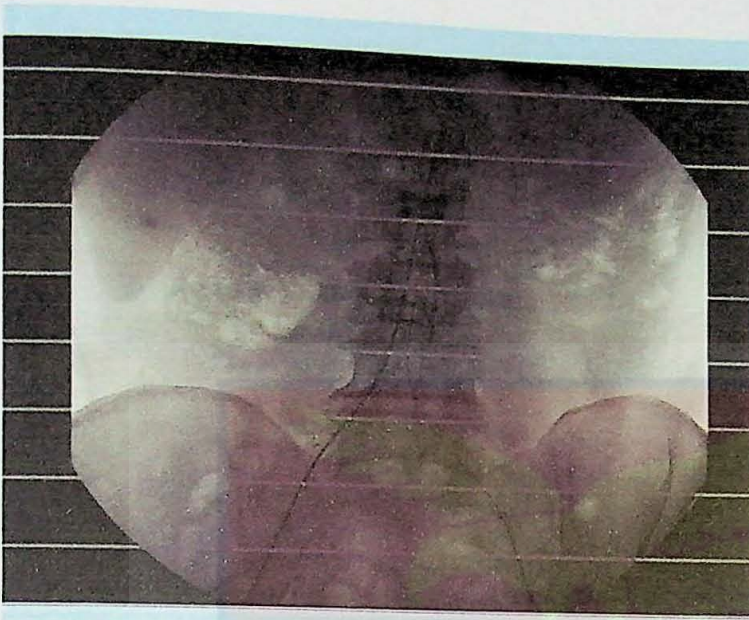


Figure 8: Definition file window (top) with DICOM image (bottom)

PCXMC - Simulation

File

---

File name:

Header text:

Age:

SkinPoint:	<input type="text" value="-5.2611"/>	<input type="text" value="10.2176"/>	<input type="text" value="25.4749"/>
Focus:	<input type="text" value="-5.2611"/>	<input type="text" value="71.0976"/>	<input type="text" value="25.4749"/>

Energy (keV):	Lot No:	Photons in the lot:
<input type="text" value="150"/>	<input type="text" value="10"/>	<input type="text" value="200000"/>

Figure 9: PCXMC image simulation window

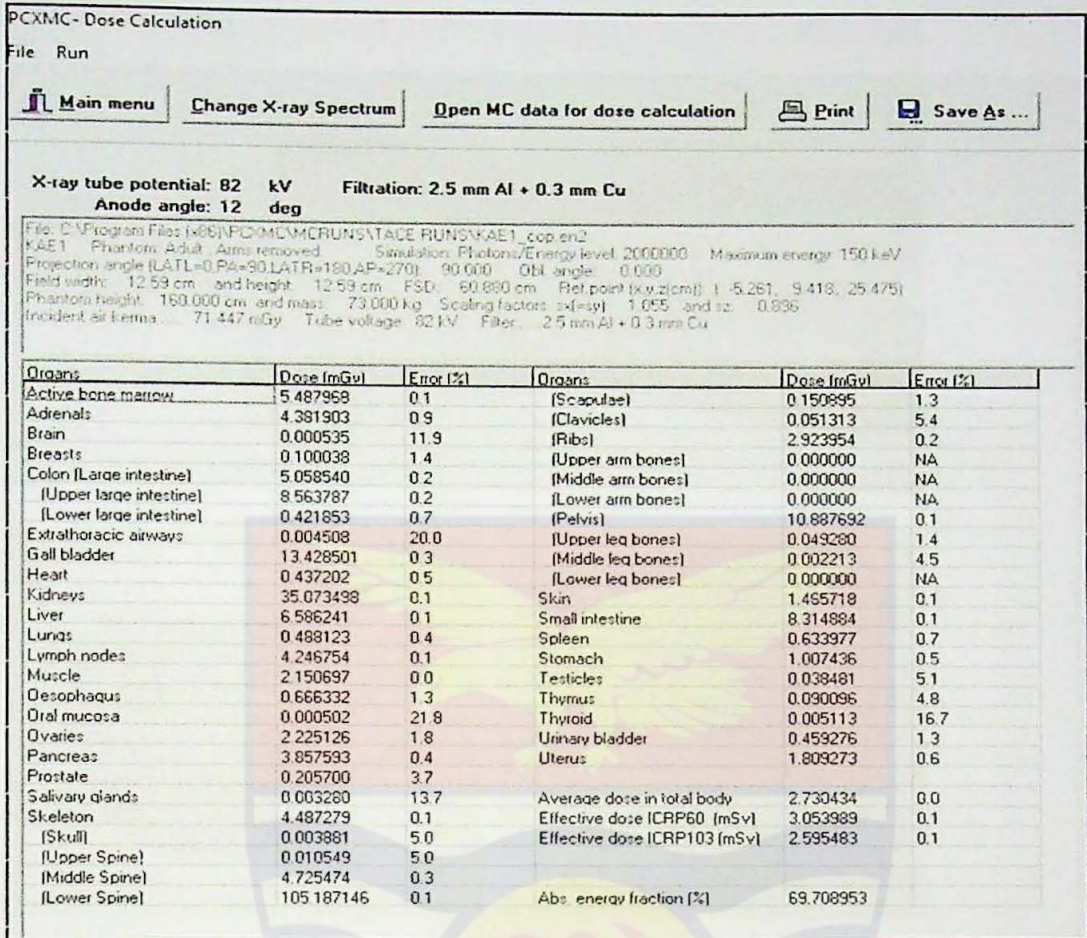
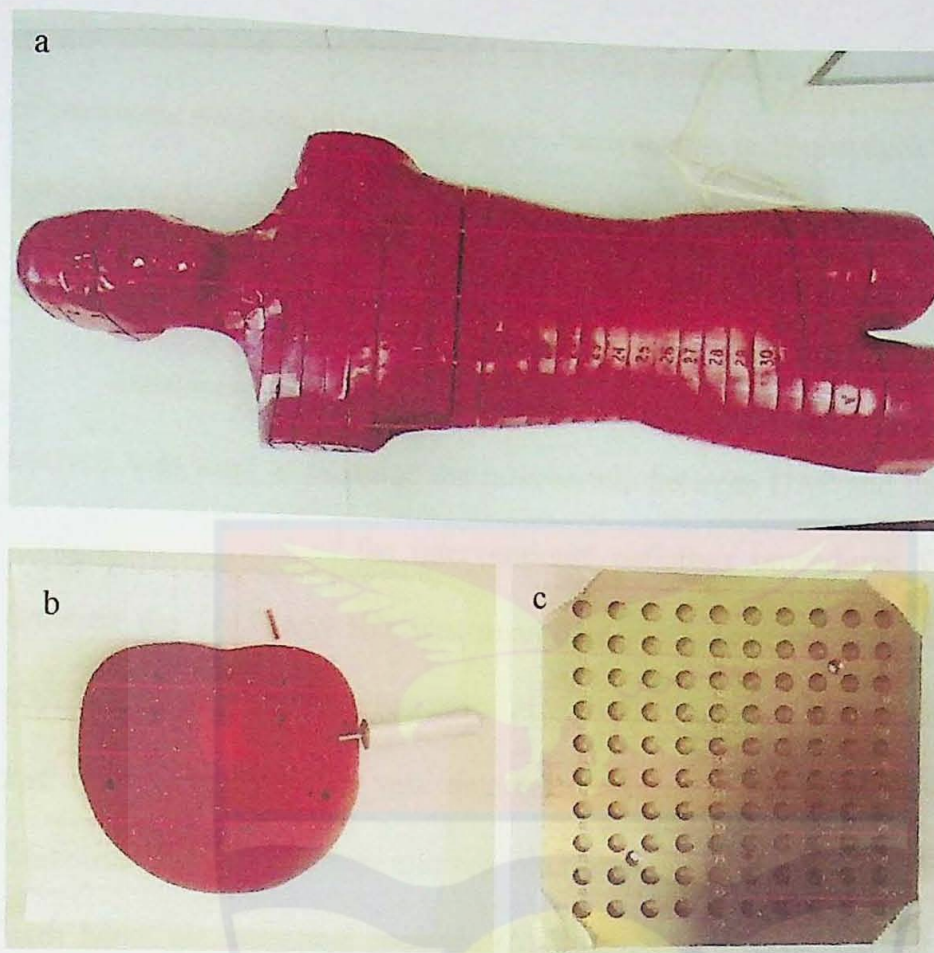


Figure 10: Dose calculation window

### Corroboration of Organ Doses Calculated with PCXMC

To corroborate the organ doses calculated with PCXMC, a physical anthropomorphic phantom (RANDO, Alderson Research Laboratories, New York, USA) and TLD chips, as displayed in Figure 11a and 6b, were used. The phantom is cut into 35 slices of transverse sections numbered 0 to 34 as shown in Figures 11a and 11b. Each section is 25 mm thick with small holes aligned on a 30 mm × 30 mm grid to enable the insertion of the TLD-100H and TLD-200 chips.



*Figure 11:* a. Physical anthropomorphic phantom (RANDO, Alderson research labs); b. a section of phantom slice; c. TLD chip cooling and organizing tray.

### **Dose Evaluation**

The PCXMC software program was used to simulate the examination procedures for each patient. Patient identifications were concealed by using alpha-numeric codes to represent each individual. Applying the codes facilitated the dose estimation and risk analysis for each individual due to their procedure.

In verification of the MC simulated results, an anthropomorphic phantom with TLD-100H and TLD-200 chips inserted in specific locations and on the surface was used. Two of the patient's procedures were repeated using the phantom with the TLD chips to measure the doses under clinical set-up conditions. The phantom used for this experiment mimics adult individual who

weighs 74.6 kg and has a height of 1.74 m. The phantom is made up of 35 slices of transverse sections numbered 0 to 34. Each section is 25 mm thick with small holes aligned on a 30 mm × 30 mm grid to enable the insertion of the TLD chips.

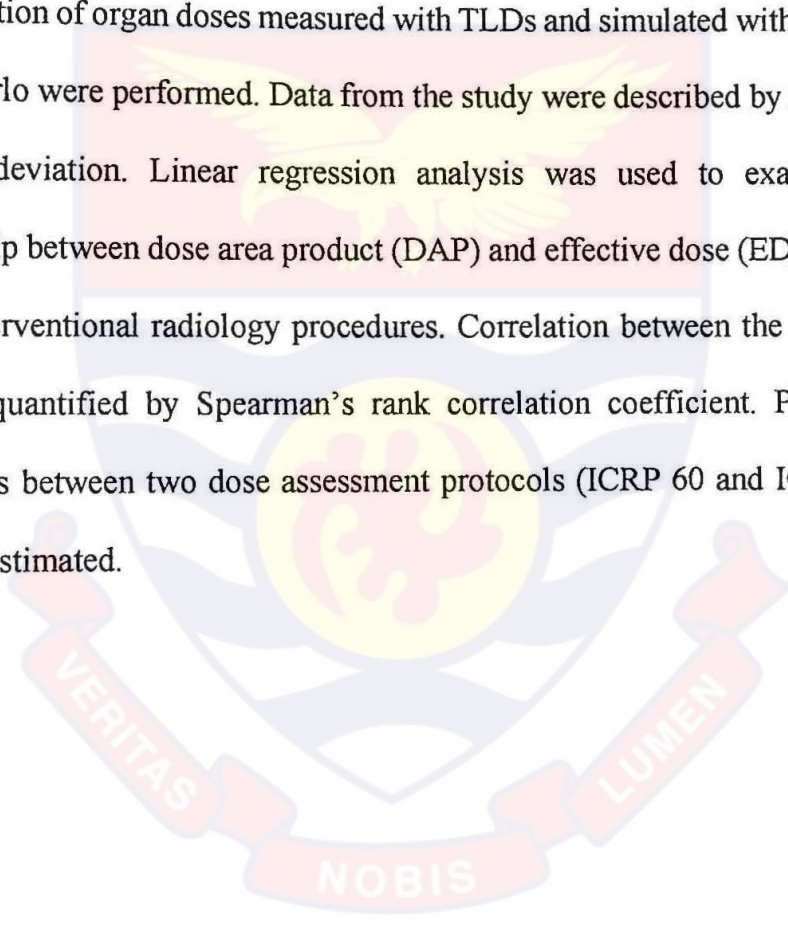
### **Statistical Analysis of Data**

Data was described by mean and standard deviation. Linear regression analysis was used to examine the relationship between DAP and the effective doses (ED) for each of the interventional radiology procedures. Correlation between the DAP and ED was quantified by Spearman's rank correlation coefficient. Association between the effective doses from PCXMC simulations and TLD measurements was determined using linear regression analysis. Statistical significance was inferred when  $P < 0.05$ . Data analysis was executed with MedCalc statistical package (MedCalc, Mariakerke, Belgium, version 18.11.3) (MedCalc Software bvba, Ostend, n.d.).

### **Summary: Chapter Three**

Materials and equipment used in this study included floor-mounted Siemens Axiom Artis FA angiographic unit, radcal ionization chamber, Leeds test phantom, anthropomorphic phantom, thermoluminescent dosimeter chips, Harshaw TLD reader, Monte Carlo PCXMC, Microsoft Excel (ver. 2017), etc. Thermoluminescent dosimeters were calibrated prior to use for dose measurement. The TLD chips were used to measure the radiation dose at 314 different points in and on the anthropomorphic phantom. A total of 99 patients examination data were retrieved from the Radiology Department of the University of Crete Hospital and used for the study. For each patient examination, data which were extracted from the DICOM report were: X-ray

tube voltage, X-ray tube current, dose area product (DAP), total fluoroscopy time, X-ray tube filtration, X-ray field size, source to skin distance, source to detector distance, tube angulation, beam projection, patient anthropometric data (i.e. age, weight and height), angiographic images, and X-ray field location on patient's body surface. The organ and effective doses were estimated using Monte Carlo PCXMC software to simulate the patient examination procedures. Corroboration of organ doses measured with TLDs and simulated with PCXMC Monte Carlo were performed. Data from the study were described by mean and standard deviation. Linear regression analysis was used to examine the relationship between dose area product (DAP) and effective dose (ED) for each of the interventional radiology procedures. Correlation between the DAP and ED was quantified by Spearman's rank correlation coefficient. Percentage differences between two dose assessment protocols (ICRP 60 and ICRP 103) was also estimated.



patients had reported with endoleaks, a condition which occurs when an aneurysmal sac continues to be pressurized despite endoluminal stent placement. The patients have been grouped based on the medical history they presented with. Table 7 presents the summary of simulated dose data for all the patients who received EVAR procedures. Scan data for each of the EVAR procedures on the 28 patients are presented in APPENDIX C (Tables A1 – A28).

### **Type I endoleak**

Table 3 presents data on patients VX, GC, KM, VI, FN, KE and SN, who presented with AAA condition of Type I endoleaks. Type I endoleak is a leak that occurs around the top or bottom of the stent graft. It is at the proximal or distal attachment sites. Because blood flowing from the top or bottom areas of the stent graft has high flow, Type I leaks are typically treated with a greater sense of urgency once they are identified. Among these seven patients, patient KE recorded highest effective dose of 43.067 mSv and 35.782 mSv using the ICRP 60 and ICRP 103 protocols respectively. This translates to 16.9 % difference in estimated effective dose based on the protocols used, similar to observation for patient VX. The observed difference in dose estimates is as a result of differences in assigned radiosensitivities of body organs in the ICRP protocols. Correspondingly, patient KE recorded the single most high organ dose of 510.996 mGy to the kidneys among the six other patients. Radiosensitivity has been defined as the relative susceptibility of cells, tissues, organs, organisms, or other substances to the injurious action of radiation. In general, it has been found that cell radiosensitivity is directly proportional to the

rate of cell division and inversely proportional to the degree of cell differentiation (NRCNA, 2006).

Table 3: Dose data for patients with Type I endoleak undergoing EVAR procedures

	Patient						
	VX	GC	KM	VI	FN	KE	SN
Active bone marrow	46.909	21.041	40.271	44.171	54.744	95.296 132.74	22.648
Adrenals	59.208	58.567	42.215	30.373	81.935	0	28.307
Brain	0.001	0.001	0.001	0.000	0.001	0.002	0.001
Breasts	0.285	0.471	0.678	0.280	0.360	0.726	0.342
Colon	16.244	11.014	24.008	22.240	19.663	38.353	11.028
Extrathoracic airways	0.003	0.001	0.004	0.000	0.004	0.002	0.001
Gall bladder	20.145	21.216	37.131	34.928	40.428	64.835	14.607
Heart	2.217	2.713	3.070	1.624	2.662	4.836	1.632
Kidneys	156.00	120.88	169.09	145.43	263.70	510.99	96.660
Liver	1	1	5	9	5	6	7.019
Lungs	8.081	10.678	16.060	12.612	14.510	31.313	1.835
Lymph nodes	2.406	2.722	3.074	1.473	2.381	5.055	10.652
Muscle	15.062	12.206	20.980	20.354	23.167	40.448	8.522
Oesophagus	16.377	8.595	14.772	14.750	18.379	35.911	3.355
Oral mucosa	5.096	5.546	5.583	3.815	7.361	11.839	0.000
Ovaries	0.001	0.000	0.000	0.000	0.000	0.002	13.457
Pancreas	26.993	9.071	22.975	23.687	18.749	45.968	16.187
Prostate	19.714	21.119	27.468	26.097	41.421	71.207	0.979
Salivary glands	5.106	0.428	1.720	2.655	1.002	2.786	0.006
Skeleton	0.009	0.004	0.006	0.002	0.005	0.013	20.119
Skin	40.165	20.740	36.653	38.912	49.562	85.669	8.818
Small intestine	19.565	8.698	13.408	14.056	21.739	41.684	22.505
Spleen	33.426	22.086	44.244	44.877	42.533	75.888	25.506
Stomach	11.952	22.826	27.902	30.177	35.159	83.759	9.533
Testicles	9.218	11.206	20.025	15.890	17.848	35.824	0.157
Thymus	0.604	0.064	0.285	0.380	0.139	0.388	0.191
Thyroid	0.234	0.279	0.344	0.204	0.306	0.588	0.010
Urinary bladder	0.013	0.013	0.014	0.007	0.012	0.026	2.359
Uterus	8.608	1.139	4.592	5.803	2.540	6.885	11.388
Average dose in total body (mGy)	30.134	6.984	19.687	22.929	15.478	39.389	10.411
Effective Dose ICRP 60 (mSv)	19.774	10.726	18.389	18.512	23.430	44.185	10.343

Effective Dose ICRP 103 (mSv)	14.830	9.645	16.721	15.807	18.995	35.782	8.922
Peak skin dose (mGy)	384.93	279.84	291.37	276.51	311.19	361.68	289.06
	3	6	9	5	9	2	6

### Type II endoleak

Type II endoleaks are the most common. These are leaks that happen when blood flows into the aneurysm sac from branches of the aorta, or other blood vessels treated with a stent. The blood flows into the aneurysm sac cavity through small branches which enter the treated aneurysm. Patients TA, AG, ZI, VS, ZK, BT and FM (Table 4) presented with Type II endoleaks. Among this set of cases, patient TA received the most dose from the EVAR procedure. Effective dose of 107.989 mSv and 92.132 mSv were estimated for ICRP 60 and ICRP 103 protocols respectively for patient TA, representing a difference of 14.7 %.

### Type III endoleak

Type III endoleak results from a defect or misalignment between the components of endografts. Similar to what happens with Type I endoleak, Type III causes systemic pressure within the aneurysm sac that increases the risk of sac rupture. These are holes, defects, or separations in the stent-graft material. Type III endoleak therefore requires urgent attention. Patient NA in this class of conditions recorded effective doses of 194.470 mSv and 159.249 mSv with ICRP 60 and ICRP 103 protocols, the highest amongst patients PI, SA, ME, KK, LG and KN (Table 5) undergoing EVAR procedures. The patient is 66 years old and received 112 exposures from the most complex of procedures performed as a result of type III endoleak condition. Average dose of 0.0006 mGy to the oral mucosa organ was the least among the seven patients.

Table 4: Dose data for patients with Type II endoleak undergoing EVAR procedures

	Patient						
	TA	AG	ZI	VS	ZK	BT	FM
Active bone marrow	267.062	68.843	23.812	14.674	32.754	34.486	15.581
Adrenals	107.819	41.502	21.170	13.548	27.105	63.530	18.593
Brain	0.005	0.001	0.000	0.000	0.001	0.001	0.000
Breasts	1.511	0.513	0.085	0.374	0.188	0.410	0.425
Colon	158.019	29.418	5.582	9.039	12.157	17.653	11.324
Extrathoracic airways	0.013	0.004	0.000	0.001	0.000	0.002	0.003
Gall bladder	203.709	33.418	11.374	15.084	23.111	34.397	15.070
Heart	8.220	2.833	0.744	1.150	1.229	2.652	1.489
Kidneys	701.141	221.597	72.806	75.552	122.281	160.617	67.666
Liver	57.287	13.381	3.081	6.984	7.204	14.124	9.004
Lungs	6.941	3.100	0.756	1.638	1.249	2.513	1.975
Lymph nodes	117.149	25.182	7.002	8.279	12.954	18.598	8.595
Muscle	79.661	22.689	6.519	5.961	10.060	12.467	6.591
Oesophagus	16.104	5.299	1.915	1.915	2.813	6.095	2.376
Oral mucosa	0.013	0.002	0.000	0.002	0.000	0.000	0.001
Ovaries	186.872	35.910	7.535	9.577	19.251	20.721	15.610
Pancreas	94.811	30.729	9.794	11.460	16.595	28.945	10.359
Prostate	19.696	5.074	0.748	0.728	1.636	1.800	1.468
Salivary glands	0.021	0.007	0.003	0.002	0.005	0.010	0.003
Skeleton	196.555	58.837	20.701	13.506	28.040	31.884	13.836
Skin	70.729	24.634	8.210	5.786	10.929	11.863	5.416
Small intestine	295.561	58.541	14.792	16.993	28.114	36.267	18.458
Spleen	76.605	35.730	5.013	14.886	14.017	22.541	14.351
Stomach	74.544	21.319	3.562	6.658	7.601	14.437	7.701
Testicles	3.290	0.710	0.100	0.116	0.239	0.278	0.214
Thymus	1.061	0.337	0.088	0.152	0.151	0.347	0.167
Thyroid	0.056	0.019	0.004	0.008	0.006	0.022	0.009
Urinary bladder	39.537	10.603	1.520	1.927	3.423	4.233	4.064
Uterus	154.340	36.309	8.113	7.624	18.659	18.493	13.789
Average dose in total body (mGy)	98.648	28.093	8.594	7.293	12.892	15.733	7.853
Effective Dose ICRP 60 (mSv)	107.989	27.133	7.412	7.604	12.800	16.423	8.818
Effective Dose ICRP 103 (mSv)	92.132	22.808	6.330	6.444	10.634	14.201	7.444
Peak skin dose (mGy)	545.449	283.664	296.899	268.571	297.835	278.733	262.477

Table 5: Dose data for patients with Type III endoleak undergoing EVAR procedures

	Patient						
	PI	SA	ME	KK	NA	LG	KN
Active bone marrow	76.951	69.224	16.633	25.399	557.176	47.924	43.584
Adrenals	123.520	3.104	16.338	23.352	91.408	52.738	31.382
Brain	0.002	0.000	0.000	0.000	0.002	0.001	0.000
Breasts	1.540	0.083	0.137	0.169	1.167	0.413	0.284
Colon	37.314	36.026	9.024	11.640	232.288	26.119	21.194
Extrathoracic airways	0.009	0.000	0.000	0.001	0.001	0.000	0.000
Gall bladder	52.155	13.245	11.862	15.644	225.162	47.444	44.086
Heart	6.337	0.401	0.826	1.126	7.085	2.329	1.933
Kidneys	291.922	48.071	65.098	79.711	979.485	226.027	267.191
Liver	25.061	4.321	4.567	6.477	58.338	18.839	11.638
Lungs	6.603	0.356	0.724	1.299	6.338	2.034	1.658
Lymph nodes	35.036	19.995	7.932	10.019	178.762	26.050	22.929
Muscle	27.227	23.704	5.974	8.214	157.661	16.704	16.485
Oesophagus	11.658	0.734	2.055	2.458	15.292	5.432	4.625
Oral mucosa	0.004	0.000	0.000	0.000	0.000	0.000	0.000
Ovaries	50.997	81.253	15.259	17.680	424.825	25.996	12.319
Pancreas	52.334	5.231	12.051	10.830	107.105	43.075	36.303
Prostate	4.613	14.529	1.434	1.292	50.032	1.639	0.634
Salivary glands	0.016	0.000	0.001	0.002	0.007	0.004	0.001
Skeleton	70.774	54.741	14.700	22.026	425.509	44.672	38.755
Skin	27.411	23.488	5.372	8.361	163.405	16.354	17.110
Small intestine	72.645	64.918	16.709	23.469	506.426	50.679	44.237
Spleen	46.380	7.158	17.042	13.927	94.660	30.880	27.127
Stomach	30.354	6.637	7.508	6.993	79.227	21.563	20.649
Testicles	0.719	1.928	0.217	0.172	6.686	0.254	0.090
Thymus	0.703	0.037	0.104	0.113	0.779	0.284	0.209
Thyroid	0.052	0.000	0.004	0.006	0.009	0.005	0.006
Urinary bladder	11.986	32.258	3.574	3.634	103.834	4.653	1.734
Uterus	50.304	101.674	14.406	18.912	421.886	24.843	9.623
Average dose in total body (mGy)	34.077	27.346	7.351	10.338	195.800	21.429	20.319
Effective Dose ICRP 60 (mSv)	34.870	27.986	8.112	10.288	194.470	22.496	20.261
Effective Dose ICRP 103 (mSv)	30.124	21.333	6.805	8.795	159.249	19.286	16.847
Peak skin dose (mGy)	294.945	402.681	271.747	274.047	399.936	283.806	333.734

## Type IV endoleak

Type IV endoleak occurs when there is blood flow through the pores of the stent graft. This type of endoleak is infrequently seen with newer generation stent graft devices. Table 6 presents dose data on patients who reported with this type of condition. Of these, patient CP's procedure was most complex and received the highest effective dose of 39.590 mSv with ICRP 60 protocol and 34.003 mSv with ICRP 103 protocol. Percentage difference in effective dose between the two protocols was 14.11 %.

Table 6: Dose data for patients with Type IV endoleak undergoing EVAR procedures

	Patient						
	MM	MN	TS	KAK	MS	CP	TG
Active bone marrow	64.030	26.736	36.818	39.522	76.052	76.697	13.785
Adrenals	97.183	60.965	68.881	59.842	109.906	125.583	37.834
Brain	0.004	0.001	0.001	0.001	0.003	0.003	0.001
Breasts	0.664	0.345	0.322	0.458	1.165	1.417	0.476
Colon	19.427	15.897	14.759	17.720	30.071	41.392	6.903
Extrathoracic airways	0.027	0.000	0.002	0.005	0.020	0.024	0.002
Gall bladder	35.004	32.186	33.377	27.192	56.692	61.161	12.673
Heart	4.137	2.085	2.180	2.634	5.499	7.714	2.118
Kidneys	221.543	186.596	181.145	156.968	296.227	357.889	78.192
Liver	14.279	14.950	13.139	14.472	24.460	34.893	7.655
Lungs	4.543	1.996	2.208	2.524	5.796	9.377	3.423
Lymph nodes	22.917	17.120	17.111	16.976	31.982	39.731	7.752
Muscle	18.303	11.300	12.382	12.785	23.040	31.443	5.750
Oesophagus	8.484	5.128	5.600	5.333	10.358	13.664	3.838
Oral mucosa	0.009	0.000	0.000	0.000	0.007	0.005	0.001
Ovaries	29.345	12.016	16.144	19.245	36.558	60.113	7.947
Pancreas	37.572	31.431	29.324	26.567	44.317	66.576	13.885
Prostate	3.470	0.634	0.844	0.990	2.551	4.562	0.525
Salivary glands	0.024	0.002	0.004	0.004	0.024	0.023	0.007
Skeleton	55.776	25.970	34.215	35.883	67.975	70.394	13.547
Skin	20.704	10.917	13.617	13.355	25.408	31.758	5.938
Small intestine	45.148	30.191	30.961	34.101	65.903	76.445	13.420
Spleen	20.905	31.767	22.173	22.889	30.549	109.108	16.794
Stomach	15.073	16.894	12.175	14.036	20.628	36.242	6.996
Testicles	0.510	0.093	0.129	0.145	0.421	0.718	0.080
Thymus	0.592	0.222	0.282	0.292	0.793	1.034	0.247
Thyroid	0.050	0.008	0.018	0.015	0.057	0.052	0.012
Urinary bladder	6.820	1.872	2.072	2.629	5.800	11.010	1.277

Uterus	33.345	9.623	12.685	15.818	32.437	50.739	6.551
Average dose in total body (mGy)	24.106	14.053	16.007	16.534	30.390	38.072	7.143
Effective Dose ICRP 60 (mSv)	23.650	15.030	15.920	16.746	30.776	39.590	7.534
Effective Dose ICRP 103 (mSv)	20.409	12.931	13.651	14.480	26.385	34.003	6.591
Peak skin dose (mGy)	375.336	277.726	303.470	312.338	323.831	303.009	277.349

### Summarized Dose Data for EVAR Procedures

Tables 3 – 6 are summarized into Table 7, presenting the maximum, minimum, mean, sum, 75<sup>th</sup> and 90<sup>th</sup> percentiles for the simulated dose data on all 28 patients who underwent the EVAR procedures. Significantly from the data, the highest individual organ dose recorded in all the EVAR procedures performed was 979.485 mGy to the kidneys. This was the case for patient NA, who presented with type III endoleak that had caused rupture in the aneurysm sac as a result of elevated pressure within. From the study, five organs receiving the highest doses in EVAR procedures are kidneys, bone marrow, small intestine, skeleton and adrenals with average dose estimates of 225.732, 69.744, 65.341, 58.218 and 58.166 mGy respectively. This observation was clearly visualized in Figure 12. ICRP 103 protocol estimated mean effective dose 15.83% less compared with ICRP 60 protocol. While average effective dose per ICRP 60 is 28.495 mSv, that for ICRP 103 is 23.985 mSv. This observation was similar to studies of Obed et al (2016) where effective and absorbed dose received by tissues and individual organs were estimated using ICRP 60 and ICRP 103 and results compared for patients undergoing CT examinations. Effective dose estimation allows for the estimation of radiation risk to the EVAR patient population. Brain, which is situated remotely (very far) from the site of the EVAR procedure, recorded the least average dose of 0.001 mGy ( $\pm$

0.001), representing a minute fraction of scattered radiation from the treatment site.

Table 7: Summary of simulated organ doses (mGy) from EVAR procedures

	Min	Max	Mean	± SD	Sum	P75	P90
Active bone marrow	13.785	557.176	69.744	± 106.775	1952.824	68.938	82.454
Adrenals	3.104	132.740	58.166	± 37.569	1628.647	84.303	113.990
Brain	0.000	0.005	0.001	± 0.001	0.035	0.001	0.003
Breasts	0.083	1.540	0.546	± 0.424	15.291	0.668	1.242
Colon	5.582	232.288	32.340	± 48.117	905.517	29.581	39.265
Extrathoracic airways	0.000	0.027	0.005	± 0.007	0.128	0.004	0.015
Gall bladder	11.374	225.162	44.191	± 50.606	1237.336	44.925	62.263
Heart	0.401	8.220	2.981	± 2.159	83.476	3.337	6.562
Kidneys	48.071	979.485	225.732	± 205.687	6320.503	264.576	403.821
Liver	3.081	58.338	16.587	± 13.973	464.425	16.755	32.387
Lungs	0.356	9.377	3.071	± 2.196	85.997	3.703	6.418
Lymph nodes	7.002	178.762	28.391	± 36.016	794.939	25.399	39.946
Muscle	5.750	157.661	22.579	± 30.177	632.224	22.777	32.783
Oesophagus	0.734	16.104	6.206	± 4.187	173.770	7.642	12.387
Oral mucosa	0.000	0.013	0.002	± 0.003	0.051	0.002	0.006
Ovaries	7.535	424.825	45.217	± 82.193	1266.073	36.072	66.455
Pancreas	5.231	107.105	33.661	± 25.241	942.506	41.835	67.965
Prostate	0.428	50.032	4.770	± 9.843	133.574	3.743	7.933
Salivary glands	0.000	0.024	0.008	± 0.007	0.213	0.009	0.022
Skeleton	13.506	425.509	58.218	± 80.315	1630.117	56.541	75.242
Skin	5.372	163.405	23.169	± 30.646	648.734	23.775	34.736
Small intestine	13.420	506.426	65.341	± 100.848	1829.537	60.135	76.055
Spleen	5.013	109.108	32.564	± 26.377	911.781	32.615	78.751
Stomach	3.562	79.227	19.655	± 18.276	550.344	20.817	35.949
Testicles	0.064	6.686	0.683	± 1.352	19.125	0.533	1.082
Thymus	0.037	1.061	0.362	± 0.280	10.143	0.407	0.783
Thyroid	0.000	0.057	0.018	± 0.018	0.514	0.020	0.052
Urinary bladder	1.139	103.834	10.371	± 20.312	290.385	7.316	18.067
Uterus	6.551	421.886	43.077	± 80.598	1206.163	34.086	66.019
Average dose in total body (mGy)	7.143	195.800	28.125	± 37.408	787.501	27.533	39.906
Effective Dose ICR P60 (mSv)	7.412	194.470	28.495	± 37.852	797.868	27.346	40.633
Effective Dose ICRP 103 (mSv)	6.330	159.249	23.985	± 31.206	671.585	21.702	34.537
Peak skin dose (mGy)	262.477	545.449	316.507	± 60.521	8862.203	326.307	389.434

Min: minimum; max: maximum; SD: standard deviation; P: percentile

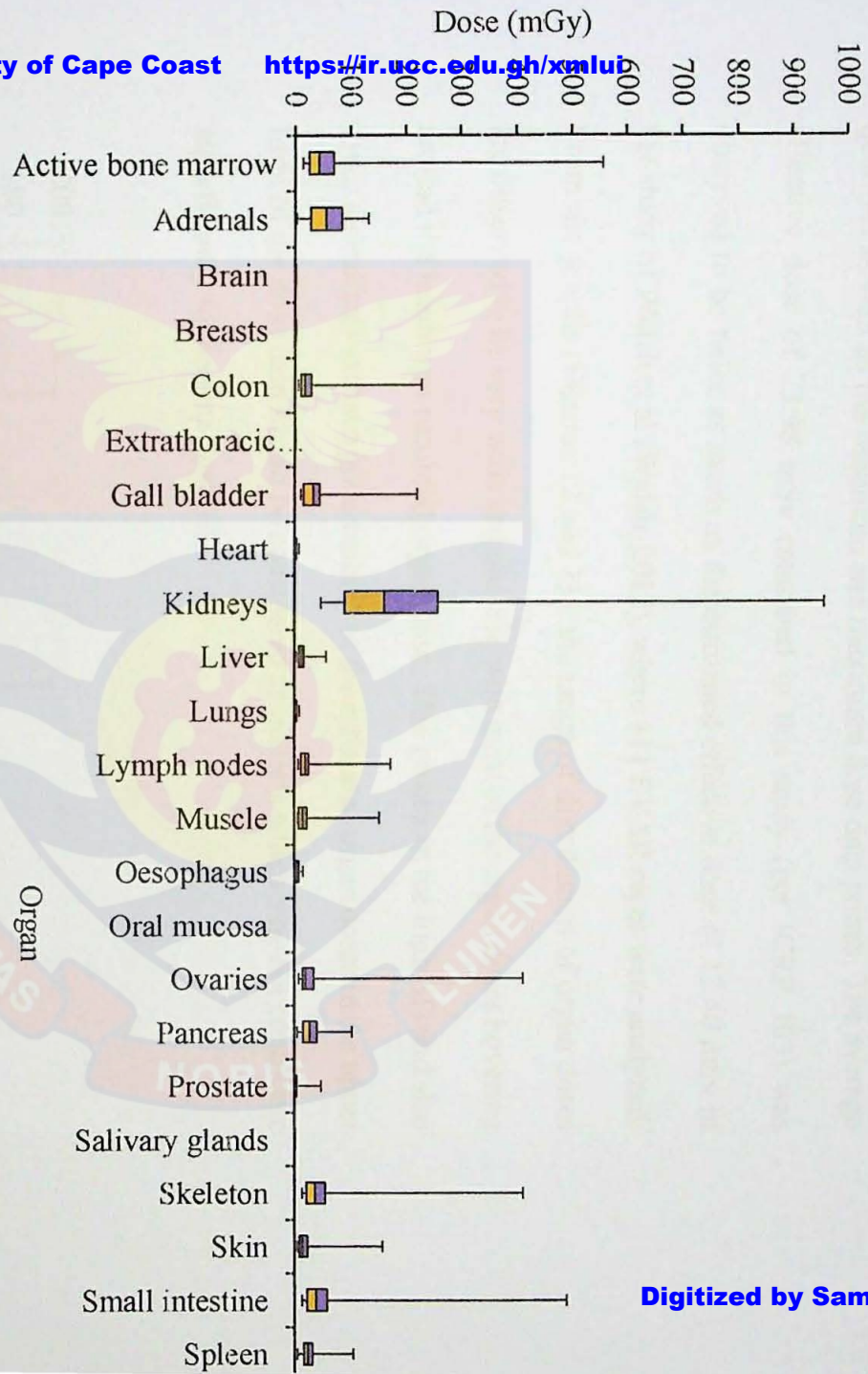


Figure 12: Box plot for simulated organ doses (mGy) from EVAR procedures

Graphically, Figures 12 and 13 present respectively box plots of the summarized organ and effective dose estimates for the 28 patients in the EVAR procedures. The box plot presents data reflecting the first, second and third quartiles as well as the minimum and maximum dose data points. The average effective dose of 23.98 mSv estimated in this study (per ICRP 103) was observed to be twice as much as the estimated effective dose of 12.40 mSv in the study of Walsh et al (Walsh, 2012), where 111 EVAR cases were analyzed. From the graphs (Figures 12 and 13), the range of distribution of organ doses are observed to be very wide and uneven, with most of the organ doses hovering around the minimum recorded organ dose. This results in the high SD and also gives an indication that a good number of the estimated organ doses in the upper limit of the dose data would be considered as outliers which may not contribute significantly to the data analysis.

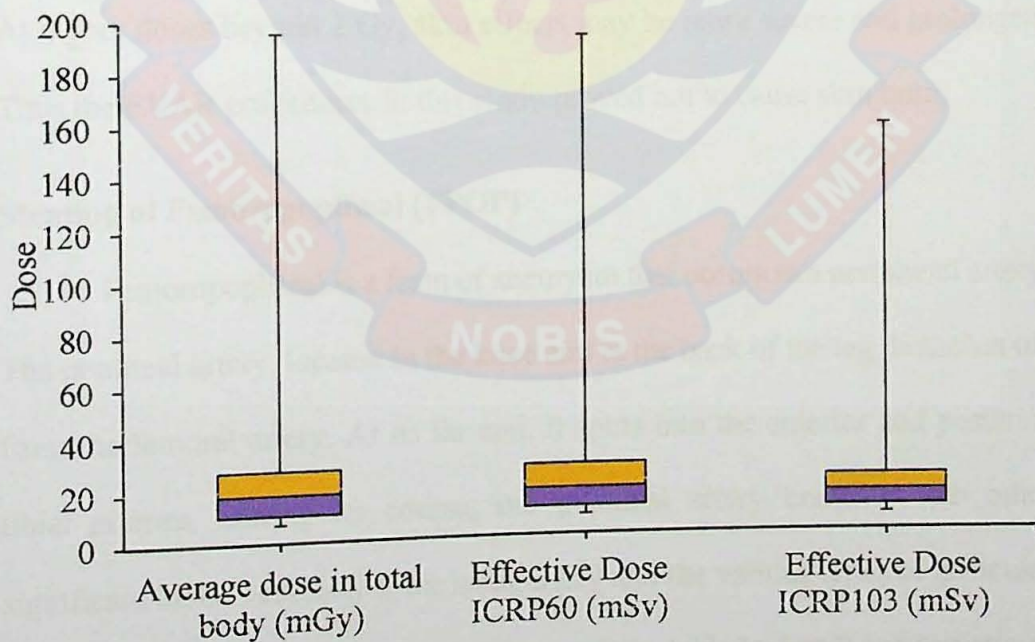


Figure 13: Box plot for average and effective doses from EVAR procedures

EVAR is a high dose procedure and emphasis on dose optimization is important. Skin dose, which allows for the assessment of the potential for an individual patient to receive a radiation skin injury as a deterministic effect, was analyzed from the study. An average of 316.507 mGy ( $\pm 60.521$ ) peak skin dose was estimated from the study. The peak skin dose was estimated from equation (19) (Walsh, 2012).

$$D(\text{mGy}) = 249 + 5.2 \times \text{DAP}(\text{Gy} \cdot \text{m}^2)$$

(19)

Of all 28 patients in the study, none had estimated peak skin dose of up to 2 Gy at any point during the procedure. This indicates an unlikely occurrence of skin injury in the EVAR procedures performed. However, early transient erythema could occur 24 - 48 hours post exposures exceeding 2 Gy, producing an injury resembling sunburn in an area matching the shape of the X-ray field. At higher doses beyond 2 Gy, skin effects may be more severe and prolonged. Thus the EVAR procedures in this study proved not to cause skin burn.

### **Stenting of Femoropopliteal (FPOP)**

Femoropopliteal is a form of aneurysm that occurs in a peripheral artery. The popliteal artery, located in the knee and at the back of the leg, branches off from the femoral artery. At its far end, it splits into the anterior and posterior tibial arteries. During its course, the popliteal artery branches into other significant blood vessels like the sural artery and the various types of genicular arteries. The popliteal artery is palpable (i.e. detectable by hand) and sometimes used to count pulses in the back of the knee. This popliteal artery sometimes

become narrowed or blocked, preventing blood flow to the lower extremities. To bypass the narrowed or blocked blood vessel, blood is redirected through either a healthy blood vessel that has been transplanted or a man-made graft material. This vessel or graft is sewn above and below the diseased artery under fluoroscopic imaging guidance so that blood flows through the new vessel or graft (Secemsky and Armstrong, 2018).

Femoropopliteal aneurysm is a bulge or weakness in the wall of the popliteal artery, which supplies blood to the knee joint, thigh and calf. A popliteal aneurysm can burst, which may cause life-threatening, uncontrolled bleeding. The aneurysm may also cause a blood clot, potentially requiring a leg amputation. True femoral aneurysm contained all three layers of the normal arterial wall and was defined as focal dilatation to at least 1.5 times the diameter of the adjacent normal artery. The popliteal artery is defined as aneurysmal when focal dilation in its diameter is more than 50 % of the normal vessel diameter. The normal diameter of the popliteal artery varies from 0.7 to 1.1 cm. These focal dilations classify as fusiform (diffuse dilation) or saccular (asymmetrical) (Secemsky and Armstrong, 2018).

Tables 8 – 13 presents results on simulated organ doses for forty-one (41) patients who reported with different popliteal aneurysm conditions and underwent FPOP stenting procedures at the University of Crete Hospital. Stenting of FPOP arterial disease is currently the most common strategy adopted by endovascular specialists. Several randomized trials have shown that stenting with nitinol self-expanding stents leads to less restenosis (recurrence of abnormal narrowing of an artery) on intermediate-term and long-term follow-

up when compared with plain old balloon angioplasty and provisional stenting (Shammas and Banerjee, 2015).

**Type I Popliteal aneurysm (single aneurysm with local pain and pulsating mass)**

This stage of popliteal aneurysm is one of the early stages of the disease where the aneurysm is localized and relatively easy to deal with. Seven of the patients (i.e. VE, PE, SK, PP, GM, SM and II) who were selected with this type of condition reported with pain and either a small pulsating mass or none at all. The FPOP procedures performed of this set of patients were simple and did not have much repeated exposures comparative to the advanced stage disease. Effective doses of  $< 1$  mSv were estimated for all the patients using both ICRP 60 and ICRP 103 protocols, as presented in Table 8. The low radiation doses received by the organs were contributions from scatter radiation during the FPOP scanning procedures. The scan location being the knee, located distant from the internal organs, only small fractions were scattered to organs such as the adrenals, brain, liver, kidney, etc. (Table 8) using the Monte Carlo simulation. Correspondingly, peak skin doses were relatively low and far below thresholds that could initiate any deterministic effects.

### **Type I Popliteal aneurysm (multiple aneurysm with local pain and pulsating mass)**

Similar to the Type I popliteal with single aneurysm, the group with Type I multiple aneurysm received similar levels of radiation to the internal organs. Patient PI who had two aneurysms in both knee regions of sizes of 1.7 and 2.0 cm received the highest effective doses of 0.407 and 0.290 mSv respectively for ICRP 60 and ICRP 103 protocols. Conversely, patient CS who had less effective dose recorded the most peak skin dose of 466.3 mGy (Table 9). This observation could have been a result of high exposure parameters or projection angle that was used during the procedure.

### **Type I Popliteal aneurysm (multiple aneurysm with acute thrombosis)**

Patients with multiple aneurysm and acute thrombosis of Type I popliteal conditions had dilations of the arteries up to 3.5 cm. The normal diameter of the popliteal artery varies from 0.7 to 1.1 cm. The focal dilations were classified as either fusiform (diffuse dilation) or saccular (asymmetrical). Patients undergoing this kind of study recorded effective doses between 0.057 – 0.292 mSv per ICRP 60 protocol and between 0.035 – 0.187 mSv per ICRP 103 protocol (Table 10). Maximum of the average dose in total body of 1.744 mGy was recorded by patient CM, similar to the effective doses.

Table 9: Dose data for patients undergoing FPOP procedures with Type I multiple aneurysm and pulsating mass

	Patient						
	PI	KN	CS	BI	SA	FG	MG
Active bone marrow	0.674	0.159	0.088	0.236	0.097	0.042	0.280
Adrenals	0.008	0.000	0.000	0.000	0.000	0.000	0.001
Brain	0.000	0.000	0.000	0.000	0.000	0.000	0.000
Breasts	0.001	0.000	0.000	0.000	0.000	0.000	0.000
Colon	0.543	0.273	0.246	0.104	0.274	0.075	0.167
Extrathoracic airways	0.000	0.000	0.000	0.000	0.000	0.000	0.000
Gall bladder	0.084	0.004	0.001	0.005	0.003	0.001	0.022
Heart	0.001	0.000	0.000	0.000	0.000	0.000	0.000
Kidneys	0.052	0.004	0.001	0.003	0.002	0.001	0.014
Liver	0.034	0.001	0.000	0.002	0.001	0.000	0.010
Lungs	0.001	0.000	0.000	0.000	0.000	0.000	0.000
Lymph nodes	0.192	0.053	0.030	0.048	0.033	0.032	0.081
Muscle	0.973	0.653	0.384	0.583	0.443	0.521	0.750
Oesophagus	0.002	0.000	0.000	0.000	0.000	0.000	0.001
Oral mucosa	0.000	0.000	0.000	0.000	0.000	0.000	0.000
Ovaries	0.972	0.343	0.112	0.311	0.140	0.062	0.417
Pancreas	0.013	0.002	0.001	0.001	0.001	0.000	0.003
Prostate	1.223	0.376	0.592	0.421	0.656	0.205	0.412
Salivary glands	0.000	0.000	0.000	0.000	0.000	0.000	0.000
Skeleton	1.440	1.337	0.714	0.954	0.715	0.968	1.332
Skin	0.948	0.739	0.408	0.563	0.448	0.668	0.834
Small intestine	0.518	0.064	0.025	0.067	0.032	0.015	0.153
Spleen	0.004	0.002	0.000	0.000	0.001	0.000	0.001
Stomach	0.012	0.004	0.001	0.001	0.002	0.001	0.002
Testicles	0.506	0.251	0.464	0.266	0.310	0.249	0.292
Thymus	0.000	0.000	0.000	0.000	0.000	0.000	0.000
Thyroid	0.000	0.000	0.000	0.000	0.000	0.000	0.000
Urinary bladder	0.777	0.267	0.236	0.251	0.379	0.076	0.277
Uterus	0.929	0.316	0.135	0.234	0.183	0.065	0.256
Average dose in total body (mGy)	0.936	0.667	0.383	0.563	0.427	0.520	0.742
Effective Dose ICRP 60 (mSv)	0.407	0.177	0.139	0.154	0.141	0.090	0.196
Effective Dose ICRP 103 (mSv)	0.290	0.118	0.091	0.099	0.098	0.052	0.128
Peak skin dose (mGy)	37.500	19.600	466.300	25.800	26.000	23.400	36.500

Table 10: Dose data for patients undergoing FPOP procedures with Type I multiple aneurysm and acute thrombosis

	DG	AD1	MP	Patient			
				KS	CM	KA	SG
Active bone marrow	0.416	0.192	0.029	0.039	0.709	0.257	0.043
Adrenals	0.002	0.000	0.000	0.000	0.002	0.335	0.000
Brain	0.000	0.000	0.000	0.000	0.000	0.000	0.000
Breasts	0.000	0.000	0.000	0.000	0.000	0.003	0.000
Colon	0.234	0.389	0.030	0.066	1.012	0.320	0.093
Extrathoracic airways	0.000	0.000	0.000	0.000	0.000	0.000	0.000
Gall bladder	0.022	0.004	0.001	0.000	0.016	0.010	0.003
Heart	0.000	0.000	0.000	0.000	0.000	0.046	0.000
Kidneys	0.013	0.003	0.000	0.000	0.013	0.113	0.001
Liver	0.007	0.001	0.000	0.000	0.003	0.006	0.001
Lungs	0.000	0.000	0.000	0.000	0.000	0.040	0.000
Lymph nodes	0.094	0.076	0.022	0.043	0.163	0.074	0.023
Muscle	0.849	1.119	0.344	0.831	1.779	0.532	0.325
Oesophagus	0.001	0.000	0.000	0.000	0.000	0.056	0.000
Oral mucosa	0.000	0.000	0.000	0.000	0.000	0.000	0.000
Ovaries	0.812	0.227	0.026	0.014	1.245	0.444	0.130
Pancreas	0.004	0.001	0.000	0.000	0.005	0.119	0.000
Prostate	0.739	0.940	0.186	0.137	1.621	0.201	0.494
Salivary glands	0.000	0.000	0.000	0.000	0.000	0.000	0.000
Skeleton	1.420	2.014	0.866	1.342	3.033	0.856	0.245
Skin	0.820	1.218	0.457	1.136	1.854	0.585	0.308
Small intestine	0.185	0.053	0.006	0.004	0.266	0.082	0.027
Spleen	0.001	0.001	0.000	0.000	0.006	0.080	0.000
Stomach	0.004	0.002	0.000	0.000	0.012	0.045	0.001
Testicles	0.345	0.665	0.137	0.111	0.652	0.089	0.201
Thymus	0.000	0.000	0.000	0.000	0.000	0.003	0.000
Thyroid	0.000	0.000	0.000	0.000	0.000	0.000	0.000
Urinary bladder	0.556	0.519	0.088	0.050	1.087	0.156	0.292
Uterus	0.699	0.322	0.033	0.021	1.252	0.155	0.177
Average dose in total body (mGy)	0.827	1.105	0.372	0.807	1.744	0.519	0.278
Effective Dose ICRP 60 (mSv)	0.292	0.270	0.057	0.092	0.587	0.191	0.085
Effective Dose ICRP 103 (mSv)	0.187	0.176	0.035	0.053	0.410	0.139	0.053
Peak skin dose (mGy)	35.800	99.200	17.000	57.200	75.400	19.700	23.400

### **Type II Popliteal aneurysm (multiple aneurysm with acute thrombosis)**

Type II popliteal multiple aneurysm with acute thrombosis is an elevated form of the Type I condition with acute thrombosis. Physical examination of such condition mostly revealed bilateral non-tender pulsatile masses of sizes between 3 cm and 5 cm diameter. Of the patients (TS, VS1, DE, LF, GN, VS2 and VA) reporting with this condition, LF recorded the highest effective dose of 0.857 mSv and 0.570 mSv per ICRP 60 and ICRP 103 respectively for a single cycle of FPOP procedure (Table 11). After first procedure for patient VS and ineffective correction of the Type II aneurysm condition, a second procedure was performed which corrected the condition. However, the cumulative dose was found to be less than the single shot dose received by patient LF. None of the patients recorded peak skin dose above 100 mGy, indicating unlikely occurrence of deterministic effect.

### **Type II Popliteal aneurysm (multiple aneurysm with peripheral embolization)**

The Type II popliteal cases that were reported with multiple aneurysm and peripheral embolization were mostly of sizes between 5 and 7 cm. Such condition cause considerable level of pain for the patients and needed to receive FPOP immediately. Of the patients (Table 12), patient DA's effective doses far outweighed that of the rest recording estimates of 4.213 and 3.141 mSv respectively for ICRP 60 and ICRP 103. Correspondingly, the average dose in total body for patient DA (5.030 mGy) was the highest, over 800 % more than the least recorded average dose in total body for patient AD2. This is as a result

of longer scanning time and high exposure parameters used in the case of DA as compared to AD2.

Table 11: Dose data for patients undergoing FPOP procedures with Type II multiple aneurysm and acute thrombosis

	TS	VS1	DE	Patient LF	GN	VS2	VA
Active bone marrow	0.451	0.291	0.550	0.962	0.119	0.251	0.088
Adrenals	0.002	0.002	0.002	0.001	0.000	0.001	0.000
Brain	0.000	0.000	0.000	0.000	0.000	0.000	0.000
Breasts	0.000	0.000	0.000	0.000	0.000	0.000	0.000
Colon	0.484	0.317	0.389	1.237	0.276	0.185	0.154
Extrathoracic airways	0.000	0.000	0.000	0.000	0.000	0.000	0.000
Gall bladder	0.029	0.015	0.030	0.037	0.001	0.012	0.001
Heart	0.000	0.000	0.000	0.001	0.000	0.000	0.000
Kidneys	0.015	0.009	0.017	0.023	0.001	0.006	0.001
Liver	0.009	0.005	0.009	0.010	0.000	0.004	0.000
Lungs	0.000	0.000	0.000	0.000	0.000	0.000	0.000
Lymph nodes	0.120	0.077	0.132	0.227	0.029	0.056	0.018
Muscle	0.726	0.689	1.055	1.766	0.409	0.511	0.218
Oesophagus	0.001	0.000	0.000	0.001	0.000	0.000	0.000
Oral mucosa	0.000	0.000	0.000	0.000	0.000	0.000	0.000
Ovaries	0.953	0.697	1.366	2.056	0.077	0.511	0.169
Pancreas	0.005	0.003	0.005	0.008	0.000	0.002	0.000
Prostate	1.358	0.896	1.325	2.566	0.738	0.681	0.183
Salivary glands	0.000	0.000	0.000	0.000	0.000	0.000	0.000
Skeleton	1.085	0.848	1.080	2.699	0.678	0.650	0.356
Skin	0.703	0.691	1.063	1.726	0.389	0.489	0.243
Small intestine	0.291	0.150	0.301	0.486	0.017	0.111	0.025
Spleen	0.003	0.002	0.002	0.008	0.000	0.001	0.001
Stomach	0.007	0.004	0.006	0.016	0.001	0.002	0.001
Testicles	0.886	0.538	0.530	1.537	0.449	0.328	0.061
Thymus	0.000	0.000	0.000	0.000	0.000	0.000	0.000
Thyroid	0.000	0.000	0.000	0.000	0.000	0.000	0.000
Urinary bladder	0.806	0.558	0.926	1.781	0.321	0.455	0.130
Uterus	1.041	0.810	1.290	2.003	0.106	0.498	0.146
Average dose in total body (mGy)	0.698	0.636	0.950	1.699	0.396	0.474	0.213
Effective Dose ICRP 60 (mSv)	0.407	0.285	0.438	0.857	0.146	0.198	0.075
Effective Dose ICRP 103 (mSv)	0.259	0.178	0.274	0.570	0.100	0.128	0.054
Peak skin dose (mGy)	23.200	28.900	97.700	48.800	21.900	23.600	15.900

Table 12: Dose data for patients undergoing FPOP procedures with Type II multiple aneurysm peripheral embolization

	AD2	ZS	Patient			
			DA	KC	LN1	LN2
Active bone marrow	0.013	0.180	8.645	0.335	0.048	0.228
Adrenals	0.000	0.000	0.103	0.000	0.000	0.001
Brain	0.000	0.000	0.000	0.000	0.000	0.000
Breasts	0.000	0.000	0.005	0.000	0.000	0.000
Colon	0.029	0.212	6.553	1.556	0.060	0.433
Extrathoracic airways	0.000	0.000	0.000	0.000	0.000	0.000
Gall bladder	0.000	0.004	0.754	0.009	0.001	0.003
Heart	0.000	0.000	0.019	0.000	0.000	0.000
Kidneys	0.000	0.002	0.852	0.006	0.000	0.003
Liver	0.000	0.001	0.197	0.002	0.000	0.001
Lungs	0.000	0.000	0.015	0.000	0.000	0.000
Lymph nodes	0.027	0.047	2.152	0.093	0.032	0.085
Muscle	0.505	0.606	5.013	1.186	0.585	1.297
Oesophagus	0.000	0.000	0.033	0.000	0.000	0.000
Oral mucosa	0.000	0.000	0.000	0.000	0.000	0.000
Ovaries	0.006	0.198	13.120	0.572	0.030	0.332
Pancreas	0.000	0.001	0.233	0.003	0.000	0.001
Prostate	0.059	1.035	8.653	2.093	0.381	0.410
Salivary glands	0.000	0.000	0.000	0.000	0.000	0.000
Skeleton	0.988	0.873	7.891	1.085	0.871	2.597
Skin	0.788	0.593	4.158	1.068	0.827	1.677
Small intestine	0.001	0.042	7.033	0.122	0.007	0.061
Spleen	0.000	0.000	0.209	0.003	0.000	0.002
Stomach	0.000	0.001	0.330	0.006	0.000	0.003
Testicles	0.072	0.776	1.843	0.862	0.253	0.279
Thymus	0.000	0.000	0.000	0.000	0.000	0.000
Thyroid	0.000	0.000	0.000	0.000	0.000	0.000
Urinary bladder	0.024	0.546	7.459	1.223	0.126	0.265
Uterus	0.008	0.260	12.466	0.631	0.042	0.218
Average dose in total body (mGy)	0.515	0.571	5.030	1.044	0.560	1.322
Effective Dose ICRP 60 (mSv)	0.056	0.216	4.213	0.510	0.092	0.258
Effective Dose ICRP 103 (mSv)	0.032	0.135	3.141	0.381	0.054	0.174
Peak skin dose (mGy)	29.200	20.100	133.000	180.300	16.500	242.200

### **Type II Popliteal aneurysm (multiple aneurysms with acute thrombosis and limb-threatening ischemia)**

The last set of patients (GA, KE, ML, FE, FV, KD, and KV) for FPOP procedures reported with multiple aneurysms with acute thrombosis and limb-threatening ischemia. This is the most advanced form of FPOP aneurysm which is mostly treated through complex procedures. Among these seven patients, patient KV recorded highest effective dose of 37.419 and 26.646 mSv based on ICRP 60 and ICRP 103 protocols respectively. Most of these dose components were received in the ovaries, uterus and the bone marrow, recording organ doses of 140.639, 139.698 and 76.089 mGy respectively. Noticeably, patient FV whose effective doses per ICRP 60 and ICRP 103 protocols (i.e. 11.888 and 8.786 mSv) were much lower than patient KV, recorded PSD of 3887.0 mGy which is about 280 times the PSD received by patient KV. This observation raises the issue of indirect correlation between effective dose and peak skin dose. The indirect relationship between PSD and the cumulative air kerma in fluoroscopic guided interventional radiology is extensively analyzed in a number of studies (Neil, 2010; Jones, 2011; Jones, 2012). This observation is an indication that aside air kerma, other factors such as the exposure time and field size (scan area) could influence the PSD. Hence cumulative air kerma alone may not be enough as a factor for predicting the PSD.

Table 13: Dose data for patients undergoing FPOP procedures with multiple aneurysm, acute thrombosis and limb-threatening ischemia

	Patient						
	GA	KE	ML	FE	FV	KD	KV
Active bone marrow	7.139	9.140	8.029	15.936	23.177	1.657	76.089
Adrenals	0.088	0.117	0.262	0.575	0.552	0.000	3.261
Brain	0.000	0.000	0.000	0.000	0.000	0.000	0.000
Breasts	0.005	0.006	0.007	0.021	0.023	0.001	0.082
Colon	5.745	6.592	5.940	12.153	17.662	1.353	40.161
Extrathoracic airways	0.000	0.000	0.000	0.000	0.000	0.000	0.000
Gall bladder	0.620	0.741	1.802	4.165	3.501	0.030	12.183
Heart	0.015	0.024	0.032	0.087	0.096	0.000	0.344
Kidneys	0.773	1.030	2.611	6.973	4.597	0.014	31.965
Liver	0.170	0.142	0.290	1.062	0.956	0.008	3.721
Lungs	0.012	0.018	0.026	0.074	0.083	0.000	0.316
Lymph nodes	1.820	2.422	2.501	5.055	6.507	0.358	19.520
Muscle	5.413	5.950	3.180	7.178	11.682	5.655	35.219
Oesophagus	0.030	0.039	0.061	0.148	0.165	0.000	0.618
Oral mucosa	0.000	0.000	0.000	0.000	0.000	0.000	0.000
Ovaries	10.037	12.540	8.461	24.073	40.840	1.004	140.639
Pancreas	0.175	0.295	0.496	1.077	1.043	0.004	4.554
Prostate	8.218	6.228	3.373	8.794	19.462	8.347	50.398
Salivary glands	0.000	0.000	0.000	0.000	0.000	0.000	0.001
Skeleton	7.828	10.966	7.239	13.011	19.114	7.698	61.122
Skin	4.786	6.480	3.001	5.614	9.346	5.407	29.508
Small intestine	5.702	7.846	8.143	16.088	21.245	0.242	62.099
Spleen	0.202	0.373	0.311	1.051	1.000	0.003	4.292
Stomach	0.322	0.526	0.523	1.502	1.473	0.007	4.057
Testicles	2.960	1.297	1.006	1.468	3.001	3.025	7.680
Thymus	0.000	0.002	0.004	0.013	0.009	0.000	0.041
Thyroid	0.000	0.000	0.000	0.000	0.000	0.000	0.000
Urinary bladder	6.317	7.169	3.493	9.934	21.497	3.681	66.751
Uterus	8.980	14.495	5.423	19.859	43.167	1.296	139.698
Average dose in total body (mGy)	5.282	6.192	3.592	7.609	11.975	5.256	36.694
Effective Dose ICRP 60 (mSv)	3.600	4.365	3.287	7.370	11.888	1.347	37.419
Effective Dose ICRP 103 (mSv)	2.709	3.245	2.597	5.738	8.786	0.905	26.646
Peak skin dose (mGy)	192.700	245.200	420.200	442.900	3887.000	483.000	13.900

### Summarized Dose Data for FPOP Procedures

Table 14 presents the summary of simulated dose data for the 41 patients who underwent the FPOP procedures and presented in Tables 8 – 13. Scan data for the individual patients are presented in APPENDIX D (Tables B1 – B41). The summarized data in Table 13, present the maximum, minimum, mean, sum, 75<sup>th</sup> and 90<sup>th</sup> percentiles for the simulated dose data for 41 patients. The highest individual organ dose of 140.639 mGy was recorded by patient KV in the ovaries. This patient had type II multi spread popliteal aneurysm with thrombosis and limb-threatening ischemia. The study identified the ovaries, uterus, skeleton, bone marrow and prostate as the five organs receiving the highest doses in FPOP procedures with average estimates of 6.456, 6.305, 4.195, 3.844 and 3.295 mGy respectively. Graphical representation of this is presented in Figure 14 where box plot of the simulated organ doses are plotted indicating the minimum, maximum, median, 25<sup>th</sup> and 75<sup>th</sup> percentiles. Average effective dose for the FPOP procedures for ICRP 60 and ICRP 103 protocols were estimated as 1.969 and 1.429 mSv respectively. This implies a 26.4 % less dose estimated with ICRP 103 compared with ICRP 60. Similar observation in CT studies have been published by Obed et al (Obed, 2016).

Table 14: Summary of simulated organ doses (mGy) from FPOP procedures

	Min	Max	Mean	± SD	Sum	P75	P90
Active bone marrow	0.013	76.089	3.844	± 12.505	157.593	0.674	8.645
Adrenals	0.000	3.261	0.130	± 0.519	5.319	0.002	0.262
Brain	0.000	0.000	0.000	± 0.000	0.000	0.000	0.000
Breasts	0.000	0.082	0.004	± 0.013	0.156	0.000	0.006
Colon	0.012	40.161	2.590	± 7.002	106.180	1.012	6.553
Extrathoracic airways	0.000	0.000	0.000	± 0.000	0.000	0.000	0.000
Gall bladder	0.000	12.183	0.589	± 2.053	24.151	0.030	0.754
Heart	0.000	0.344	0.016	± 0.057	0.669	0.000	0.032
Kidneys	0.000	31.965	1.199	± 5.103	49.152	0.017	1.030
Liver	0.000	3.721	0.162	± 0.612	6.662	0.009	0.197
Lungs	0.000	0.316	0.014	± 0.052	0.589	0.000	0.026
Lymph nodes	0.011	19.520	1.038	± 3.260	42.540	0.163	2.422
Muscle	0.193	35.219	2.493	± 5.759	102.194	1.297	5.655
Oesophagus	0.000	0.618	0.028	± 0.101	1.158	0.001	0.056
Oral mucosa	0.000	0.000	0.000	± 0.000	0.000	0.000	0.000
Ovaries	0.006	140.639	6.456	± 22.822	264.694	1.004	12.540
Pancreas	0.000	4.554	0.197	± 0.739	8.066	0.005	0.295
Prostate	0.059	50.398	3.295	± 8.424	135.101	1.621	8.347
Salivary glands	0.000	0.001	0.000	± 0.000	0.001	0.000	0.000
Skeleton	0.245	61.122	4.195	± 9.950	171.982	2.597	7.891
Skin	0.226	29.508	2.279	± 4.800	93.428	1.677	5.407
Small intestine	0.001	62.099	3.219	± 10.431	131.987	0.291	7.846
Spleen	0.000	4.292	0.185	± 0.697	7.573	0.006	0.311
Stomach	0.000	4.057	0.217	± 0.702	8.893	0.012	0.523
Testicles	0.061	7.680	0.839	± 1.350	34.399	0.862	1.843
Thymus	0.000	0.041	0.002	± 0.007	0.072	0.000	0.003
Thyroid	0.000	0.000	0.000	± 0.000	0.001	0.000	0.000
Urinary bladder	0.024	66.751	3.406	± 10.867	139.654	1.087	7.169
Uterus	0.008	139.698	6.305	± 22.711	258.513	1.252	12.466
Average dose in total body (mGy)	0.195	36.694	2.533	± 5.992	103.863	1.322	5.282
Effective Dose ICRP 60 (mSv)	0.029	37.419	1.969	± 6.128	80.722	0.510	4.213
Effective Dose ICRP 103 (mSv)	0.017	26.646	1.429	± 4.396	58.574	0.381	3.141
Peak skin dose (mGy)	7.900	3887.000	188.100	± 606.969	7714.100	99.200	420.200

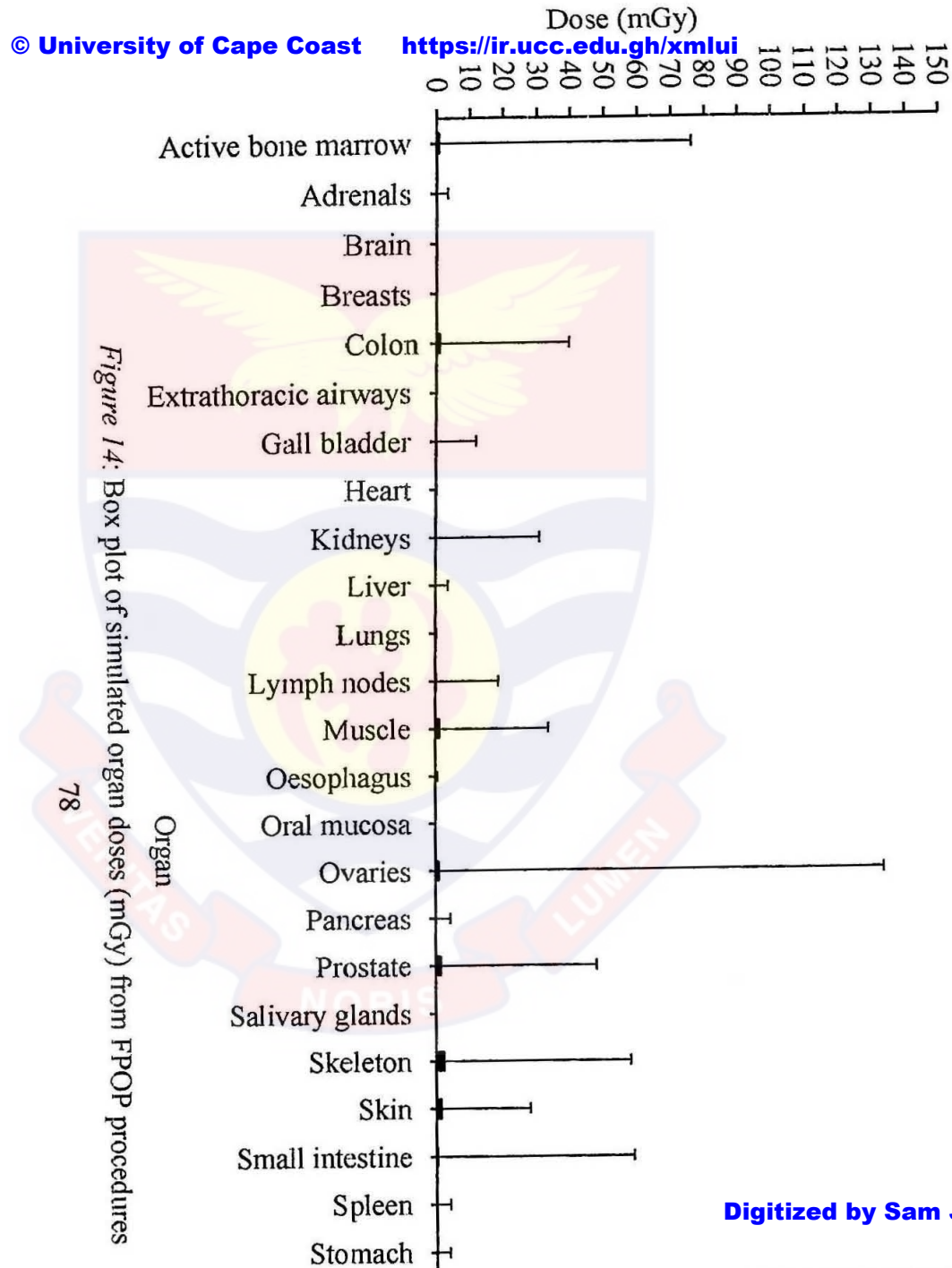


Figure 14: Box plot of simulated organ doses (mGy) from FPDP procedures

Figure 15 present box plot for the effective dose estimates of the 41 patients in the FPOP procedures. The estimated average effective dose of 1.429 mSv per ICRP 103 was comparable to the estimated effective dose of 1.600 mSv in the study of (Qi et al, 2016), which assessed radiation dose to lower extremities of patients in CT angiography. The graphical representation reveals an uneven distribution of the simulated between the minimum and maximum dose data points. A high proportion of outliers were observed in the distribution, giving indication that most of the dose data were skewed towards the minimum dose limit.

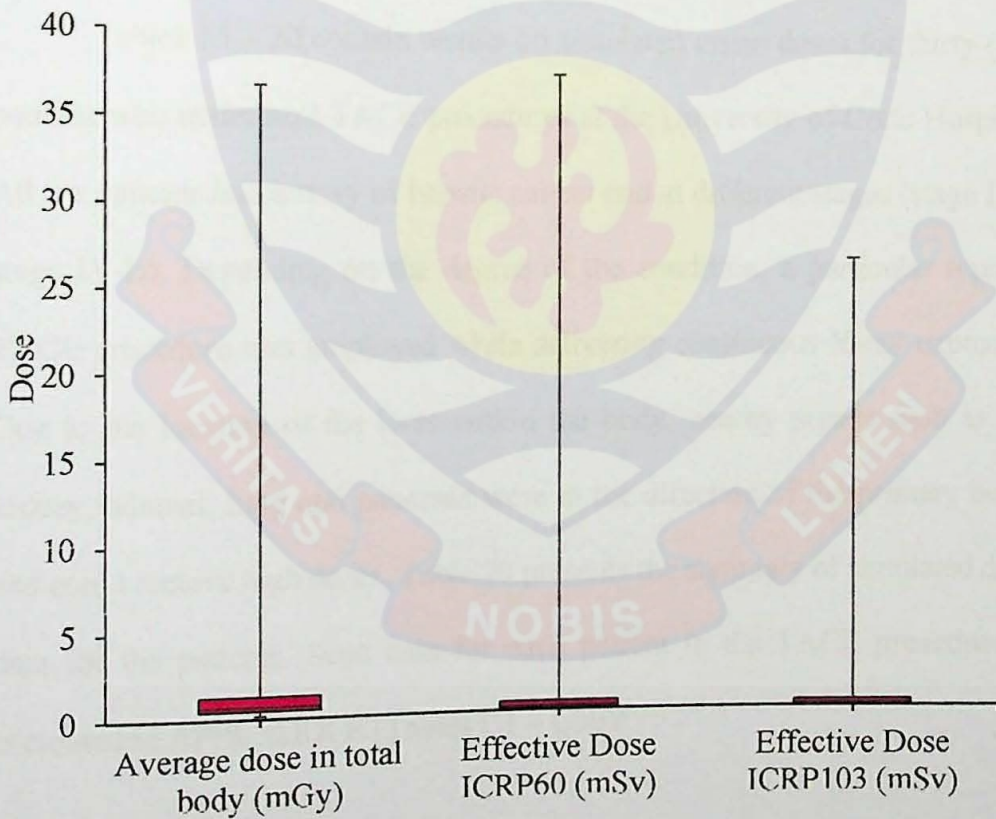


Figure 15: Box plot for average and effective doses from FPOP procedures

### **Transarterial Chemoembolization (TACE)**

TACE is minimally invasive, non-surgical procedure performed in radiology by interventional radiologists to combine local delivery of chemotherapy and embolization in the treatment of cancer, most often of the liver (Wang et al., 2010). The procedure is performed under X-ray imaging to place chemotherapy and embolic agent into blood vessel feeding the cancerous tumor to cut off the tumor's blood supply and trap the chemotherapy within the tumor. Chemoembolization procedures performed on the patients were either standalone treatment or in combination with surgery, ablation, chemotherapy or radiation therapy.

Tables 15 – 20 contain results on simulated organ doses for thirty (30) patients who underwent TACE procedures at the University of Crete Hospital. All the patients had history of hepatic cancer and at different stages (stage II to stage IV-B). Depending on the degree of the condition, a particular type of TACE procedure was employed while delivering continuous X-ray exposure. Due to the location of the liver within the body, nearby organs such as the kidney, adrenal, lung and pancreas were in the direction of the primary beam and could receive high doses. Table 20 presents the summary of simulated dose data for the patients. Scan data for each patient in the TACE procedure is presented in APPENDIX E (Tables C1 – C30).

### Stage II Hepatic Cancer

The stage II hepatic cancers identified in this set of patients either had a single tumour larger than 2 cm and grown into blood vessels or had more than one tumour with none larger than 5 cm diameter. These cancers had not spread to nearby lymph nodes or to distant sites. For the group of cases, as presented in Table 15, patient KAE received two cycles of the procedure and consequently received the highest effective dose. Consequently, same patient received the highest peak skin dose of 881.684 mGy. Effective doses ranged between 5.755 – 17.057 mSv for ICRP 60 protocol and 5.266 - 15.122 mSv per ICRP 103 protocol. Kidneys and adrenals were found to be the organs receiving most of the radiation in this procedure with estimated range of doses of 57.673 – 169.358 mGy and 42.894 - 151.471 mGy, respectively.

Table 15: Dose data for patients undergoing TACE procedures with stage II hepatic cancer

	Patient					
	KAE	NIK	KRI	KAE2	KAG	VEG
Active bone marrow	14.994	10.508	14.731	17.477	8.255	7.431
Adrenals	151.471	42.894	91.682	112.767	45.358	58.609
Brain	0.076	0.001	0.003	0.007	0.002	0.002
Breasts	2.923	0.831	1.303	2.308	0.863	0.723
Colon	3.612	6.512	6.022	8.535	3.122	5.144
Extrathoracic airways	0.417	0.012	0.022	0.071	0.023	0.016
Gall bladder	29.390	40.980	22.021	46.123	13.860	38.974
Heart	5.373	2.852	6.540	7.733	2.930	2.866
Kidneys	109.080	145.715	95.055	169.358	57.673	124.690
Liver	52.120	35.756	38.047	99.165	24.710	59.129
Lungs	20.840	5.508	11.874	23.880	7.139	5.079

Lymph nodes	9.229	10.126	9.504	13.351	4.958	8.537
Muscle	8.378	6.675	7.419	11.872	4.035	6.290
Oesophagus	8.238	4.009	9.909	9.814	4.741	4.131
Oral mucosa	0.224	0.002	0.009	0.035	0.006	0.006
Ovaries	0.964	1.592	1.682	2.038	0.815	0.974
Pancreas	15.774	16.156	19.198	18.719	8.970	13.491
Prostate	0.071	0.083	0.099	0.141	0.056	0.065
Salivary glands	0.438	0.008	0.024	0.058	0.015	0.015
Skeleton	23.903	12.384	17.998	23.598	10.279	9.920
Skin	9.535	6.561	7.953	13.550	4.347	6.401
Small intestine	4.491	9.330	9.079	10.523	4.299	5.905
Spleen	1.488	11.746	4.784	1.810	1.781	1.348
Stomach	2.347	5.902	5.327	3.131	1.987	2.617
Testicles	0.011	0.014	0.014	0.028	0.011	0.008
Thymus	2.367	0.413	0.959	1.618	0.517	0.547
Thyroid	0.918	0.023	0.079	0.216	0.059	0.044
Urinary bladder	0.179	0.267	0.295	0.374	0.140	0.183
Uterus	0.757	1.294	1.360	1.540	0.652	0.772
Average dose in total body (mGy)	11.840	8.623	9.896	16.154	5.566	8.415
Effective Dose ICRP 60 (mSv)	13.106	9.614	10.130	17.057	5.755	9.332
Effective Dose ICRP 103 (mSv)	11.324	8.022	9.436	15.122	5.266	7.677
Peak skin dose (mGy)	688.936	525.011	681.713	881.684	473.318	512.817

### Stage III-A Hepatic Cancer

The patients in this group were diagnosed with more than one tumour, with at least one tumour larger than 5 cm diameter. These cancers were localized and not spread to nearby lymph nodes or to distant sites. In treating such condition the chemotherapy and embolic agent were injected into multiple sites in the liver due to the multiple tumour sites. The procedures were a little

extended than the stage II cases. Patient PES received two separate cycles of the treatment when it was realized that the first cycle did not completely destroy the tumour. The second treatment cycle produced effective doses of 21.447 and 19.240 mSv per ICRP 60 and ICRP 103 protocols respectively (Table 16), the highest amongst all the stage III-A hepatic cancer TACE procedures performed. Consequently, same patient recorded the highest peak skin dose of 858.549 mGy. With organ doses, the kidneys were estimated to have received the most doses ranging between 105.898 - 225.466 mGy.

Table 16: Dose data for patients undergoing TACE procedures with stage III-A hepatic cancer

	Patient					
	LEA	SFA	SOM	TEG	PES1	PES2
Active bone marrow	5.689	24.986	26.986	23.435	17.388	16.318
Adrenals	59.940	189.528	205.647	125.604	178.651	204.313
Brain	0.003	0.008	0.004	0.005	0.017	0.034
Breasts	1.064	1.739	1.555	3.457	2.328	3.201
Colon	2.895	5.018	8.222	9.101	4.159	6.423
Extrathoracic airways	0.016	0.073	0.031	0.048	0.118	0.246
Gall bladder	20.276	29.270	60.904	48.664	35.692	54.739
Heart	2.674	7.682	7.776	9.023	7.721	10.701
Kidneys	105.898	121.451	217.941	174.199	156.670	225.466
Liver	55.766	62.781	69.324	84.234	69.852	155.101
Lungs	12.995	14.792	11.021	19.673	19.700	27.087
Lymph nodes	5.218	12.548	18.057	15.327	11.521	15.119
Muscle	6.020	9.486	11.608	11.557	9.121	12.796
Oesophagus	2.984	17.599	17.113	13.679	12.860	12.544
Oral mucosa	0.018	0.034	0.015	0.013	0.058	0.127
Ovaries	0.709	1.292	1.756	1.856	1.516	2.278
Pancreas	5.163	33.678	43.024	28.497	23.730	24.578
Prostate	0.025	0.113	0.127	0.158	0.179	0.254
Salivary glands	0.034	0.055	0.027	0.048	0.117	0.225
Skeleton	8.911	31.928	32.683	29.006	24.139	24.048
Skin	7.927	10.482	11.533	11.826	10.225	14.578
Small intestine	3.390	6.577	10.501	11.337	5.442	8.036

Spleen	0.365	5.766	7.872	15.508	3.582	1.928
Stomach	0.776	5.011	9.533	7.856	4.372	3.784
Testicles	0.007	0.020	0.016	0.019	0.032	0.055
Thymus	0.726	1.462	1.220	1.653	1.886	3.135
Thyroid	0.087	0.143	0.090	0.145	0.300	0.566
Urinary bladder	0.106	0.287	0.338	0.361	0.350	0.550
Uterus	0.508	1.122	1.514	1.523	1.207	1.871
Average dose in total body (mGy)	7.996	14.141	16.474	16.273	13.163	18.631
Effective Dose ICRP 60 (mSv)	8.715	15.888	17.746	17.535	15.554	21.447
Effective Dose ICRP 103 (mSv)	7.304	13.755	16.270	16.126	13.509	19.240
Peak skin dose (mGy)	683.928	720.838	804.110	789.212	684.276	858.549

### Stage III--B Hepatic Cancer

The patients who fell within the stage III-B hepatic cancer group had at least one tumour of any size that had grown into a major branch of a large vein of the liver (hepatic vein). Here the cancer had not spread to nearby lymph nodes or to distant sites. As presented in Table 17, two patients (i.e. FAP and PRN) received two separate cycles of the treatment in this case. Peak skin doses in these procedures were slightly elevated comparative to stage III-A as a result of much extended period of scanning under X-ray exposure. However, the peak skin doses were within the 2 Gy level which could initiate deterministic effects. The single procedure which produced the most effective dose was the first cycle of patient PRN, where effective doses of 27.226 and 24.265 mSv were estimated per ICRP 60 and ICRP 103 respectively. The single most high organ dose for these patients was 265.640 mGy which was received by the adrenals of patient PRN in the first cycle of the procedure.

Table 17: Dose data for patients undergoing TACE procedures with stage III-B hepatic cancer

	Patient					
	FAP	FAP 2	PRN 1	PRN 2	MOM	KOA
Active bone marrow	14.691	23.504	31.179	6.609	16.056	12.136
Adrenals	135.103	124.185	265.640	38.201	181.704	102.921
Brain	0.008	0.006	0.007	0.003	0.011	0.005
Breasts	1.894	1.654	4.045	1.435	2.593	1.374
Colon	4.095	12.462	7.542	1.537	5.029	5.550
Extrathoracic airways	0.073	0.048	0.073	0.035	0.093	0.040
Gall bladder	24.813	50.990	63.813	15.642	43.479	36.321
Heart	6.358	6.006	15.736	3.332	7.559	4.496
Kidneys	117.385	206.696	255.415	74.204	189.241	153.511
Liver	74.760	112.264	144.064	86.688	171.155	69.760
Lungs	19.120	13.816	36.177	15.270	21.602	13.370
Lymph nodes	9.479	14.931	20.410	4.661	11.856	9.345
Muscle	7.925	14.318	16.943	5.241	12.380	8.336
Oesophagus	9.808	9.439	22.322	3.510	9.383	6.544
Oral mucosa	0.030	0.032	0.029	0.016	0.045	0.022
Ovaries	1.363	3.258	1.508	0.295	1.195	1.332
Pancreas	18.247	21.636	41.193	5.796	18.561	13.156
Prostate	0.099	0.259	0.074	0.010	0.066	0.091
Salivary glands	0.053	0.041	0.057	0.022	0.080	0.036
Skeleton	19.639	27.998	43.149	10.567	24.211	16.239
Skin	9.049	16.455	19.665	7.262	15.473	9.442
Small intestine	6.202	15.599	9.214	1.724	5.967	6.860
Spleen	4.021	3.490	6.651	0.480	1.582	1.341
Stomach	4.099	4.261	8.163	0.962	2.936	2.144
Testicles	0.013	0.044	0.015	0.002	0.015	0.012
Thymus	1.462	1.297	2.718	0.939	1.945	1.001
Thyroid	0.155	0.167	0.215	0.083	0.229	0.094
Urinary bladder	0.265	0.654	0.278	0.057	0.241	0.261
Uterus	1.096	2.492	1.226	0.245	0.951	1.052
Average dose in total body (mGy)	11.601	19.114	24.442	8.296	18.495	11.389
Effective Dose ICRP 60 (mSv)	13.825	18.956	27.226	8.655	20.745	12.317
Effective Dose ICRP 103 (mSv)	12.072	16.413	24.265	8.290	17.856	10.645
Peak skin dose (mGy)	1060.975	694.214	1354.354	645.817	1030.950	747.612

### Stage IV-A Hepatic Cancer

The stage IV-A hepatic cancer patients had either single or multiple tumours of any size that had spread to nearby lymph nodes but not distant sites. While patient PIG received two separate cycles of the TACE procedure, patient AGG received three. These were done to shrink the tumor sizes in succession till they were completely ablated. Patient AGG had cancer in both lobes of the liver and hence had to be treated one at a time. Effective doses for the patients ranged between 9.828 – 35.523 mSv and 8.156 – 30.390 mSv respectively per ICRP 60 and ICRP 103 protocols. Patient PIG, in the cycle of the TACE procedure received peak skin dose of 2847.658 mGy, exceeding the 2 mGy threshold limit. Such patient had a tendency for onset development of skin reaction few days after the procedure. However, follow up was not made on the patient. Patient PIG also recorded the single most elevated organ dose of 407.920 mGy in the kidneys.

Table 18: Dose data for patients undergoing TACE procedures with stage IV-A hepatic cancer

	Patient					
	PIG	PIG2	GIV	AGG1	AGG2	AGG3
Active bone marrow	22.998	22.097	31.701	26.967	16.323	7.914
Adrenals	177.249	129.372	227.185	127.967	91.825	68.052
Brain	0.012	0.019	0.007	0.030	0.012	0.005
Breasts	3.539	4.212	2.280	4.758	1.930	0.943
Colon	7.865	11.392	6.344	13.071	13.005	5.110
Extrathoracic airways	0.108	0.185	0.075	0.246	0.104	0.038
Gall bladder	65.069	86.468	31.494	69.062	61.982	26.766
Heart	10.433	11.061	11.585	11.449	5.534	2.893
Kidneys	286.964	407.920	113.301	349.066	334.103	127.841
Liver	199.742	327.381	59.521	313.825	203.834	61.353
Lungs	33.394	30.232	22.222	38.288	13.717	9.134
Lymph nodes	17.353	20.653	15.425	19.809	15.622	6.948

Muscle	16.728	21.346	11.229	22.815	17.480	7.094
Oesophagus	13.265	12.705	20.985	13.476	7.565	3.784
Oral mucosa	0.065	0.100	0.030	0.104	0.050	0.023
Ovaries	1.920	2.764	11.756	3.850	4.103	1.344
Pancreas	25.093	25.928	37.608	22.800	18.241	8.184
Prostate	0.107	0.199	1.912	0.294	0.305	0.116
Salivary glands	0.107	0.135	0.054	0.223	0.108	0.049
Skeleton	31.651	31.195	38.064	38.918	21.764	10.830
Skin	20.409	25.186	11.892	28.346	20.083	8.453
Small intestine	9.687	13.101	10.974	15.772	15.538	6.481
Spleen	2.494	2.406	5.301	2.189	2.075	0.678
Stomach	4.106	4.778	6.217	3.991	3.531	1.258
Testicles	0.013	0.041	0.260	0.044	0.048	0.013
Thymus	2.596	3.178	1.920	3.471	1.575	0.789
Thyroid	0.327	0.384	0.172	0.566	0.246	0.098
Urinary bladder	0.365	0.544	4.744	0.734	0.754	0.249
Uterus	1.486	2.119	14.430	2.782	2.799	1.032
Average dose in total body (mGy)	24.251	31.540	16.412	33.288	23.552	9.309
Effective Dose ICRP 60 (mSv)	25.443	35.523	20.375	34.153	25.915	9.828
Effective Dose ICRP 103 (mSv)	23.449	29.716	17.027	30.390	20.124	8.156
Peak skin dose (mGy)	1427.117	2847.658	841.108	1722.222	1290.123	708.711

### Stage IV-B Hepatic Cancer

The stage IV-B hepatic cancer is the terminal stage of the liver cancer disease. The patients in this group had either single or multiple tumours of any size and had spread to nearby lymph nodes as well as spread to distant organs such as the bones or lungs. Treatment of these patients were in combination with other treatment options such as radiotherapy. Complex and elongated procedures were applied in treating patients in this group. The simulated effective doses to the patients ranged between 11.928 – 49.941 mSv and 9.830 – 43.156 mSv per ICRP 60 and ICRP 103 respectively. Only patient VLG recorded peak skin dose exceeding 2 Gy (2138.826 mGy). This was the same patient that received the highest effective dose in the group. The kidneys,

adrenals and the liver were the organs that received the most doses during the procedure. The single most elevated organ dose of 451.938 mGy was received by patient VLG in the kidneys.

Table 19: Dose data for patients undergoing TACE procedures with stage IV-B hepatic cancer

	Patient					
	MIS	MIS 2	KAI	SIE	STI	VLG
Active bone marrow	30.207	25.732	9.186	7.780	54.395	46.709
Adrenals	164.432	301.921	51.481	65.119	430.694	448.713
Brain	0.026	0.010	0.002	0.003	0.011	0.053
Breasts	6.649	4.105	0.616	0.847	3.138	7.065
Colon	9.741	7.030	92.394	21.371	11.858	16.880
Extrathoracic airways	0.233	0.077	0.015	0.013	0.084	0.372
Gall bladder	83.634	69.939	17.486	18.347	93.817	97.982
Heart	18.435	11.799	3.051	2.819	15.523	19.923
Kidneys	249.168	328.160	68.454	68.503	430.846	451.938
Liver	388.020	213.025	32.034	45.252	129.521	341.206
Lungs	49.361	35.352	5.609	7.971	28.531	57.176
Lymph nodes	23.786	18.734	8.228	5.398	30.180	31.176
Muscle	21.598	17.543	13.161	6.416	22.707	30.147
Oesophagus	19.719	15.085	5.014	4.104	32.701	27.172
Oral mucosa	0.101	0.062	0.010	0.010	0.055	0.197
Ovaries	2.297	1.866	3.684	1.038	3.448	5.381
Pancreas	36.062	29.859	12.359	8.643	72.076	49.445
Prostate	0.145	0.108	182.780	45.139	0.226	0.455
Salivary glands	0.191	0.073	0.014	0.019	0.089	0.348
Skeleton	43.327	37.829	12.365	10.832	66.605	62.734
Skin	26.518	21.845	6.716	5.514	25.285	35.427
Small intestine	11.947	8.830	9.374	3.115	16.166	22.031
Spleen	4.996	3.446	4.442	0.964	10.616	6.121
Stomach	7.956	5.395	3.872	1.424	12.073	8.643
Testicles	0.042	0.010	77.820	20.020	0.040	0.077
Thymus	5.066	2.627	0.455	0.619	2.631	5.579
Thyroid	0.594	0.264	0.042	0.064	0.267	0.868
Urinary bladder	0.465	0.318	23.390	6.118	0.660	1.071
Uterus	1.886	1.333	4.702	1.313	2.771	4.130
Average dose in total body (mGy)	34.619	26.263	13.355	8.078	32.498	43.747
Effective Dose ICRP 60 (mSv)	38.763	30.075	26.940	11.928	35.859	49.941

Effective Dose ICRP 103 (mSv)	35.343	26.461	21.877	9.830	31.187	43.156
Peak skin dose (mGy)	1574.667	1357.026	734.311	543.908	1742.066	2138.826

### Summarized Dose Data for TACE Procedures

Table 20 summarizes the data as presented in Tables 15 – 19. The table presents the maximum, minimum, mean, sum, 75<sup>th</sup> and 90<sup>th</sup> percentiles for the simulated dose data on all 30 patients who underwent the TACE procedures. The highest individual organ dose recorded in all the TACE procedures performed on the 30 patients was 451.938 mGy to the kidneys and this was received by patient VLG, who had terminal stage liver cancer with multiple spread. From the simulated results, as presented in Table 20 and the box plot in Figure 16, five organs receiving the highest doses in TACE procedures were kidneys (197.197 mGy), adrenals (153.274 mGy), liver (125.980 mGy), gall bladder (46.600 mGy) and skeleton (26.557 mGy), while the five organs receiving the least doses (all with < 1 mGy) were the thyroid, extrathoracic airways, salivary gland, oral mucosa and the brain. In terms of proximity, the organs situated close to the cancerous site (i.e. the liver) were those that received the most dose because they were directly in the path of the primary beam. Comparing results in this study to Hidajat et al (Hidajat, 2006), where radiation exposure to 65 patients in hepatic chemoembolization was performed, it was observed that the highest organ dose was received by the liver (79.86 mSv) while effective dose was estimated as 13.98 mSv.

Table 20: Summary of simulated organ doses (mGy) from TACE procedures

	Min	Max	Mean	± SD	Sum	P75	P90
Active bone marrow	5.689	54.395	19.813	± 11.500	594.380	25.545	31.231
Adrenals	38.201	448.713	153.274	± 103.105	4598.229	187.572	269.268
Brain	0.001	0.076	0.013	± 0.017	0.393	0.012	0.030
Breasts	0.616	7.065	2.512	± 1.664	75.373	3.393	4.266
Colon	1.537	92.394	10.701	± 16.035	321.044	10.979	13.452
Extrathoracic airways	0.012	0.417	0.100	± 0.105	3.003	0.107	0.246
Gall bladder	13.860	97.982	46.600	± 24.239	1397.996	63.355	83.917
Heart	2.674	19.923	8.062	± 4.810	241.862	10.971	15.544
Kidneys	57.673	451.938	197.197	± 112.857	5915.911	253.853	354.952
Liver	24.710	388.020	125.980	± 101.437	3779.387	167.142	315.180
Lungs	5.079	57.176	20.998	± 13.015	629.930	28.170	36.388
Lymph nodes	4.661	31.176	13.916	± 6.889	417.489	17.881	20.966
Muscle	4.035	30.147	12.622	± 6.391	378.663	16.889	21.709
Oesophagus	2.984	32.701	11.807	± 7.384	354.202	14.733	21.119
Oral mucosa	0.002	0.224	0.051	± 0.054	1.526	0.061	0.106
Ovaries	0.295	11.756	2.329	± 2.124	69.874	2.647	3.876
Pancreas	5.163	72.076	23.862	± 14.556	715.865	29.519	41.376
Prostate	0.010	182.780	7.792	± 34.053	233.756	0.247	0.601
Salivary glands	0.008	0.438	0.092	± 0.101	2.764	0.108	0.224
Skeleton	8.911	66.605	26.557	± 14.731	796.716	32.494	43.167
Skin	4.347	35.427	14.265	± 7.967	427.938	19.979	25.408
Small intestine	1.724	22.031	9.250	± 4.587	277.491	11.246	15.616
Spleen	0.365	15.508	4.042	± 3.562	121.270	5.224	8.147
Stomach	0.776	12.073	4.615	± 2.729	138.450	5.775	8.211
Testicles	0.002	77.820	3.292	± 14.541	98.767	0.043	0.095
Thymus	0.413	5.579	1.879	± 1.286	56.372	2.620	3.208
Thyroid	0.023	0.918	0.250	± 0.234	7.503	0.292	0.569
Urinary bladder	0.057	23.390	1.487	± 4.339	44.597	0.628	1.439
Uterus	0.245	14.430	2.065	± 2.540	61.964	2.061	2.932
Average dose in total body (mGy)	5.566	43.747	17.914	± 9.666	537.421	24.076	32.577
Effective Dose ICRP 60 (mSv)	5.755	49.941	20.278	± 10.760	608.346	26.684	35.557
Effective Dose ICRP 103 (mSv)	5.266	43.156	17.644	± 9.396	529.308	23.056	30.469
Peak skin dose (mGy)	473.318	2847.658	1025.535	± 545.265	30766.057	1338.296	1724.206

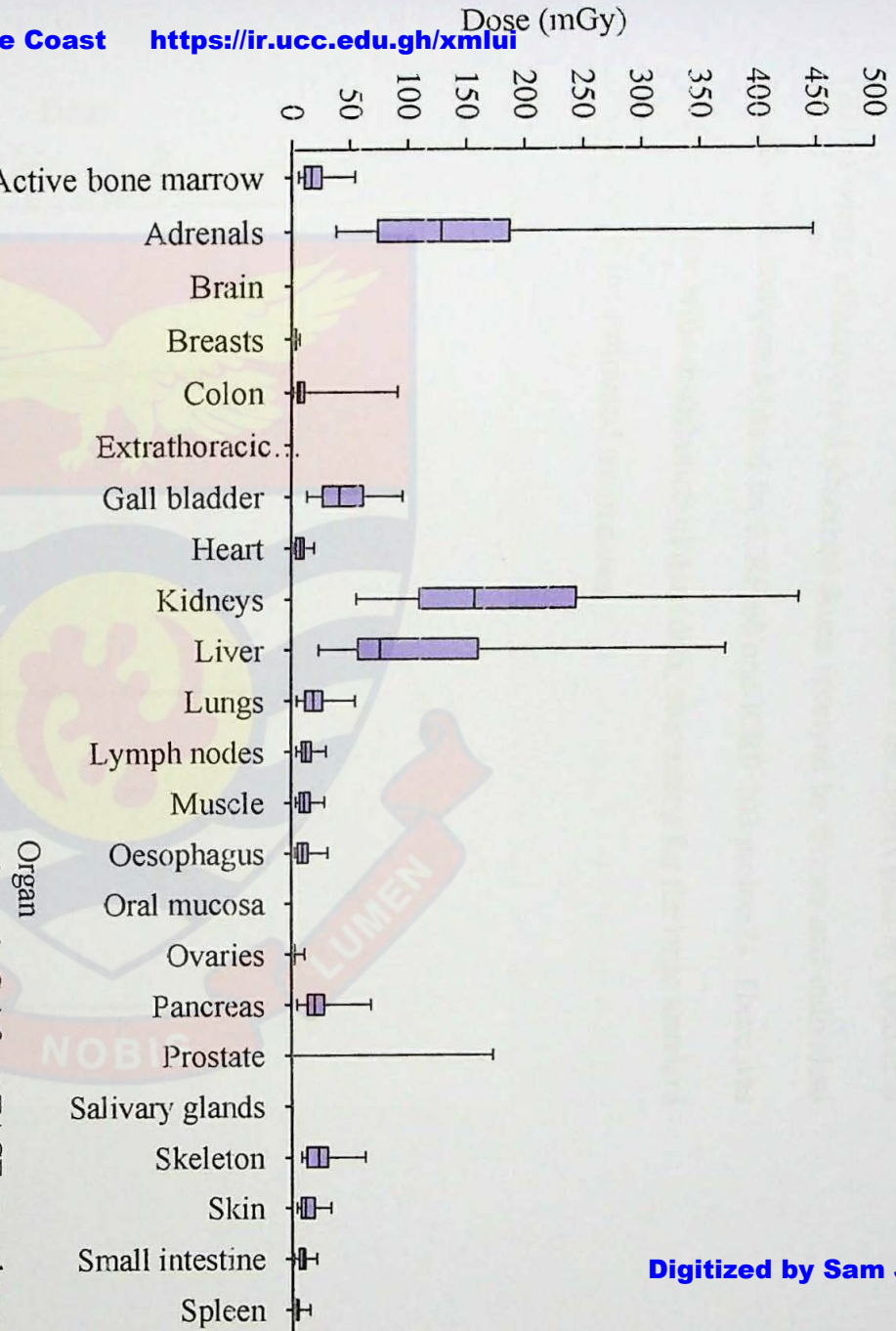


Figure 16: Box plot of simulated organ doses (mGy) from TACE procedures

The mean effective doses estimated per ICRP 60 and ICRP 103 were 20.278 and 17.644 mGy respectively, a percentage difference of 14.9 %. This observation was reflected in Figure 17, similar to the observation by Obed et al (2016) where effective and absorbed doses received by tissues and individual organs were compared based on ICRP 60 and ICRP 103 protocols. There was observed to be wide distribution of dose data, accounting for the large standard deviations in the estimated mean doses.

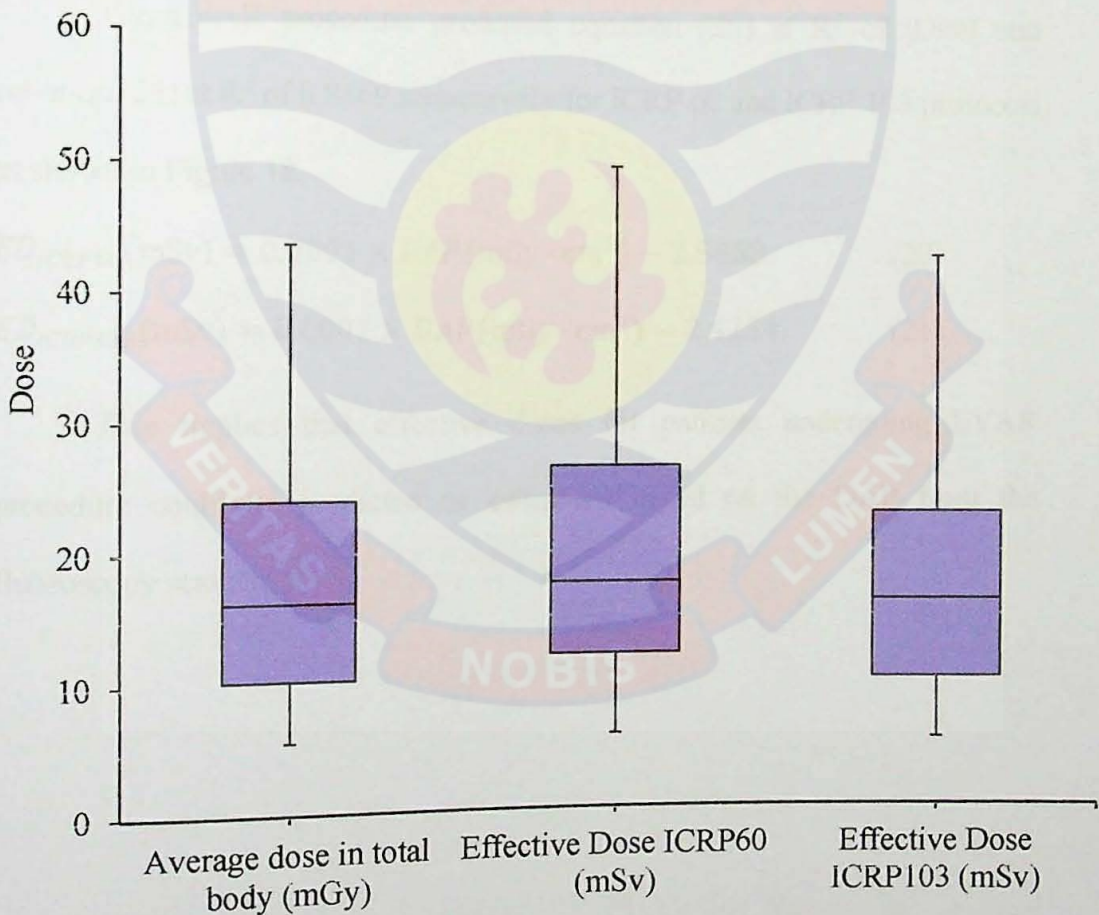


Figure 17: Box plot for average and effective doses from TACE procedures

### Relationships between Dose Area Product (DAP) and Effective Dose (ED)

In the analysis of the simulated dose data, relationships between the dose area product (DAP) and the effective doses (ED) were established. The study found linear relationships between DAP and ED for each of the procedures (i.e. EVAR, FPOP and TACE) with different levels of correlation ( $R^2$ ). From the derived relationships for the treatment procedures, the effective doses could be estimated directly from the DAP values as derived from the imaging procedures.

### Endovascular Aortic Aneurysm Repair

The EVAR procedure produced equation (20) at  $R^2$  of 0.859 and equation (21) at  $R^2$  of 0.8469 respectively for ICRP 60 and ICRP 103 protocols as shown in Figure 18.

$$ED_{ICRP60}(\text{mSv}) = 0.0001 \times DAP(\text{mGy} \cdot \text{cm}^2) - 2.8858 \quad (20)$$

$$ED_{ICRP103}(\text{mSv}) = 0.0001 \times DAP(\text{mGy} \cdot \text{cm}^2) - 2.4254 \quad (21)$$

This implies that effective doses for patients undergoing EVAR procedure could be predicted or estimated based on the DAP from the fluoroscopy scanner.

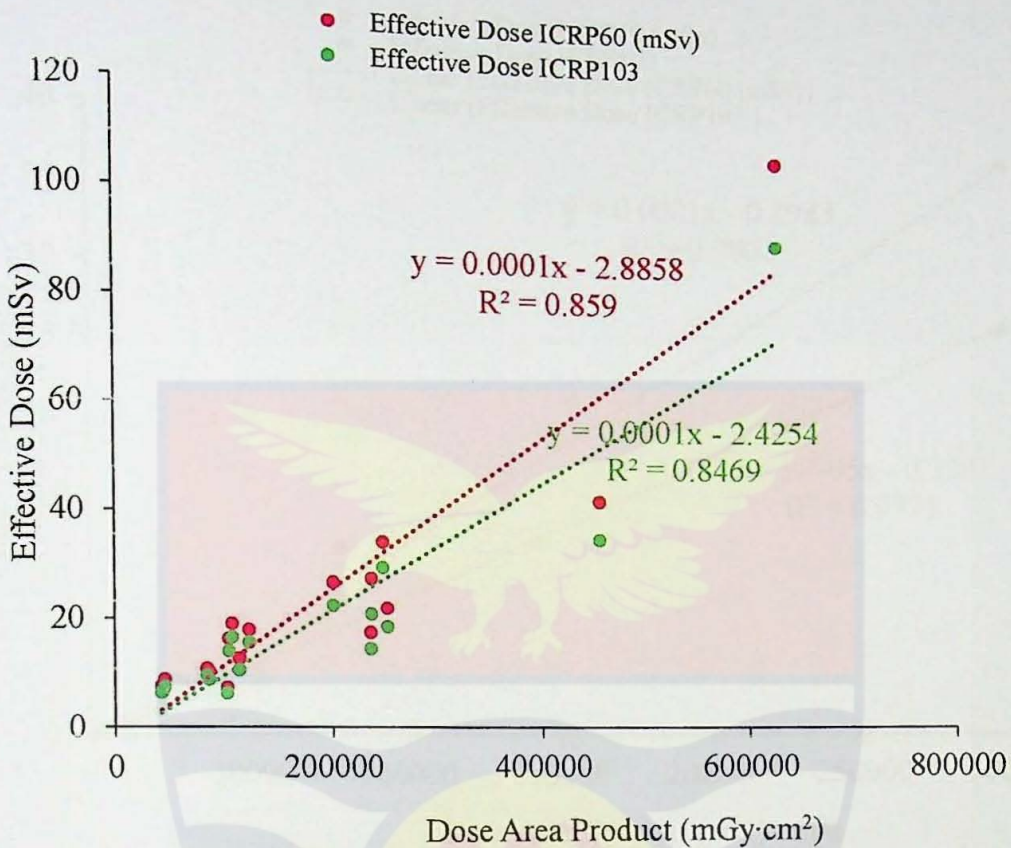


Figure 18: Relationship between DAP and ED for EVAR procedure

### Stenting of Femoropopliteal

The FPOP procedure produced equation (22) at  $R^2$  of 0.9802 and equation (23) at  $R^2$  of 0.9771 respectively for ICRP 60 and ICRP 103 protocols as presented in Figure 19.

$$ED_{ICRP60}(\text{mSv}) = 0.0001 \times DAP(\text{mGy} \cdot \text{cm}^2) - 0.4983 \quad (22)$$

$$ED_{ICRP103}(\text{mSv}) = 0.00009 \times DAP(\text{mGy} \cdot \text{cm}^2) - 0.3381 \quad (23)$$

This implies that effective doses for patients undergoing FPOP procedure could be predicted or estimated based on the DAP from the fluoroscopy scanner

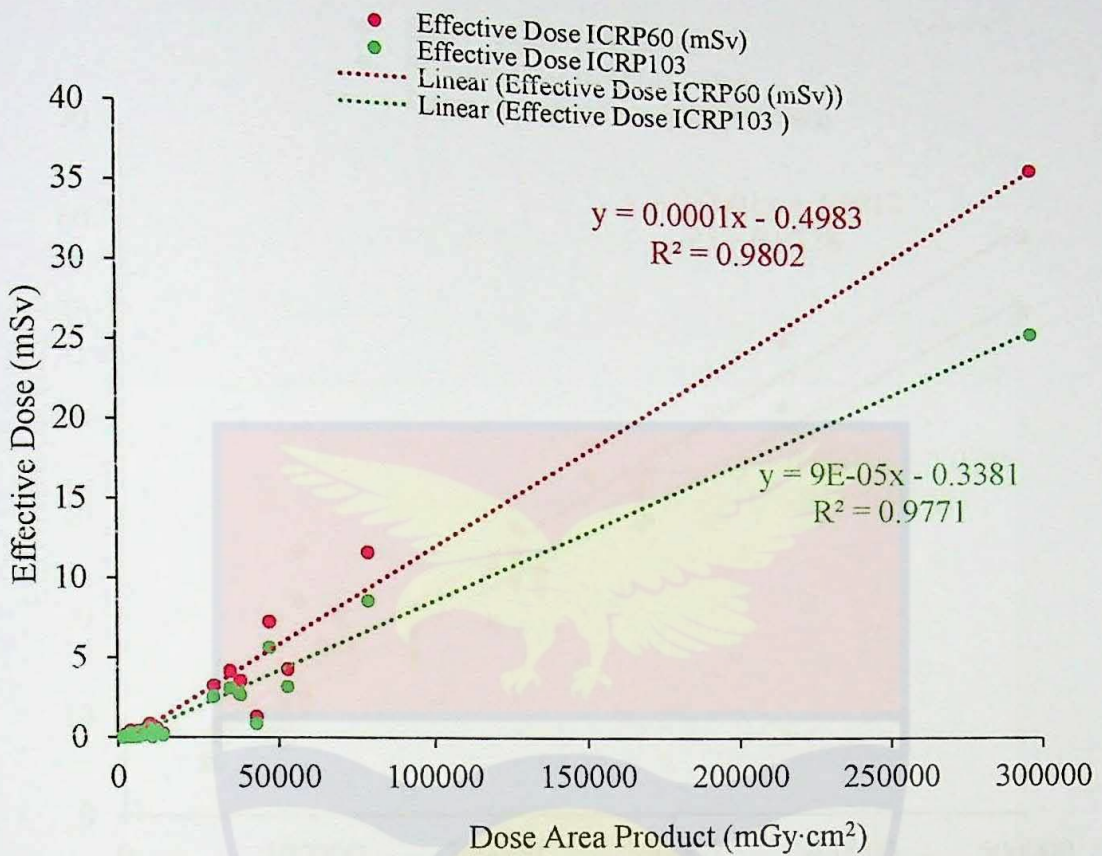


Figure 19: Relationship between DAP and ED for FPOP procedure

### Transarterial Chemoembolization

The TACE procedure produced equation (24) at  $R^2$  of 0.9228 and equation (25) at  $R^2$  of 0.9278 respectively for ICRP 60 and ICRP 103 protocols, as presented in Figure 20.

$$ED_{ICRP60}(\text{mSv}) = 0.0001 \times DAP(\text{mGy} \cdot \text{cm}^2) - 0.4983 \quad (24)$$

$$ED_{ICRP103}(\text{mSv}) = 0.00009 \times DAP(\text{mGy} \cdot \text{cm}^2) - 0.3381 \quad (25)$$

This implies that effective doses for patients undergoing TACE procedure could be predicted or estimated based on the DAP from the fluoroscopy scanner.

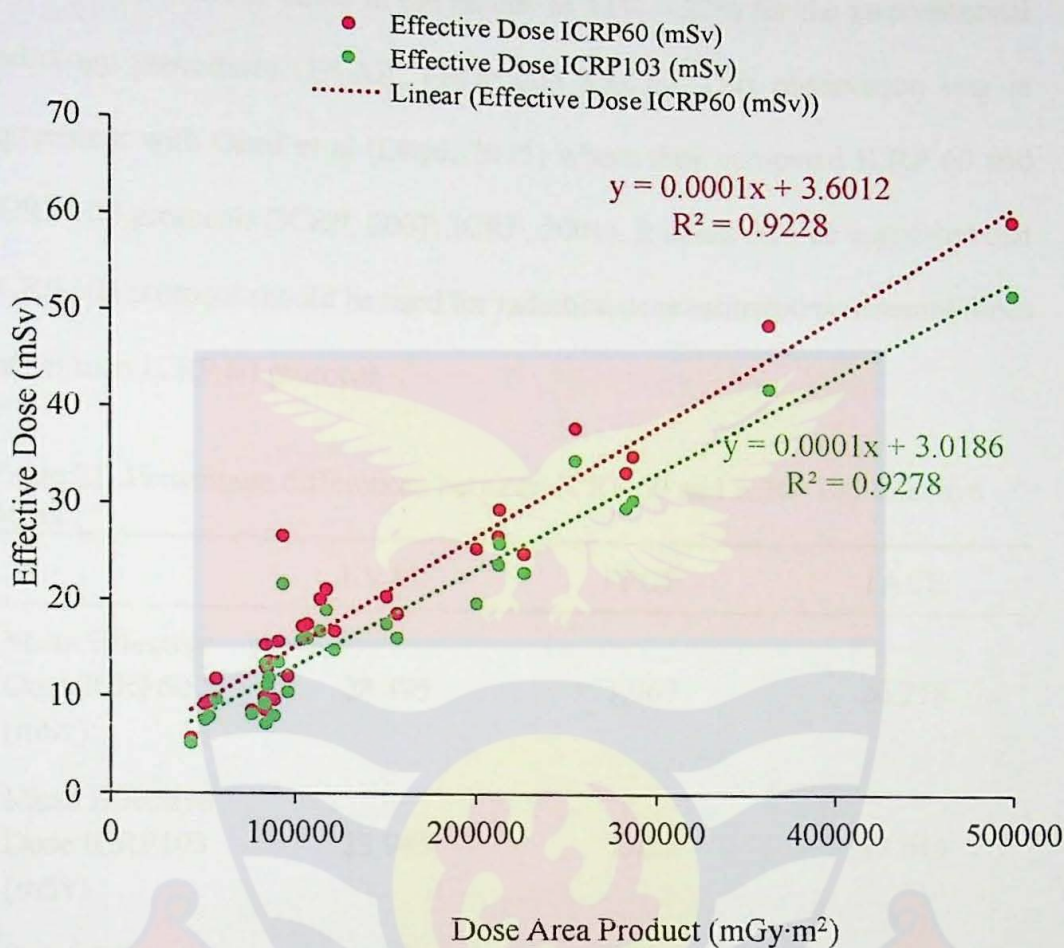


Figure 20: Relationship between DAP and ED for TACE procedure

### Comparison of ICRP 60 and ICRP 103 Estimated Effective Doses

Percentage differences between the estimated effective doses per ICRP 60 and ICRP 103 were analyzed for each of the procedures. The results (Table 21) revealed that ICRP 103 estimated effective doses were all lower (EVAR, 15.8 %; FPOP, 27.4 %; TACE, 13.0 %) than ICRP 60. This is a consequence of the changes in radiation weighting factors ( $W_R$ ) and tissue weighting factors ( $W_T$ ) as recommended by ICRP 103 in 2007. Based on recommendations by ICRP 103 that some tissues and organs may not be as radiosensitive as predicted by ICRP 60, it was seen that by the latter for dose estimations, there is seen to

be overestimation of doses in the ranges of 13% – 27% for the interventional radiology procedures (EVAR, FPOP and TACE). This observation was in agreement with Obed et al (Obed, 2015) where they compared ICRP 60 and ICRP 103 protocols (ICRP, 2007; ICRP, 2001). It could then be suggested that ICRP 103 protocol should be used for radiation dose estimations in recent times rather than ICRP 60 protocol.

Table 21: Percentage differences between ICRP 60 and ICRP 103 effective doses

	EVAR	FPOP	TACE
Mean Effective Dose ICRP60 (mSv)	28.495	1.969	20.278
Mean Effective Dose ICRP103 (mSv)	23.985	1.429	17.644
Percentage Difference %	15.8	27.4	13.0

#### Summary: Chapter Four

Organ and effective doses were assessed and a mathematical relation for predicting effective dose from dose-area-product was established for each of the three interventional radiology procedures (EVAR, FPOP and TACE). The study revealed that mean effective doses for endovascular aneurysm repair, stenting of femoropopliteal and transarterial chemoembolization were 28.495, 1.969 and 20.278 mSv; 23.985, 1.429 and 17.644 mSv; respectively for ICRP 60 and ICRP 103 protocols. By comparing mean effective doses for EVAR, FPOP and TACE

between the ICRP60 and ICRP30 protocols, percentage differences of 15.8, 27.4 and 13.0% respectively were observed.

In the establishment of relationship between dose area product (DAP) and effective dose (ED), EVAR produced the equations:

$$ED_{ICRP60}(\text{mSv}) = 0.0001 \times DAP(\text{mGy} \cdot \text{cm}^2) - 2.8858$$

$$ED_{ICRP103}(\text{mSv}) = 0.0001 \times DAP(\text{mGy} \cdot \text{cm}^2) - 2.4254$$

FPOP produced the equations:

$$ED_{ICRP60}(\text{mSv}) = 0.0001 \times DAP(\text{mGy} \cdot \text{cm}^2) - 0.4983$$

$$ED_{ICRP103}(\text{mSv}) = 0.00009 \times DAP(\text{mGy} \cdot \text{cm}^2) - 0.3381$$

TACE produced the equations:

$$ED_{ICRP60}(\text{mSv}) = 0.0001 \times DAP(\text{mGy} \cdot \text{cm}^2) - 0.4983$$

$$ED_{ICRP103}(\text{mSv}) = 0.00009 \times DAP(\text{mGy} \cdot \text{cm}^2) - 0.3381$$

## CHAPTER FIVE

### SUMMARY, CONCLUSIONS AND RECOMMENDATIONS

#### Summary

Interventional radiology procedures result in high radiation dose delivery to the body organs of patients due to extended periods of exposure to X-rays. This is often seen as drawback for the treatment technique and hence a need to evaluate the organ and effective doses associated with these procedures. The objective of this study was to assess organ and effective doses of patients from the selected interventional radiology procedures and propose effective dose prediction strategies as one of the means ensuring patient safety. This objective was achieved by surveying dose area product (DAP) and peak skin doses (PSD) for EVAR, TACE and FPOP procedures. Organ and effective doses to patients receiving the procedures were assessed. Also, the relationship between DAP and ED was established as a means of predicting the ED prior to performance of the interventional radiology procedures. The effective dose estimates using ICRP 60 and ICRP 103 protocols were then compared.

Scan data on patients undergoing EVAR, FPOP and TACE interventional procedures were retrieved from the database of the University of Crete Hospital and the data used as input parameters for simulation with a Monte Carlo PCXMC program. Anthropomorphic phantom was used to simulate a real patient procedure as a means of validating the results. Calibrated TLDs were used for the phantom measurements.

Estimation of organ and effective doses in the EVAR, FPOP and TACE procedures were performed with Monte Carlo software, using input parameters of X-ray tube voltage, filtration, beam width, beam height, focus-skin distance, projection, beam angle and DAP values received from the fluoroscopy procedures. By simulating every single exposure for each patient, the estimation of organ and effective doses were made. Effective dose (the radiation dose parameter associated with risk of stochastic effects) and peak skin dose (the radiation dose parameter that provides a good indicator of the potential for deterministic injury) were estimated.

Conditions upon which EVAR procedures were performed on 28 patients were Type I – Type IV endoleaks. The results of the study indicated that the highest individual organ dose recorded in all the EVAR procedures performed was 979.485 mGy to the kidneys. Five organs receiving the highest doses in EVAR procedures were kidneys, bone marrow, small intestine, skeleton and adrenals with average dose estimates of 225.732, 69.744, 65.341, 58.218 and 58.166 mGy respectively. The ICRP 103 protocol estimated mean effective dose 15.83% less compared with ICRP 60 protocol for this procedure.

With FPOP, conditions under which the interventional procedures were performed on 41 patients were Type I and II popliteal aneurysms with varying degrees of complications. The highest individual organ dose of 140.639 mGy was recorded by patient KV in the ovaries in this procedure. The patient had type II multi spread popliteal aneurysm with thrombosis and limb-threatening ischemia. The study identified the ovaries, uterus, skeleton, bone marrow and

prostate as the five organs receiving the most doses in FPOP procedures with average estimates of 6.456, 6.305, 4.195, 3.844 and 3.295 mGy respectively. Average effective dose for the FPOP procedures for ICRP 60 and ICRP 103 protocols were estimated as 1.969 and 1.429 mSv respectively, translating into 26.4% less dose estimated with ICRP 103 compared with ICRP 60.

The TACE interventional procedures were performed on 30 patients with varying conditions of stage II, Stage III-A, Stage III-B, Stage IV-A and Stage IV-B hepatic cancers. The highest individual organ dose recorded was 451.938 mGy to the kidneys of a patient who had terminal stage liver cancer with multiple spread. From the simulated results, five organs receiving the highest doses in TACE procedures were kidneys (197.197 mGy), adrenals (153.274 mGy), liver (125.980 mGy), gall bladder (46.600 mGy) and skeleton (26.557 mGy).

The established relationships between the dose area product (DAP) and the effective doses (ED) for the interventional radiology procedures (i.e. EVAR, FPOP and TACE) are presented below.

Endovascular Aortic Aneurysm Repair:

$$ED_{ICRP60}(\text{mSv}) = 0.0001 \times DAP(\text{mGy} \cdot \text{cm}^2) - 2.8858$$

$$ED_{ICRP103}(\text{mSv}) = 0.0001 \times DAP(\text{mGy} \cdot \text{cm}^2) - 2.4254$$

Stenting of Femoropopliteal:

$$ED_{ICRP60}(\text{mSv}) = 0.0001 \times DAP(\text{mGy} \cdot \text{cm}^2) - 0.4983$$

$$ED_{ICRP103}(\text{mSv}) = 0.00009 \times DAP(\text{mGy} \cdot \text{cm}^2) - 0.3381$$

Transarterial Chemoembolization:

$$ED_{ICRP60}(\text{mSv}) = 0.0001 \times DAP(\text{mGy} \cdot \text{cm}^2) - 0.4983$$

$$ED_{ICRP103}(\text{mSv}) = 0.00009 \times DAP(\text{mGy} \cdot \text{cm}^2) - 0.3381$$

## Conclusions

Assessment of radiation doses in interventional radiology procedures is incredibly important due to the potential harm they could pose if the risk outweighs the benefits. The study has successfully assessed patient organ and effective doses from EVAR, FPOP and TACE procedures. For EVAR procedure, three radiosensitive organs that received the most radiation were kidneys, bone marrow and small intestine with mean doses of 225.732 ( $\pm 205.687$ ) mGy, 69.744 ( $\pm 106.775$ ) mGy and 65.341 ( $\pm 100.848$ ) mGy respectively. For FPOP procedure, three of the organs receiving the most dose were ovaries, uterus and the skeleton with mean doses of 6.456 ( $\pm 22.822$ ) mGy, 6.305 ( $\pm 22.711$ ) mGy and 4.195 ( $\pm 9.950$ ) mGy respectively. The organs receiving the most doses in TACE procedures were kidneys, adrenals and liver with mean doses of 197.197 ( $\pm 112.857$ ) mGy, 153.274 ( $\pm 103.105$ ) mGy and 125.980 ( $\pm 101.437$ ) mGy. The large deviations observed were due to the dispersed nature of the radiation dose distribution.

The study has proposed a straight-forward and simple approach for estimating mean effective dose from dose-area-product (DAP). The study has established mathematical equations for estimating (predicting) the effective doses associated with patients undergoing EVAR, FPOP and TACE procedures,

if only the DAP value associated with the radiological procedure is known or provided by the fluoroscopy unit. This is a departure from the ordinary laborious way of estimating effective doses. This would serve as one radiation protection tool for determining effective doses even before the procedure is performed on patients.

Also, the study has made comparisons of effective dose estimates between ICRP 60 and ICRP 103 dose evaluation protocols for the three interventional radiology procedures. It has been proven from the studies that ICRP 60 protocol overestimated effective doses by between 13 – 27% comparative to ICRP 103 protocol. This was associated with the changes in tissue and radiation weighting factors. From the study, percentage differences between estimated effective doses for EVAR, FPOP and TACE, per the two protocols were 15.8, 24.7 and 13.0% respectively.

## **Recommendations**

To staff of interventional radiology centers

- The derived mathematical equation could be adopted and used as predictor tool to estimate effective doses of patients even before the interventional radiology procedure is undertaken.
- In assessment of radiation doses in interventional radiology procedures, ICRP 103 protocol should be used rather than ICRP 60 protocol.

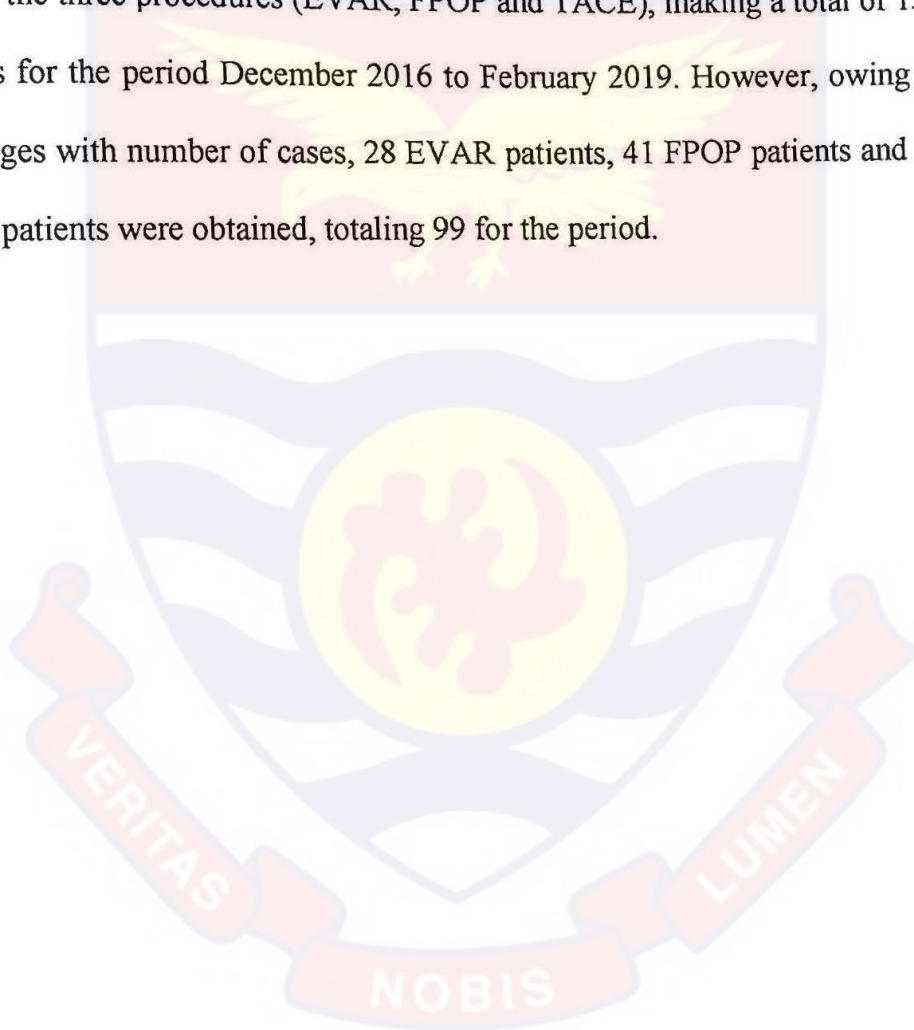
To the Research Community

- Further study could be undertaken to analyze the effect of radiation exposure time and angulation to the absorbed dose and effective dose.

- Other dose evaluation tools could also be used and findings compared with the Monte Carlo (PCXMC) software version 2.1.0.4.

## Limitations

At the conception stage, the study was planned to have 50 patients for each of the three procedures (EVAR, FPOP and TACE), making a total of 150 patients for the period December 2016 to February 2019. However, owing to challenges with number of cases, 28 EVAR patients, 41 FPOP patients and 30 TACE patients were obtained, totaling 99 for the period.



## REFERENCES

- Administration FaD (1995). *Recording information in the patient's medical record that identifies the potential for serious X-ray induced skin injuries*. Center for Devices and Radiological Health, Rockville MD, Center for Devices and Radiological Health, Rockville MD
- Badger S. A., Jones C., Boyd C. S. & Soong C.V. (2010). *Determinants of radiation exposure during EVAR*. *Eur J Vasc Endovasc Surg* 40:320–325.
- Bartal G., Vano E., Paulo G. & Miller D. (2013). *Management of Patient and Staff Radiation Dose in Interventional Radiology: Current Concepts*. *Cardiovascular and Interventional Radiology*.;37(2):289-298.
- Camphausen K. A. & Lawrence R. C. (2008). *Principles of Radiation Therapy, in Pazdur R, Wagman L.D, Camphausen K.A, Hoskins W.J. (Eds). Cancer Management: A Multidisciplinary Approach*. (11<sup>th</sup> ed.).
- Castleman E. & Tobis J. (1985). *Digital Subtraction Angiography*. *Chest*.; 87(2):253-255.
- European Commission. *Guidance on diagnostic reference levels for medical exposures; Radiation protection 109 (1999)*. Office for Official Publications of the European Communities, Luxembourg.
- Dance D., Christofides S., Maidment A. & McLean I. Ng K. (2014). *Diagnostic Radiology Physics: A Handbook for Teachers and Students*. Vienna: International Atomic Energy Agency;183-205.
- Duncan J., Balter S., Becker G., Brady J., Brink J., Bulas D et al. (2011). *Optimizing Radiation Use During Fluoroscopic Procedures:*

- Proceedings from a Multidisciplinary Consensus Panel. *Journal of Vascular and Interventional Radiology*;22(4):425-429.
- El-Serag H. B. (2012). *Epidemiology of viral hepatitis and hepatocellular carcinoma*. AGA Institute. *Gastroenterology*, 142, 1264–1273.
- Faulkner K. (2001). *Dose Display and Record Keeping*. *Radiat. Prot. Dosim.* 94, 105-114.
- Finch A. (2001). *Assurance of quality in the diagnostic image department*. Prepared by quality assurance working group of the radiation protection committee of the British Institute of Radiology (2<sup>nd</sup> ed.) p, p.55.
- Foerth M., Seidenbusch M. C., Sadeghi-Azandaryani M., Lechel U., Treitl K. M. & Treitl M. (2015). *Typical exposure parameters, organ doses and effective doses for endovascular aortic aneurysm repair: Comparison of Monte Carlo simulations and direct measurements with an anthropomorphic phantom*. *Eur Radiol.*;25 (9):2617–26
- Food and Drugs Administration. Fluoroscopy (2014). Retrieved January 31, 2016, from: <http://www.fda.gov/RadiationEmittingProducts/RadiationEmittingProductsandProcedures/MedicalImaging/MedicalXRays/ucm115354.html>
- Fossaceca R., Brambilla M., Guzzardi G., Cerini P., Renghi A., Valzano S., Brustia P. & Carriero A. (2012). *The impact of radiological equipment on patient radiation exposure during endovascular aortic aneurysm repair*. *Eur Radiol* 22:2424–2431.
- Geijer H., Larzon T., Popek R., Beckman K.W. (2005). *Radiation exposure in stent-grafting of abdominal aortic aneurysms*. *Br J Radiol* 78:906–912.

- Gingold E. & Jefferson T. (n.d.). *Modern Fluoroscopy Imaging Systems*. Retrieved April 28, 2019, from <https://www.imagewisely.org/imaging-modalities/fluoroscopy/modern-imaging-systems/>
- Greenhalgh R. (2004). *Comparison of Endovascular Aneurysm Repair with Open Repair in Patients with Abdominal Aortic Aneurysm (EVAR trial 1), 30-day Operative Mortality Results: Randomised Controlled Trial*. *The Lancet*, 364(9437):843-848.
- Guan Y. S. (2012). *Transcatheter Arterial Chemoembolization: History for More than 30 Years*. *ISRN Gastroenterology*, vol. 2012, Article ID 480650, 8 pages.
- Hidajat N., Wust P. & Felix R. (2006). *Schroder RJ. Radiation Exposure to Patient and Staff in Hepatic Chemoembolization: Risk Estimation of Cancer and Deterministic Effects*. *Cardiovasc Intervent Radiol* 29:791–796.
- Hirshfeld J.W. Jr., Balter S., Brinker J.A., Kern M.J., Klein L.W., Lindsay B.D., et al. (2005). *ACCF/AHA/HRS/SCAI clinical competence statement on physician knowledge to optimize patient safety and image quality in fluoroscopically guided invasive cardiovascular procedures: a report of the American College of Cardiology Foundation/American Heart Association/American College of Physicians Task Force on Clinical Competence and Training* *Circulation*, 111 (4), pp. 511-532.
- Horikawa M. (2015). *Development of Conventional Transarterial Chemoembolization for Hepatocellular Carcinomas in Japan*:

*Historical, Strategic, and Technical Review.* AJR, Vascular and Interventional Radiology • Review, 205, 764–773.

Howells P., Eaton R., Patel A., Taylor P. & Modarai B. (2012). Risk of Radiation Exposure during Endovascular Aortic Repair. *European Journal of Vascular and Endovascular Surgery*;43(4):393-397.

International Commission on Radiological Protection (2001). *Avoidance of Radiation Injuries from Medical Interventional Procedures.* ICRP Publication 85, Ann. ICRP 30 (2).

International Commission on Radiological Protection (1991). 1990 *Recommendations of the International Commission on Radiological Protection.* ICRP Publication 60. Ann. ICRP 21 (1 - 3).

International Commission on Radiological Protection (2007). *The 2007 Recommendations of the International Commission on Radiological Protection.* ICRP Publication 103, Ann. ICRP 37 (2-4).

International Atomic Energy Agency Tech. Rep. (2007). *Dosimetry in diagnostic radiology: an interventional code of practice,* Technical Report Series No 457 (IAEA) pp: 20-25. IAEA, Vienna.

International Electrotechnical Commission IEC (2000). *Particular Requirements for Safety of x-Ray Equipment for interventional Procedures. Medical Electrical Equipment* (Geneva: IEC) International Standards 60601-2-43. Part 2-43:).

*Interventional Radiology* (n.d.). Retrieved September 14, 2018, from: [https://en.wikipedia.org/wiki/Interventional\\_radiology](https://en.wikipedia.org/wiki/Interventional_radiology)

- Kim J. H., Won H. J., Shin Y. M. et al. (2011). *Medium-sized (3.1–5.0 cm) hepatocellular carcinoma: transarterial chemoembolization plus radiofrequency ablation versus radiofrequency ablation alone*, *Annals of Surgical Oncology*, vol. 18, no. 6, pp. 1624–1629,.
- Jackson, R. (2012). *Comparison of Long-term Survival After Open vs Endovascular Repair of Intact Abdominal Aortic Aneurysm Among Medicare Beneficiaries*. *JAMA*. 307 (15): 1621–8.
- Jia Z Tu J., Cao C., Wang W., Zhou W. et. Al. (2018). *Liver abscess following transarterial chemoembolization for the treatment of hepatocellular carcinoma: A retrospective analysis of 23 cases*. *Journal of Cancer Research and Therapeutics*. vol: 14 (10) pp: 628
- John Hopkins medicine* (n.d.). Retrieved December 10, 2018, from [https://www.hopkinsmedicine.org/interventional-radiology/what\\_is\\_IR.html](https://www.hopkinsmedicine.org/interventional-radiology/what_is_IR.html).
- Jones A. K., and Pasciak A. S. (2011). *Calculating the peak skin dose resulting from fluoroscopically guided interventions. Part I: Methods*. *J Appl Clin Med Phys*. 12(4): 231–244.
- Jones A. K. and Pasciak A. S. (2012). *Calculating the peak skin dose resulting from fluoroscopically-guided interventions. Part II: Case studies*. *J Appl Clin Med Phys*. 13(1): 174–186.
- Jones C., Badger S. A., Boyd C. S., Soong C. V. (2010). *The impact of radiation dose exposure during endovascular aneurysm repair on patient safety*. *J Vasc Surg* 52:298–302.

- Kalef-Ezra J. A., Karavasilis S., Ziogas D., Dristiliaris D., Michalis L. K., Matsagas M. (2009). *Radiation burden of patients undergoing endovascular abdominal aortic aneurysm repair*. *J Vasc Surg* 49:283–287.
- Kern M. (2011) *Angiographic Projections Made Simple: An Easy Guide to Understanding Oblique Views* (1<sup>st</sup> ed.). Retrieved April 21, 2019, from <http://www.cathlabdigest.com/files/KernAugust11.pdf>
- Khoury H. J. (2015). *Radiation Exposure to Patients and Medical Staff in Hepatic Chemoembolisation Interventional Procedures in Recife, Brazil*. *Radiation Protection Dosimetry*, 1-5.
- Klein L.W., Miller D.L., Balter S., Laskey W., Haines D., Norbash A., et al. (2009). *Occupational health hazards in the interventional laboratory: time for a safer environment*. *J Vasc Interv Radiol*, 20 (7 Suppl) pp. S278-S283.
- Koutouzi G., Henrikson O., Roos H., Zachrisson K. & Falkenberg M. (2015); *EVAR Guided by 3D Image Fusion and CO<sub>2</sub> DSA: A New Imaging Combination for Patients With Renal Insufficiency*. *Journal of Endovascular Therapy*. 22(6):912-917.
- Landberg T., Almond P., Burgers J. M. V., Busch M., Joslin C. A., Paunier J. P., ICRU Reports, *Journal of the International Commission on Radiation Units and Measurements*, Volume 0515, Issue 2, 1 April 1978, Pages 19–20, <https://doi.org/10.1093/jicru/os15.2.19s>

- Locham S., Rizwan M., Dakour-Aridi H., Faateh M., Nejim B. & Malas M. (n.d.) (2018). *Outcomes after elective abdominal aortic aneurysm repair in obese versus nonobese patients.*
- Martin C. & Sutton D. (2002). *Practical Radiation Protection in Healthcare.* Oxford: Oxford University Press; 258-285.
- Medical University of South Carolina (n.d.). Retrieved December 9, (2018), from <http://academicdepartments.musc.edu/radiology/divisions/interventional/patient.html>
- McParland BJ. Dec. (1998). Entrance skin dose estimates derived from dose-area product measurements in interventional radiological procedures. *Br J Radiol.* ;71(852):1288-95. doi: 10.1259/bjr.71.852.10319003.
- Miller D., Balter .S, Cole P., Lu H., Schueler B., Geisinger M. et al. (2003a). *Radiation Doses in Interventional Radiology Procedures: The RAD-IR Study Part I: Overall Measures of Dose.* *Journal of Vascular and Interventional Radiology.* 14(6):711-727.
- Miller D., Vaño E., Bartal G., Balter S., Dixon R., Padovani R. et al. (2010). *Occupational Radiation Protection in Interventional Radiology: A Joint Guideline of the Cardiovascular and Interventional Radiology Society of Europe and the Society of Interventional Radiology.* *Journal of Vascular and Interventional Radiology.* 21(5):607-615.
- Miller D. L., Balter S., Cole P. E., Lu H. T., Berenstein A., Albert R. et al. (2003b). *Radiation doses in interventional radiology procedures: the*

- RAD-IR study: part II: skin dose.* J Vasc Interv Radiol, 14 (8) pp. 977-990.
- Mohapatra A., Greenberg R. K., Mastracci T. M., Eagleton M. G. & Thomsberry B. (2013). *Radiation exposure to operating room personnel and patients during endovascular procedures.* J Vasc Surg 58:702–709.
- Molyvda-Athanasopoulou E., Karlatira M., Gotzamani-Psarrakou A., Koulouris C. & Siountas A. (2011). *Radiation exposure to patients and radiologists during interventional procedures.* Radiat Prot Dosim 147:86–89.
- National Research Council of the National Academies (2006). *Health Risks from Exposure to Low Levels of Ionizing Radiation: BEIR VII Phase 2.* Washington, DC: National Academies Press.
- Neil S., Padgham C. & Martin C. J. (n.d.). A study of the relationship between peak skin dose and cumulative air kerma in interventional neuroradiology and cardiology. *Journal of Radiological Protection* 30(4):659-72. DOI: [10.1088/0952-4746/30/4/002](https://doi.org/10.1088/0952-4746/30/4/002).
- Obed R. I., Ogbole G. I. & Majolagbe B. (2016). *Comparison of the ICRP 60 and ICRP 103 Recommendations on the Determination of the Effective Dose from Abdominopelvic Computed Tomography.* Int Journ of Med Phys, Clin Eng and Rad Onc. 04(02):172-176.
- Oliveira N., Gonçalves F., Hoeks S., Josee van Rijn M., Ultee K. et. al. (2018). *Long-term outcomes of standard endovascular aneurysm repair in patients with severe neck angulation.* Journal of Vascular Surgery vol: 68 (6) pp: 1725-173.

Pantos, I., Patatoukas, G., Katritsis, D. & Efstathopoulos, E. (2009); *Patient Radiation Doses in Interventional Cardiology Procedures*. Current Cardiology Reviews. 5(1):1-11.

Percutaneous Coronary Intervention (n.d.). Retrieved October 16, 2018 from [https://en.wikipedia.org/wiki/Percutaneous\\_coronary\\_intervention](https://en.wikipedia.org/wiki/Percutaneous_coronary_intervention)

Radiology Key. Retrieved December 05, 2020 from <https://radiologykey.com/>.

Rehani M., Ciraj-Bjelac O., Vaňo E., Miller D., Walsh S., Giordano B. et. al. (2010); *Radiological Protection in Fluoroscopically Guided Procedures Performed Outside the Imaging Department*. Annals of the ICRP. 40(6):1-102.

Rexius H. (2013); *Endovaskulär kirurgi - Kärl-Thorax, Sahlgrenska Universitetssjukhuset*.

Secemsky E. & Armstrong E. (2018). *Femoropopliteal Stent Implantation*. Circulation: Cardiovascular Interventions. vol: 11 (8) pp: e007134.

Shammas N. W. & Banerjee S. (2015). *Should we routinely stent the femoropopliteal Artery? An interventionalist's perspective*. J Invasive Cardiol. 27(11):E258-61.

Stecker M. S., Balter S., Towbin R. B., Miller D. L., Vano, G. E., Bartal et al. (2009), *Guidelines for patient radiation dose management* J Vasc Interv Radiol, 20 (7 Suppl), pp. S263-S273.

Strauss K. S. (2006). *The ALARA (As Low As Reasonably Achievable) Concept in Pediatric Interventional and Fluoroscopic Imaging: Striving to Keep Radiation Doses as Low as Possible During Fluoroscopy of Pediatric*

*Patients—a White Paper Executive Summary*. Paediatric Radiology 36(S2):110-112.

Swedish Radiation Safety Authority (2008). Retrieved November 20, 2018, from:

<http://www.stralsakerhetsmyndigheten.se/Global/Publikationer/Forfattning/SSMFS/2008/SSMFS2008-20.pdf>

Thakor A. S., Winterbottom A., Mercuri M., Cousins C., Gaunt M. E. (2011).

*The radiation burden from increasingly complex endovascular aortic aneurysm repair*. Insights Imaging 2:699–704.

Qi L, Tang L.J, Xu Y, Zhu X.M, Zhang Y.D, Shi H.B, Yu R.B. (2016). The

Diagnostic Performance of Coronary CT Angiography for the Assessment of Coronary Stenosis in Calcified Plaque. <https://doi.org/10.1371/journal.pone.0154852>

Wah T. M. (2017). *Image-guided ablation of renal cell carcinoma*. *Clinical radiology*. Elsevier BV. 72 (8): 636–644. doi:10.1016/j.crad.2017.03.007. ISSN 0009-9260. PMID 28527529.

Walsh C., O’Callaghan A., Moore D. et al. (2012). *Measurement and optimization of patient radiation doses in endovascular aneurysm repair*. *Eur J Vasc Endovasc Surg* 43:534–539.

Wang W., Shi J. & Xie W. F. (2010). *Transarterial chemoembolization in combination with percutaneous ablation therapy in unresectable hepatocellular carcinoma: a meta-analysis*, *Liver International*, vol. 30, no. 5, pp. 741–749.

Weerakkody R. A., Walsh R., Cousins C., Goldstone K. E., Tang T. Y. & Gaunt M. E. (2008). *Radiation exposure during endovascular aneurysm repair*. *Br J Surg* 95:699–702

Wikipedia. <https://en.wikipedia.org/wiki/Angiography>. December 10, 2018.

Wikipedia. [https://en.wikipedia.org/wiki/Interventional\\_radiology](https://en.wikipedia.org/wiki/Interventional_radiology). December 10, 2018.



# APPENDIX A: Ethical clearance obtained from University of Crete



## OFFICIAL TRANSLATION FROM THE GREEK LANGUAGE

MINISTRY OF HEALTH  
7<sup>TH</sup> SANITARY REGION OF CRETE  
UNIVERSITY GENERAL HOSPITAL OF HERAKLION "VENIZELIO"

### SCIENTIFIC COUNCIL

Heraklion, 25.04.2018  
Prot. No. 3650

CHAIRMAN  
Karanthas Apostolos  
Professor  
Director of Medical  
Depiction Laboratory

TO: Dir. of Medical Service  
Prof. G. Velegrakis  
Cc Administrator of University Hospital PaGNI  
Prof. Mr. I. Damilakis  
Non-medical Scientist Mrs C. Engmann.

REGULAR MEMBERS  
1-1

SECRETARIAL  
Maria Benetou  
Tel. 1-1

Subject: Approval of the scientific protocol to be carried out in the Laboratory of Medical Physics of the PaGNI in the framework of a doctoral dissertation of the non-medical scientist Mrs C. Engmann.

The S.C. at its meeting on 25.04.2018 after having taken into consideration the letter of Prof. I. Damilakis and of the non-medical scientist Mrs C. Engmann with the prot. No. 3650/15.03.2018, the favourable recommendation of the working group of the Ethics and Deontology Committee, as well as the attached documents, recommends the Board of Administration to approve the research protocol with the title "Study on occupational exposure and patient exposure to radiation in fluoroscopically guided interventions" that will be carried out at the Laboratory of Medical Physics of our hospital within the framework of the doctoral dissertation of the non-medical scientist Mrs C. Engmann.

The recommendation of the S.C. does not hold the place of a resolution and under no circumstances must be used as such.

For the Scientific Council  
/signature/  
Prof. Georgios Mpriasoulis

True and certified translation in accordance with the P.D.  
169/17.06.2002.  
Heraklion, 22.04.2019  
The Translator  
Member of PEEMPIP-FIT  
Member of BDU-FIT

DECISION NO. 121/05  
CORFU FIRST INSTANCE COURT

Georgia Tsikalidilaki-Hasiaki  
Certified Translator  
Ionian University Graduate  
7, Zografou Street, 4th floor  
GR 712 01 Heraklion  
Tel: 30 2810 288032 Fax: 30 2810 285846

APPENDIX B: Ethical approval obtained from University of Cape Coast

UNIVERSITY OF CAPE COAST

INSTITUTIONAL REVIEW BOARD SECRETARIAT

TEL: 0558091443 / 0568878309 / 0244207014

E-MAIL: [irba@ucc.edu.gh](mailto:irba@ucc.edu.gh)

OUR REF: UCC/IRB/A/2016/661

YOUR REF:

OMB NO: 0990-0279

IORG #: IORG0009096



C/O Directorate of Research, Innovation and Consultancy

21<sup>ST</sup> MAY, 2020

Ms. Cynthia Kaikor Engmann  
Department of Physics  
University of Cape Coast

Dear Ms. Engmann,

**ETHICAL CLEARANCE – ID (UCCIRB/CANS/2020/01)**

The University of Cape Coast Institutional Review Board (UCCIRB) has granted Provisional Approval for the implementation of your research protocol Estimation of Radiation Doses to Internal Organs of Patients from Selected Procedures in Interventional Radiology. This approval is valid from 21<sup>st</sup> May, 2020 to 20<sup>th</sup> May, 2021. You may apply for a renewal subject to submission of all the required documents that will be prescribed by the UCCIRB.

Please note that any modification to the project must be submitted to the UCCIRB for review and approval before its implementation. You are required to submit periodic review of the protocol to the Board and a final full review to the UCCIRB on completion of the research. The UCCIRB may observe or cause to be observed procedures and records of the research during and after implementation.

You are also required to report all serious adverse events related to this study to the UCCIRB within seven days verbally and fourteen days in writing.

Always quote the protocol identification number in all future correspondence with us in relation to this protocol.

Yours faithfully,

Samuel Asiedu Owusu, PhD

UCCIRB Administrator  
-----  
ADMINISTRATOR  
INSTITUTIONAL REVIEW BOARD  
UNIVERSITY OF CAPE COAST

### APPENDIX C: Patients Scan and Dose Data for Endovascular Aortic Aneurysm Repair (EVAR)

Table A1: Scan and Dose data for Patient 1 in EVAR procedure

Patient ID	Exam Type	Dose Area Product (mGy·cm <sup>2</sup> )	Effective Dose ICRP 60 (mSv)	Effective Dose ICRP 103 (mSv)
VX	O	16566	1.531	1.351
	O	22689	2.109	1.663
	O	50969	3.696	2.961
	FA	17795	1.214	0.910
	FA	17540	1.192	1.112
	FA	17482	1.168	1.095
	FA	36139	2.639	2.234
	FA	17828	1.409	1.119
	FA	38260	2.884	2.382

Table A2: Scan and Dose data for Patient 2 in EVAR procedure

Patient ID	Exam Type	Dose Area Product (mGy·cm <sup>2</sup> )	Effective Dose ICRP 60 (mSv)	Effective Dose ICRP 103 (mSv)
GC	O	5026	0.955	0.924
	O	3692	0.706	0.692
	O	8231	1.389	1.210
	O	10979	1.794	1.555
	S	337	0.042	0.033
	S	312	0.037	0.032
	FA	2967	0.308	0.292
	FA	8756	0.910	0.873
	FA	4851	0.537	0.489
	FA	2789	0.297	0.235
	FA	2795	0.286	0.238
	FA	12752	1.407	1.246
	FA	9692	1.120	0.948
	FA	9867	1.083	0.879

Table A3: Scan and Dose data for Patient 3 in EVAR procedure

Patient ID	Exam Type	Dose Area Product (mGy·cm <sup>2</sup> )	Effective Dose ICRP 60 (mSv)	Effective Dose ICRP 103 (mSv)
KM	O	5291	1.226	1.189
	O	4948	1.330	1.299
	O	4538	1.236	1.074
	O	5023	1.265	1.125
	O	7633	1.426	1.151
	O	6880	2.000	1.627
	O	4953	1.233	1.024
	FA	2947	0.442	0.417
	FA	26365	3.889	3.434
	FA	2908	0.358	0.323
	FA	5865	0.700	0.559
	FA	16164	2.153	1.896
	FA	12431	1.985	1.604

Table A4: Scan and Dose data for Patient 4 in EVAR procedure

Patient ID	Exam Type	Proj. angle (°)	Dose Area Product (mGy·cm <sup>2</sup> )	Effective Dose ICRP 60 (mSv)	Effective Dose ICRP 103 (mSv)
VI	O	90	4954	1.038	0.955
	O	92	7937	1.503	1.251
	O	61	9215	1.847	1.579
	O	90	9069	1.786	1.494
	O	90	6086	1.166	0.961
	O	59	8623	1.498	1.263
	S	108	324	0.044	0.037
	S	90	613	0.071	0.065
	S	90	249	0.034	0.027
	S	59	402	0.047	0.039
	FA	90	6600	0.822	0.755
	FA	58	4076	0.571	0.544
	FA	85	3552	0.389	0.411
	FA	51	8590	1.205	1.063
	FA	78	9390	1.188	1.022
	FA	75	2653	0.324	0.268
	FA	108	2803	0.345	0.295
	FA	92	5708	0.697	0.618
	FA	92	2642	0.315	0.282
	FA	92	8291	0.990	0.901

FA	92	11113		
FA	90	2646	1.242	1.104
FA	90	6163	0.313	0.231
			0.706	0.642

Table A5: Scan and Dose data for Patient 5 in EVAR procedure

Patient ID	Exam Type	Dose Area Product (mGy·cm <sup>2</sup> )	Effective Dose ICRP 60 (mSv)	Effective Dose ICRP 103 (mSv)
FN	O	14864	1.654	1.576
	O	14618	1.543	1.468
	O	24111	2.470	1.998
	O	72331	6.340	5.080
	O	21530	2.165	1.750
	S	837	0.075	0.071
	S	1197	0.095	0.080
	S	646	0.047	0.037
	S	881	0.077	0.062
	FA	4623	0.437	0.414
	FA	4936	0.390	0.388
	FA	5059	0.558	0.492
	FA	7850	0.632	0.535
	FA	14716	1.181	1.011
	FA	10035	0.659	0.516
	FA	4299	0.333	0.284
	FA	5677	0.474	0.392
	FA	20276	1.479	1.255
	FA	4913	0.387	0.313
	FA	5091	0.371	0.299
FA	12701	1.090	0.974	

Table A6: Scan and Dose data for Patient 6 in EVAR procedure

Patient ID	Exam Type	Dose Area Product (mGy·cm <sup>2</sup> )	Effective Dose ICRP 60 (mSv)	Effective Dose ICRP 103 (mSv)
	O	10608	1.407	1.245
	O	22678	2.281	1.949
	O	11398	1.662	1.463
	O	11773	1.776	1.613
	O	21344	2.089	1.843
	O	16875	1.554	1.260

KE	O	23945		
	O	21667	3.037	2.520
	O	50867	2.748	2.280
	O	53126	4.209	3.476
	S	893	4.350	3.653
	FA	7684	0.064	0.053
	FA	18823	0.710	0.631
	FA	8396	2.184	1.703
	FA	8125	0.901	0.768
	FA	7711	0.775	0.742
	FA	7711	0.577	0.484
	FA	28632	2.319	1.807
	FA	33312	2.630	2.187
	FA	16477	1.315	1.039
	FA	16601	1.267	1.002
FA	64129	5.211	4.062	

Table A7: Scan and Dose data for Patient 7 in EVAR procedure

Patient ID	Exam Type	Dose Area Product (mGy·cm <sup>2</sup> )	Effective Dose ICRP 60 (mSv)	Effective Dose ICRP 103 (mSv)
SN	O	8578	1.386	1.314
	O	4553	0.821	0.753
	O	7215	1.271	1.018
	O	28315	3.865	3.253
	S	725	0.075	0.070
	S	251	0.019	0.015
	S	401	0.042	0.033
	FA	4850	0.492	0.411
	FA	3829	0.263	0.210
	FA	3912	0.316	0.256
	FA	22124	1.792	1.588

Table A8: Scan and Dose data for Patient 8 in EVAR procedure

Patient ID	Exam Type	Dose Area Product (mGy·cm <sup>2</sup> )	Effective Dose ICRP 60 (mSv)	Effective Dose ICRP 103 (mSv)
TA	O	46611	8.213	7.636
	O	90479	17.189	13.957
	O	68172	11.626	9.369
	S	1214	0.225	0.209
	S	1192	0.190	0.183
	S	4233	0.566	0.445
				121

S	2607	0.453	0.400
FA	102904	16.219	13.502
FA	103798	18.921	17.299
FA	103211	15.073	12.093
FA	102683	19.313	17.041

Table A9: Scan and Dose data for Patient 9 in EVAR procedure

Patient ID	Exam Type	Dose Area Product (mGy·cm <sup>2</sup> )	Effective Dose ICRP 60 (mSv)	Effective Dose ICRP 103 (mSv)
AG	O	7329	1.410	1.122
	O	4312	0.926	0.734
	O	6339	1.122	1.070
	O	11772	2.217	1.865
	O	11067	2.021	1.655
	S	330	0.040	0.034
	S	2037	0.243	0.184
	FA	4157	0.459	0.386
	FA	4060	0.497	0.364
	FA	9326	0.919	0.746
	FA	12152	1.354	1.113
	FA	8458	0.740	0.611
	FA	8554	0.740	0.590
	FA	4015	0.426	0.323
	FA	4165	0.513	0.488
	FA	4698	0.548	0.426
	FA	4462	0.772	0.633
	FA	4090	0.707	0.597
	FA	4364	0.757	0.644
	FA	3999	0.424	0.362
	FA	4545	0.675	0.587
	FA	10218	1.436	1.253
	FA	12813	2.148	1.955
	FA	8751	0.978	0.777
	FA	4062	0.463	0.366
	FA	4040	0.415	0.333
	FA	12624	1.477	1.281
	FA	14548	1.759	1.503
	FA	4007	0.447	0.364
	FA	4695	0.499	0.441

Table A10: Scan and Dose data for Patient 10 in EVAR procedure

Patient ID	Exam Type	Dose Area Product (mGy·cm <sup>2</sup> )	Effective Dose ICRP 60 (mSv)	Effective Dose ICRP 103 (mSv)
ZI	O	7153	0.660	0.582
	O	5096	0.497	0.448
	O	10703	1.233	1.029
	O	7254	0.800	0.697
	O	9815	0.922	0.784
	S	984	0.055	0.043
	S	469	0.030	0.026
	FA	14727	0.734	0.609
	FA	15016	0.842	0.672
	FA	14790	0.785	0.677
	FA	15316	0.854	0.762

Table A11: Scan and Dose data for Patient 11 in EVAR procedure

Patient ID	Exam Type	Dose Area Product (mGy·cm <sup>2</sup> )	Effective Dose ICRP 60 (mSv)	Effective Dose ICRP 103 (mSv)
VS	O	3497	0.812	0.808
	O	3709	0.940	0.821
	O	6118	1.549	1.296
	O	8318	1.428	1.143
	S	217	0.031	0.025
	S	203	0.029	0.023
	FA	3692	0.497	0.440
	FA	1523	0.234	0.198
	FA	1533	0.240	0.188
	FA	5044	0.773	0.658
	FA	7545	1.072	0.844

Table A12: Scan and Dose data for Patient 12 in EVAR procedure

Patient ID	Exam Type	Dose Area Product (mGy·cm <sup>2</sup> )	Effective Dose ICRP 60 (mSv)	Effective Dose ICRP 103 (mSv)
ZK	O	7832	1.309	1.067
	O	15149	2.444	2.064
	O	22453	3.257	2.647
	S	926	0.082	0.067
	S	577	0.044	0.035
	S	681	0.066	0.052
	S	818	0.082	0.069
	FA	7446	0.626	0.559
	FA	13764	1.213	0.993
	FA	6752	0.483	0.390
	FA	6735	0.608	0.474
	FA	29564	2.588	2.217

Table A13: Scan and Dose data for Patient 13 in EVAR procedure

Patient ID	Exam Type	Dose Area Product (mGy·cm <sup>2</sup> )	Effective Dose ICRP 60 (mSv)	Effective Dose ICRP 103 (mSv)
BT	O	4981	0.920	0.869
	O	4695	0.884	0.836
	O	5292	1.264	1.043
	O	6300	1.190	1.079
	O	6114	1.422	1.286
	O	12150	2.132	1.792
	O	3227	0.653	0.590
	O	3344	0.726	0.635
	O	3601	0.736	0.624
	S	172	0.020	0.016
	S	196	0.023	0.022
	S	295	0.042	0.034
	FA	3605	0.424	0.328
	FA	3575	0.365	0.294
	FA	3656	0.364	0.292
	FA	24841	3.023	2.551
	FA	8966	1.256	1.065
	FA	7914	0.979	0.845

Table A14: Scan and Dose data for Patient 14 in EVAR procedure

Patient ID	Exam Type	Dose Area Product (mGy·cm <sup>2</sup> )	Effective Dose ICRP 60 (mSv)	Effective Dose ICRP 103 (mSv)
FM	O	3086		
	O	2625	0.651	0.627
	O	4205	0.555	0.533
	FA	1019	0.889	0.854
	S	71	0.137	0.118
	O	1813	0.01	0.008
	O	2955	0.453	0.374
	FA	6743	0.742	0.611
	FA	1052	0.923	0.734
	FA	1051	0.152	0.123
	FA	1051	0.133	0.106
	S	238	0.033	0.027
	FA	5465	0.695	0.553
	O	4175	1.028	0.826
	O	2186	0.562	0.453
	O	3548	0.912	0.735
	S	167	0.026	0.02
O	3660	0.917	0.742	

Table A15: Scan and Dose data for Patient 15 in EVAR procedure

Patient ID	Exam Type	Dose Area Product (mGy·cm <sup>2</sup> )	Effective Dose ICRP 60 (mSv)	Effective Dose ICRP 103 (mSv)
PI	FA	5626	0.662	0.608
	O	6734	1.327	1.307
	O	7690	1.544	1.525
	O	5859	1.176	1.162
	FA	5708	0.683	0.657
	FA	4818	0.557	0.514
	S	419	0.053	0.047
	FA	4776	0.574	0.503
	S	318	0.044	0.039
	FA	19543	2.350	2.057
	FA	36002	4.366	4.029
	S	551	0.070	0.064
	O	12795	2.429	1.974
	FA	5630	0.578	0.447
	FA	6483	0.724	0.602
	FA	5365	0.719	0.650
	FA	5655	0.689	0.607
	FA	4795	0.559	0.480

FA	4806		
RM	27808	0.549	0.456
FA	4865	3.230	2.689
O	550	0.579	0.454
O	557	0.106	0.085
FA	5892	0.107	0.086
FA	14640	0.690	0.569
FA	5120	1.834	1.509
O	16202	0.591	0.468
O	28189	2.917	2.340
		5.164	4.196

Table A16: Scan and Dose data for Patient 16 in EVAR procedure

Patient ID	Exam Type	Dose Area Product (mGy·cm <sup>2</sup> )	Effective Dose ICRP 60 (mSv)	Effective Dose ICRP 103 (mSv)
SA	O	22581	3.211	2.597
	O	28466	2.769	2.206
	O	10113	1.651	1.337
	O	22214	2.188	1.756
	FA	95186	10.51	7.759
	FA	21053	2.700	2.006
	FA	18470	2.476	1.837
	FA	18349	2.481	1.836

Table A17: Scan and Dose data for Patient 17 in EVAR procedure

Patient ID	Exam Type	Dose Area Product (mGy·cm <sup>2</sup> )	Effective Dose ICRP 60 (mSv)	Effective Dose ICRP 103 (mSv)
ME	FA	2919	0.393	0.374
	FA	948	0.139	0.117
	O	5724	1.254	1.100
	O	5280	1.157	1.017
	FA	834	0.094	0.075
	FA	884	0.127	0.102
	FA	6135	0.890	0.716
	FA	4701	0.579	0.483
	O	8955	1.922	1.558
	O	7366	1.557	1.262

Table A18: Scan and Dose data for Patient 18 in EVAR procedure

Patient ID	Exam Type	Dose Area Product (mGy·cm <sup>2</sup> )	Effective Dose ICRP 60 (mSv)	Effective Dose ICRP 103 (mSv)
KK	O	6516	1.013	0.954
	O	6333	0.950	0.874
	FA	2230	0.199	0.188
	FA	2109	0.174	0.143
	O	647	0.088	0.073
	S	311	0.029	0.024
	FA	2127	0.176	0.144
	FA	2674	0.230	0.187
	FA	9110	0.810	0.662
	FA	2293	0.235	0.196
	FA	4483	0.448	0.396
	FA	9985	0.914	0.846
	O	8951	1.370	1.109
	O	17047	2.495	1.991
	FA	2602	0.260	0.217
	FA	2463	0.269	0.245
	FA	4471	0.423	0.383
	FA	2354	0.204	0.162

Table A19: Scan and Dose data for Patient 19 in EVAR procedure

Patient ID	Exam Type	Dose Area Product (mGy·cm <sup>2</sup> )	Effective Dose ICRP 60 (mSv)	Effective Dose ICRP 103 (mSv)
NA	FA	12612	0.926	0.724
	O	89673	6.632	5.430
	FA	13029	1.368	0.992
	FA	17847	1.716	1.144
	FA	13086	1.274	0.882
	FA	16711	1.505	1.039
	FA	13100	1.275	0.899
	FA	12659	3.198	2.139
	FA	39803	3.562	2.597
	FA	12927	1.001	0.779
	FA	13567	1.053	0.844
	FA	12578	0.895	0.668
	FA	15355	1.206	0.913
	FA	12674	1.081	0.867
	O	27707	2.965	2.573
	O	32355	3.603	3.103

FA	14161		
FA	40542	1.605	1.421
FA	12936	3.301	3.012
S	1173	0.913	0.725
S	1034	0.082	0.065
FA	14092	0.078	0.062
S	1058	1.027	0.814
FA	13712	0.069	0.058
FA	65337	1.232	1.082
FA	12629	7.136	5.783
FA	25878	1.336	1.004
S	1829	2.616	2.025
FA	52715	0.148	0.123
S	1513	5.430	4.478
O	37091	0.123	0.095
O	64062	3.839	3.019
O	59527	6.244	4.954
O	36109	5.802	4.603
O	41155	3.740	2.958
FA	14265	5.039	4.052
O	43688	0.918	0.771
S	1473	4.912	4.101
FA	30276	0.202	0.159
FA	29056	3.315	2.910
FA	12705	5.287	3.969
FA	15544	2.282	1.711
S	1471	1.661	1.546
FA	51212	0.113	0.088
FA	24286	5.269	4.944
FA	57179	3.089	2.813
FA	14270	6.128	5.736
FA	14226	1.969	1.397
S	7034	1.414	1.292
FA	67151	0.520	0.434
S	4146	6.388	5.252
S	1277	0.362	0.298
FA	26770	0.127	0.095
S	2017	2.464	2.168
O	46675	0.161	0.127
O	43087	5.875	4.688
FA	167506	5.048	3.934
O	41847	13.143	11.357
O	37659	4.663	3.801
O	22776	3.377	2.750
O	28223	2.084	1.697
O	29617	3.201	2.734
O	66211	4.183	3.341
		5.965	4.659

O	47754		
FA	72268	5.574	4.571
O	41835	7.163	6.032
		4.590	3.952

Table A20: Scan and Dose data for Patient 20 in EVAR procedure

Patient ID	Exam Type	Dose Area Product (mGy·cm <sup>2</sup> )	Effective Dose ICRP 60 (mSv)	Effective Dose ICRP 103 (mSv)
LG	FA	4744	0.781	0.660
	O	4863	1.162	1.113
	FA	4913	0.806	0.709
	O	10801	2.169	1.947
	FA	5013	0.840	0.740
	FA	4809	0.660	0.540
	FA	6081	0.941	0.890
	FA	4980	0.771	0.729
	FA	5128	0.700	0.558
	FA	5183	0.926	0.757
	FA	4827	0.789	0.652
	FA	4602	0.693	0.572
	S	188	0.031	0.026
	FA	15365	2.416	2.014
	FA	9372	1.411	1.171
	FA	9360	1.366	1.157
	FA	4653	0.769	0.656
	O	7942	2.143	1.771
	O	14348	3.122	2.624

Table A21: Scan and Dose data for Patient 21 in EVAR procedure

Patient ID	Exam Type	Dose Area Product (mGy·cm <sup>2</sup> )	Effective Dose ICRP 60 (mSv)	Effective Dose ICRP 103 (mSv)
KN	O	24283	2.714	2.262
	O	17176	1.934	1.648
	FA	14677	1.510	1.272
	FA	6462	0.522	0.432
	S	695	0.056	0.046
	FA	42624	3.712	3.041
			129	

FA	6535	0.611	0.494
FA	27004	2.391	2.007
FA	21371	2.108	1.791
S	1005	0.088	0.072
O	14222	1.957	1.623
O	19485	2.660	2.157

Table A22: Scan and Dose data for Patient 22 in EVAR procedure

Patient ID	Exam Type	Dose Area Product (mGy·cm <sup>2</sup> )	Effective Dose ICRP 60 (mSv)	Effective Dose ICRP 103 (mSv)
MM	O	21362	2.966	2.713
	FA	9556	0.898	0.733
	S	1320	0.127	0.104
	FA	41826	3.639	3.163
	FA	40479	4.245	3.615
	FA	21175	1.706	1.457
	O	29459	4.591	4.028
	O	51338	5.280	4.433
	S	2145	0.196	0.163

Table A23: Scan and Dose data for Patient 23 in EVAR procedure

Patient ID	Exam Type	Dose Area Product (mGy·cm <sup>2</sup> )	Effective Dose ICRP 60 (mSv)	Effective Dose ICRP 103 (mSv)
MN			0.136	0.116
	S	994	1.035	0.921
	O	4822	1.605	1.469
	O	7539	1.556	1.377
	FA	11467	0.486	0.396
	FA	4340	0.028	0.023
	S	230	0.546	0.45
	FA	4682	0.700	0.660
	FA	5307	0.575	0.489
	FA	4347	130	

FA	8976	1.089	0.904
FA	4365	0.520	0.457
S	313	0.041	0.036
FA	18319	2.344	1.924
O	9276	1.636	1.410
S	519	0.064	0.055
O	7426	1.445	1.189
S	273	0.037	0.030
O	6244	1.186	1.026

Table A24: Scan and Dose data for Patient 24 in EVAR procedure

Patient ID	Exam Type	Dose Area Product (mGy·cm <sup>2</sup> )	Effective Dose ICRP 60 (mSv)	Effective Dose ICRP 103 (mSv)
TS	O	8476	1.396	1.262
	FA	4221	0.439	0.384
	FA	4996	0.463	0.451
	FA	4207	0.389	0.374
	FA	4110	0.380	0.314
	FA	20820	1.851	1.704
	FA	17562	1.589	1.368
	FA	3965	0.357	0.294
	FA	26147	2.469	1.986
	S	773	0.078	0.065
	O	12504	1.917	1.630
	O	12428	1.906	1.620
	O	24844	2.553	2.090
	S	1597	0.134	0.108

Table A25: Scan and Dose data for Patient 25 in EVAR procedure

Patient ID	Exam Type	X-ray beam height (cm)	Dose Area Product (mGy·cm <sup>2</sup> )	Effective Dose ICRP 60 (mSv)	Effective Dose ICRP 103 (mSv)
KAK	O	21	12240	1.649	1.594
	FA	21	4987	0.531	0.504
	FA	18	5064	0.655	0.611
	FA	17	3829	0.373	0.304
	FA	17	25044	2.716	2.287
	FA	17	19862	2.063	1.721
	FA	22	9346	0.958	0.851
	FA	22	16354	1.718	1.514
	FA	22	4666	0.433	0.378
	O	22	15829	2.756	2.349
	O	22	16763	2.894	2.367

Table A26: Scan and Dose data for Patient 26 in EVAR procedure

Patient ID	Exam Type	Dose Area Product (mGy·cm <sup>2</sup> )	Effective Dose ICRP 60 (mSv)	Effective Dose ICRP 103 (mSv)
MS	O	9613	1.867	1.795
	S	3206	0.354	0.322
	O	896	0.122	0.113
	F	12007	1.327	1.206
	F	6691	0.710	0.647
	F	18689	2.565	2.223
	F	8646	0.926	0.842
	F	6731	0.754	0.668
	F	23557	3.237	2.715
	S	1258	0.173	0.145
	F	13629	1.494	1.260
	F	29883	3.236	2.613
	F	36599	4.322	3.505
	F	13832	1.358	1.230
	S	1238	0.143	0.121
	O	31006	4.395	3.895
	O	27157	3.792	3.085

Table A27: Scan and Dose data for Patient 27 in EVAR procedure

Patient ID	Exam Type	Dose Area Product (mGy·cm <sup>2</sup> )	Effective Dose ICRP 60 (mSv)	Effective Dose ICRP 103 (mSv)
CP	F	5517	0.650	0.525
	F	5789	0.846	0.699
	O	242	0.056	0.053
	S	308	0.043	0.040
	O	6632	1.231	1.155
	O	7765	1.469	1.380
	O	7701	1.457	1.369
	F	12053	1.422	1.300
	F	5531	0.662	0.622
	F	5602	0.674	0.552
	S	612	0.081	0.067
	F	5574	0.606	0.481
	S	462	0.058	0.046
	F	12810	1.619	1.468
	F	11153	1.061	0.886
	S	1255	0.174	0.139
	O	15715	3.520	2.875
	O	29377	4.428	3.595
	O	17648	4.044	3.339
	O	12104	2.596	2.160
O	10307	2.211	1.839	
O	18221	3.412	2.794	
F	30141	3.796	3.510	
O	26749	3.472	3.106	

Table A28: Scan and Dose data for Patient 28 in EVAR procedure

Patient ID	Exam Type	Dose Area Product (mGy·cm <sup>2</sup> )	Effective Dose ICRP 60 (mSv)	Effective Dose ICRP 103 (mSv)
TG	F	17027	1.762	1.592
	F	1643	0.180	0.170
	O	6253	1.243	1.204
	F	2197	0.241	0.227
	F	4432	0.451	0.413
	F	1648	0.183	0.148
	O	6943	1.320	1.092
	O	13228	1.956	1.581
	O	723	0.146	0.124
	S	425	0.051	0.043

Table B3: Scan and Dose data for Patient 3 in FPOP procedure

Patient ID	Exam Type	Dose Area Product (mGy·cm <sup>2</sup> )	Effective Dose ICRP 60 (mSv)	Effective Dose ICRP 103 (mSv)
KA	O	1406	0.129	0.095
	O	169	0.005	0.004
	O	87	0.001	0.001
	O	157	0.001	0.001
	F	356	0.002	0.001
	O	124	0.001	0.001
	F	211	0.001	0.001
	O	194	0.002	0.001
	F	195	0.001	0.001
	O	216	0.002	0.001
	F	470	0.004	0.002
	O	712	0.013	0.008
	O	228	0.003	0.002
	O	112	0.025	0.022

Table B4: Scan and Dose data for Patient 4 in FPOP procedure

Patient ID	Exam Type	Dose Area Product (mGy·cm <sup>2</sup> )	Effective Dose ICRP 60 (mSv)	Effective Dose ICRP 103 (mSv)
KS	F	614	0.005	0.003
	F	572	0.004	0.002
	F	569	0.003	0.001
	O	188	0.002	0.001
	O	64	0.001	0.000
	RM	631	0.003	0.002
	RM	585	0.003	0.002
	F	566	0.003	0.002
	F	2658	0.016	0.008
	F	1761	0.018	0.011
	O	1512	0.028	0.018
	O	118	0.001	0.001
	O	102	0.001	0.001
	O	86	0.001	0.000
	O	49	0.000	0.000
	O	286	0.002	0.001

Table B5: Scan and Dose data for Patient 5 in FPOP procedure

Patient ID	Exam Type	Dose Area Product (mGy·cm <sup>2</sup> )	Effective Dose ICRP 60 (mSv)	Effective Dose ICRP 103 (mSv)
KN	O	396	0.100	0.075
	O	143	0.009	0.005
	O	153	0.003	0.001
	O	93	0.001	0.001
	F	295	0.003	0.002
	F	135	0.001	0.001
	O	83	0.003	0.002
	O	341	0.014	0.009
	O	268	0.005	0.003
	F	216	0.005	0.003
	O	377	0.010	0.005
	O	155	0.003	0.001
	F	66	0.002	0.001
	F	83	0.001	0.001
	O	501	0.015	0.008
	O	125	0.002	0.001

Table B6: Scan and Dose data for Patient 6 in FPOP procedure

Patient ID	Exam Type	Dose Area Product (mGy·cm <sup>2</sup> )	Effective Dose ICRP 60 (mSv)	Effective Dose ICRP 103 (mSv)
KD	RM	801	0.015	0.010
	F	748	0.016	0.010
	F	2240	0.043	0.026
	F	1458	0.011	0.006
	F	791	0.013	0.008
	F	2647	0.039	0.025
	F	754	0.018	0.012
	F	3891	0.043	0.024
	F	2276	0.041	0.027
	O	798	0.032	0.021
	O	2185	0.075	0.050
	O	7641	0.379	0.267
	F	1210	0.036	0.025
	S	563	0.017	0.012
	F	914	0.026	0.017
	S	124	0.004	0.003
	O	1905	0.107	0.071

S	135		
S	281	0.004	0.003
F	725	0.012	0.008
F	795	0.006	0.003
F	3631	0.020	0.012
O	3049	0.256	0.178
O	341	0.102	0.069
F	720	0.005	0.003
F	752	0.005	0.003
F	740	0.006	0.003
O	156	0.006	0.003
O	294	0.002	0.001
O	195	0.004	0.002
O	195	0.002	0.001
O	79	0.001	0.000

Table B7: Scan and Dose data for Patient 7 in FPOP procedure

Patient ID	Exam Type	Dose Area Product (mGy·cm <sup>2</sup> )	Effective Dose ICRP 60 (mSv)	Effective Dose ICRP 103 (mSv)
BI	RM	117	0.006	0.004
	F	107	0.008	0.005
	F	208	0.002	0.001
	O	737	0.035	0.025
	O	204	0.007	0.005
	O	172	0.002	0.001
	F	535	0.030	0.020
	O	452	0.019	0.013
	O	250	0.003	0.002
	F	94	0.001	0.001
	O	268	0.010	0.007
	O	111	0.001	0.001
	S	20	0.001	0.000
	O	392	0.010	0.005
	F	164	0.001	0.001
	F	211	0.005	0.003
	O	351	0.010	0.005
	O	300	0.003	0.002

Table B8: Scan and Dose data for Patient 8 in FPOP procedure

Patient ID	Exam Type	Dose Area Product (mGy·cm <sup>2</sup> )	Effective Dose ICRP 60 (mSv)	Effective Dose ICRP 103 (mSv)
PI	F	135	0.009	0.006
	F	155	0.010	0.008
	O	1875	0.242	0.183
	O	212	0.022	0.015
	O	264	0.004	0.002
	RM	714	0.015	0.009
	O	578	0.033	0.022
	F	469	0.006	0.004
	O	362	0.023	0.015
	O	215	0.007	0.005
	O	290	0.026	0.017
	O	93	0.002	0.001
	O	117	0.001	0.001
	O	105	0.001	0.001
	F	97	0.001	0.000
	F	102	0.001	0.000
	F	235	0.002	0.001
	F	120	0.001	0.001
	F	99	0.001	0.000

Table B9: Scan and Dose data for Patient 9 in FPOP procedure

Patient ID	Exam Type	Dose Area Product (mGy·cm <sup>2</sup> )	Effective Dose ICRP 60 (mSv)	Effective Dose ICRP 103 (mSv)
PE	F	619	0.067	0.053
	F	221	0.021	0.016
	F	220	0.020	0.014
	F	228	0.002	0.001
	F	228	0.028	0.017
	F	1830	0.023	0.013
	F	1728	0.004	0.002
	F	419	0.002	0.001
	F	229	0.007	0.004
	F	469	0.007	0.017
	F	715	0.029	0.017
	F	715	0.002	0.001
	F	98	0.002	0.001
	O	98	0.001	0.000
	O	59	0.001	0.000

Table B12: Scan and Dose data for Patient 12 in FPOP procedure

Patient ID	Exam Type	Dose Area Product (mGy·cm <sup>2</sup> )	Effective Dose ICRP 60 (mSv)	Effective Dose ICRP 103 (mSv)
GM	O	582	0.073	0.053
	O	253	0.013	0.009
	O	203	0.004	0.002
	O	47	0.001	0.000
	F	792	0.006	0.003
	F	517	0.004	0.002
	F	349	0.002	0.001
	O	132	0.002	0.001
	O	42	0.000	0.000
	F	254	0.002	0.001
	O	113	0.001	0.001
	F	626	0.004	0.002
	O	273	0.005	0.003
	O	214	0.004	0.002
	O	188	0.003	0.002
	O	180	0.002	0.001
	O	46	0.001	0.000

Table B13: Scan and Dose data for Patient 13 in FPOP procedure

Patient ID	Exam Type	Dose Area Product (mGy·cm <sup>2</sup> )	Effective Dose ICRP 60 (mSv)	Effective Dose ICRP 103 (mSv)
SM	F	52	0.003	0.002
	O	273	0.045	0.033
	O	163	0.006	0.003
	O	158	0.002	0.001
	O	126	0.001	0.001
	F	264	0.002	0.001
	O	148	0.002	0.001
	RM	327	0.003	0.001
	O	96	0.002	0.001
	O	82	0.002	0.001
	F	375	0.003	0.002
	O	75	0.002	0.001
	O	42	0.001	0.000
	O	33	0.000	0.000
	O	97	0.001	0.001

Table B14: Scan and Dose data for Patient 14 in FPOP procedure

Patient ID	Exam Type	Dose Area Product (mGy·cm <sup>2</sup> )	Effective Dose ICRP 60 (mSv)	Effective Dose ICRP 103 (mSv)
II	F	389	0.026	0.017
	F	78	0.004	0.002
	O	883	0.107	0.071
	O	659	0.039	0.028
	O	104	0.002	0.001
	O	146	0.002	0.001
	O	213	0.002	0.001
	F	991	0.006	0.003
	F	1022	0.007	0.004
	F	253	0.001	0.001
	O	300	0.003	0.002
	F	94	0.001	0.000
	O	520	0.006	0.003
	F	122	0.001	0.000
	F	165	0.003	0.001
	O	362	0.015	0.009

Table B15: Scan and Dose data for Patient 15 in FPOP procedure

Patient ID	Exam Type	Dose Area Product (mGy·cm <sup>2</sup> )	Effective Dose ICRP 60 (mSv)	Effective Dose ICRP 103 (mSv)
TS	F	97	0.011	0.007
	O	647	0.136	0.091
	O	128	0.010	0.006
	O	97	0.002	0.001
	F	517	0.011	0.006
	O	655	0.155	0.099
	O	256	0.006	0.003
	F	311	0.013	0.008
	O	614	0.047	0.030
	O	210	0.014	0.007
	O	82	0.001	0.001
	O	55	0.001	0.000

Table B16: Scan and Dose data for Patient 16 in FPOP procedure

Patient ID	Exam Type	Dose Area Product (mGy·cm <sup>2</sup> )	Effective Dose ICRP 60 (mSv)	Effective Dose ICRP 103 (mSv)
VSI	O	1042	0.128	0.083
	O	144	0.003	0.002
	O	148	0.002	0.001
	O	139	0.001	0.001
	F	1367	0.019	0.010
	O	849	0.097	0.062
	O	331	0.017	0.010
	F	191	0.007	0.004
	F	190	0.002	0.001
	O	303	0.007	0.004

Table B17: Scan and Dose data for Patient 17 in FPOP procedure

Patient ID	Exam Type	Dose Area Product (mGy·cm <sup>2</sup> )	Effective Dose ICRP 60 (mSv)	Effective Dose ICRP 103 (mSv)
DE	F	344	0.022	0.014
	F	405	0.029	0.017
	F	332	0.024	0.014
	O	2144	0.201	0.135
	O	628	0.031	0.019
	O	154	0.002	0.001
	F	1876	0.093	0.056
	F	363	0.002	0.001
	F	1146	0.009	0.005
	F	1743	0.019	0.010
	F	320	0.002	0.001
	F	331	0.003	0.002

Table B18: Scan and Dose data for Patient 18 in FPOP procedure

Patient ID	Exam Type	Dose Area Product (mGy·cm <sup>2</sup> )	Effective Dose ICRP 60 (mSv)	Effective Dose ICRP 103 (mSv)
LF	F	153	0.018	0.011
	F	135	0.016	0.011
	O	1081	0.231	0.152
	O	265	0.021	0.014
	O	107	0.002	0.001
	O	148	0.001	0.001
	O	1029	0.150	0.104
	O	163	0.006	0.003
	O	97	0.002	0.001
	O	78	0.001	0.001
	F	145	0.001	0.001
	F	1036	0.027	0.016
	O	671	0.100	0.064
	O	292	0.009	0.005
	O	144	0.002	0.001
	F	274	0.005	0.003
	O	163	0.005	0.003
	O	144	0.003	0.002
	F	133	0.001	0.001
	O	114	0.002	0.001
	F	464	0.005	0.002
	O	155	0.010	0.005
	O	77	0.001	0.001
	F	446	0.030	0.021
	O	1006	0.184	0.132
	O	354	0.015	0.007
	O	133	0.002	0.001
	F	418	0.004	0.002
	O	104	0.002	0.001

Table B19: Scan and Dose data for Patient 19 in FPOP procedure

Patient ID	Exam Type	Dose Area Product (mGy·cm <sup>2</sup> )	Effective Dose ICRP 60 (mSv)	Effective Dose ICRP 103 (mSv)
KE	F	1829	0.179	0.130
	O	15622	2.267	1.652
	O	2614	0.360	0.277
	O	855	0.046	0.025
	O	159	0.003	0.001
	F	4109	0.318	0.251
	O	8848	1.037	0.824
	F	5081	0.039	0.022
	F	12856	0.102	0.056
	O	177	0.003	0.002
	S	12	0.000	0.000
	O	186	0.003	0.002
	O	174	0.003	0.002
	O	79	0.001	0.001
	O	161	0.004	0.002

Table B20: Scan and Dose data for Patient 20 in FPOP procedure

Patient ID	Exam Type	Dose Area Product (mGy·cm <sup>2</sup> )	Effective Dose ICRP 60 (mSv)	Effective Dose ICRP 103 (mSv)
VS2	F	136	0.010	0.007
	F	104	0.005	0.004
	O	397	0.048	0.033
	O	231	0.006	0.004
	O	136	0.002	0.001
	O	110	0.001	0.001
	F	393	0.013	0.008
	O	381	0.032	0.021
	F	794	0.020	0.012
	SEL	452	0.053	0.034
	SEL	226	0.003	0.002
	F	101	0.001	0.000
	SEL	113	0.003	0.001

Table B21: Scan and Dose data for Patient 21 in FPOP procedure

Patient ID	Exam Type	Dose Area Product (mGy·cm <sup>2</sup> )	Effective Dose ICRP 60 (mSv)	Effective Dose ICRP 103 (mSv)
VA	F	55	0.004	0.003
	RM	84	0.005	0.004
	F	39	0.003	0.003
	F	239	0.020	0.014
	F	501	0.031	0.023
	F	304	0.003	0.002
	F	134	0.001	0.001
	F	29	0.000	0.000
	O	113	0.002	0.001
	F	87	0.001	0.000
	O	83	0.002	0.001
	F	33	0.000	0.000
	O	83	0.001	0.001
	O	83	0.001	0.001

Table B22: Scan and Dose data for Patient 22 in FPOP procedure

Patient ID	Exam Type	Dose Area Product (mGy·cm <sup>2</sup> )	Effective Dose ICRP 60 (mSv)	Effective Dose ICRP 103 (mSv)
DG	F	242	0.019	0.013
	O	674	0.101	0.066
	O	152	0.004	0.002
	F	744	0.008	0.005
	O	612	0.059	0.039
	O	238	0.003	0.002
	F	234	0.009	0.006
	O	766	0.063	0.042
	F	318	0.003	0.002
	O	192	0.003	0.002
	F	337	0.002	0.001
	O	611	0.010	0.005
	O	206	0.003	0.002
	F	439	0.003	0.002

Table B23: Scan and Dose data for Patient 23 in FPOP procedure

Patient ID	Exam Type	Dose Area Product (mGy·cm <sup>2</sup> )	Effective Dose ICRP 60 (mSv)	Effective Dose ICRP 103 (mSv)
AD1	O	731	0.101	0.072
	O	138	0.004	0.002
	O	83	0.001	0.001
	F	513	0.009	0.005
	RM	1673	0.015	0.008
	O	666	0.027	0.015
	O	287	0.007	0.004
	O	567	0.014	0.008
	O	128	0.002	0.001
	F	976	0.008	0.004
	O	747	0.059	0.043
	O	128	0.009	0.006
	F	223	0.003	0.002
	O	108	0.004	0.003
	O	89	0.001	0.001
	O	64	0.001	0.001
	F	464	0.003	0.002
	O	77	0.001	0.001

Table B24: Scan and Dose data for Patient 24 in FPOP procedure

Patient ID	Exam Type	Dose Area Product (mGy·cm <sup>2</sup> )	Effective Dose ICRP 60 (mSv)	Effective Dose ICRP 103 (mSv)
MP	O	270	0.030	0.019
	O	131	0.003	0.002
	O	95	0.001	0.001
	F	305	0.003	0.001
	O	300	0.005	0.003
	O	139	0.003	0.002
	O	70	0.001	0.001
	F	286	0.002	0.001
	O	149	0.003	0.002
	O	72	0.001	0.001
	F	305	0.003	0.001
	O	119	0.002	0.001

Table B25: Scan and Dose data for Patient 25 in FPOP procedure

Patient ID	Exam Type	Dose Area Product (mGy·cm <sup>2</sup> )	Effective Dose ICRP 60 (mSv)	Effective Dose ICRP 103 (mSv)
FE	F	539	0.052	0.032
	F	548	0.058	0.042
	O	5009	0.894	0.739
	O	5956	0.973	0.810
	O	9688	1.332	1.098
	O	2327	0.409	0.304
	O	221	0.010	0.005
	O	121	0.002	0.001
	F	696	0.077	0.061
	RM	694	0.089	0.063
	F	578	0.140	0.084
	SIN	315	0.035	0.033
	F	2867	0.343	0.326
	F	612	0.068	0.053
	F	4159	1.054	0.681
	F	623	0.086	0.062
	F	5271	0.804	0.588
	O	4223	0.773	0.630
	F	1945	0.112	0.082
	F	608	0.060	0.043

Table B26: Scan and Dose data for Patient 26 in FPOP procedure

Patient ID	Exam Type	Dose Area Product (mGy·cm <sup>2</sup> )	Effective Dose ICRP 60 (mSv)	Effective Dose ICRP 103 (mSv)
CM	F	325	0.027	0.018
	F	310	0.032	0.023
	F	727	0.049	0.035
	F	300	0.025	0.019
	O	741	0.129	0.095
	O	225	0.012	0.008
	O	155	0.003	0.002
	O	128	0.002	0.001
	O	280	0.005	0.003
	O	452	0.013	0.007
	O	117	0.002	0.001
	O	73	0.001	0.001
	O	136	0.002	0.001
	F	288	0.002	0.001

F	276		
F	1457	0.002	0.001
O	729	0.096	0.075
O	298	0.079	0.058
RM	504	0.009	0.005
O	410	0.013	0.007
F	788	0.013	0.007
O	118	0.007	0.004
F	488	0.003	0.001
F	760	0.005	0.003
O	132	0.007	0.004
O	260	0.003	0.002
O	318	0.006	0.003
F	490	0.007	0.004
O	396	0.009	0.005
		0.024	0.017

Table B27: Scan and Dose data for Patient 27 in FPOP procedure

Patient ID	Exam Type	Dose Area Product (mGy·cm <sup>2</sup> )	Effective Dose ICRP 60 (mSv)	Effective Dose ICRP 103 (mSv)
ML	RM	3012	0.309	0.276
	F	11207	1.297	1.172
	F	1160	0.158	0.112
	F	9983	1.090	0.742
	O	512	0.106	0.073
	F	3327	0.324	0.221
	O	67	0.001	0.001
	O	80	0.001	0.001
	O	32	0.000	0.000

Table B28: Scan and Dose data for Patient 28 in FPOP procedure

Patient ID	Exam Type	Dose Area Product (mGy·cm <sup>2</sup> )	Effective Dose ICRP 60 (mSv)	Effective Dose ICRP 103 (mSv)
SG	F	293	0.006	0.004
	RM	251	0.004	0.003
	RM	253	0.005	0.003
	F	1017	0.026	0.017
	O	537	0.035	0.022
	O	304	0.005	0.003
	O	223	0.004	0.002

Table B29: Scan and Dose data for Patient 29 in FPOP procedure

Patient ID	Exam Type	Dose Area Product (mGy·cm <sup>2</sup> )	Effective Dose ICRP 60 (mSv)	Effective Dose ICRP 103 (mSv)
VE	O	119	0.011	0.007
	O	71	0.002	0.001
	F	535	0.005	0.002
	O	111	0.004	0.002
	O	90	0.002	0.001
	SIN	13	0.000	0.000
	F	185	0.001	0.001
	O	107	0.002	0.001
	SIN	11	0.000	0.000
	O	76	0.001	0.001
	O	83	0.001	0.001
	SIN	9	0.000	0.000

Table B30: Scan and Dose data for Patient 30 in FPOP procedure

Patient ID	Exam Type	Dose Area Product (mGy·cm <sup>2</sup> )	Effective Dose ICRP 60 (mSv)	Effective Dose ICRP 103 (mSv)
FV	O	18329	3.004	2.447
	O	19822	3.293	2.609
	O	2678	0.217	0.149
	O	230	0.008	0.004
	F	10837	2.339	1.420
	F	8291	1.158	0.801
	F	7885	0.926	0.664
	F	10395	0.942	0.693

Table B31: Scan and Dose data for Patient 31 in FPOP procedure

Patient ID	Exam Type	Dose Area Product (mGy·cm <sup>2</sup> )	Effective Dose ICRP 60 (mSv)	Effective Dose ICRP 103 (mSv)
CS	F	85	0.008	0.006
	O	303	0.045	0.033
	O	99	0.005	0.003
	O	163	0.003	0.002
	O	91	0.001	0.001
	RM	216	0.007	0.003
	F	376	0.009	0.006
	O	371	0.049	0.031
	O	93	0.007	0.005
				149

O	80		
F	87	0.001	0.001
O	146	0.001	0.000
		0.002	0.001

Table B32: Scan and Dose data for Patient 32 in FPOP procedure

Patient ID	Exam Type	Dose Area Product (mGy·cm <sup>2</sup> )	Effective Dose ICRP 60 (mSv)	Effective Dose ICRP 103 (mSv)
KV	F	3394	0.305	0.225
	RM	6875	0.549	0.436
	F	45446	3.917	2.866
	O	13677	2.497	2.013
	O	12624	1.717	1.386
	F	8871	0.899	0.653
	F	11401	1.387	0.956
	F	40057	6.565	4.384
	F	7689	1.093	0.782
	F	3652	0.371	0.306
	F	26216	3.628	2.299
	F	3364	0.505	0.374
	F	6615	0.676	0.456
	F	6667	1.269	0.722
	F	3836	0.507	0.365
	F	14481	1.777	1.339
	F	15488	2.206	1.353
	F	3525	0.352	0.265
	F	3966	0.527	0.376
	F	3938	0.512	0.342
	O	16682	2.493	1.925
	F	3551	0.296	0.215
	F	3316	0.166	0.122
	O	5605	0.352	0.251
	F	7801	0.408	0.290
	O	14480	2.307	1.852
	O	2779	0.137	0.094

Table B33: Scan and Dose data for Patient 33 in FPOP procedure

Patient ID	Exam Type	Dose Area Product (mGy·cm <sup>2</sup> )	Effective Dose ICRP 60 (mSv)	Effective Dose ICRP 103 (mSv)
SA	F	692	0.059	0.046
	O	598	0.055	0.038
	O	234	0.011	0.006
	F	1798	0.016	0.009

Table B34: Scan and Dose data for Patient 34 in FPOP procedure

Patient ID	Exam Type	Dose Area Product (mGy·cm <sup>2</sup> )	Effective Dose ICRP 60 (mSv)	Effective Dose ICRP 103 (mSv)
FG	F	216	0.016	0.012
	O	1063	0.031	0.018
	O	298	0.004	0.002
	O	340	0.004	0.002
	F	483	0.003	0.002
	O	286	0.011	0.006
	F	213	0.001	0.001
	O	584	0.013	0.007
	O	347	0.004	0.002
	O	180	0.002	0.001
	O	57	0.001	0.000

Table B35: Scan and Dose data for Patient 35 in FPOP procedure

Patient ID	Exam Type	Dose Area Product (mGy·cm <sup>2</sup> )	Effective Dose ICRP 60 (mSv)	Effective Dose ICRP 103 (mSv)
MG	F	156	0.012	0.008
	O	775	0.097	0.068
	O	125	0.006	0.003
	O	36	0.001	0.000
	O	50	0.001	0.000
	F	1059	0.016	0.009
	O	367	0.023	0.015
	O	173	0.008	0.005
	F	624	0.009	0.005
	O	74	0.001	0.001
	F	141	0.001	0.001
	F	1169	0.013	0.007
	O	80	0.001	0.001
	O	38	0.001	0.000
	F	307	0.002	0.001
	F	136	0.001	0.001
	RM	144	0.001	0.001
	F	135	0.001	0.001
	O	62	0.001	0.000
	O	44	0.001	0.000
O	53	0.001	0.000	

Table B36: Scan and Dose data for Patient 36 in FPOP procedure

Patient ID	Exam Type	Dose Area Product (mGy·cm <sup>2</sup> )	Effective Dose ICRP 60 (mSv)	Effective Dose ICRP 103 (mSv)
AD2	F	386	0.010	0.007
	O	234	0.005	0.003
	F	790	0.005	0.003
	O	747	0.009	0.005
	RM	1126	0.009	0.005
	O	453	0.007	0.004
	SIN	26	0.000	0.000
	O	266	0.005	0.002
	O	192	0.002	0.001
	O	56	0.001	0.000
	O	81	0.001	0.001

Table B37: Scan and Dose data for Patient 37 in FPOP procedure

Patient ID	Exam Type	Dose Area Product (mGy·cm <sup>2</sup> )	Effective Dose ICRP 60 (mSv)	Effective Dose ICRP 103 (mSv)
ZS	F	68	0.005	0.003
	F	102	0.002	0.001
	O	518	0.057	0.038
	O	345	0.012	0.006
	F	57	0.001	0.000
	F	515	0.018	0.011
	F	100	0.001	0.001
	O	244	0.029	0.019
	O	219	0.020	0.011
	O	144	0.008	0.004
	O	149	0.002	0.001
	F	190	0.005	0.003
	O	337	0.039	0.026
	O	185	0.016	0.009

Table B38: Scan and Dose data for Patient 38 in FPOP procedure

Patient ID	Exam Type	Dose Area Product (mGy·cm <sup>2</sup> )	Effective Dose ICRP 60 (mSv)	Effective Dose ICRP 103 (mSv)
DA	O	12009	1.851	1.369
	O	12854	1.876	1.467
	O	867	0.076	0.051
	RM	1492	0.060	0.039
	O	975	0.110	0.065
	O	246	0.032	0.021
	O	127	0.002	0.001
	O	109	0.001	0.001
	RM	4502	0.151	0.096
	O	96	0.002	0.001
	O	73	0.001	0.001
	O	106	0.002	0.001
	O	360	0.034	0.020
	O	262	0.006	0.003
	O	114	0.002	0.001
	O	98	0.001	0.001
	O	133	0.002	0.001
	O	237	0.003	0.002

Table B39: Scan and Dose data for Patient 39 in FPOP procedure

Patient ID	Exam Type	Dose Area Product (mGy·cm <sup>2</sup> )	Effective Dose ICRP 60 (mSv)	Effective Dose ICRP 103 (mSv)
KC	F	231	0.013	0.010
	F	359	0.017	0.013
	O	1212	0.119	0.087
	F	446	0.023	0.019
	F	2226	0.133	0.104
	F	829	0.039	0.029
	F	681	0.031	0.022
	O	827	0.049	0.037
	O	1226	0.079	0.058
	O	277	0.004	0.002
	O	100	0.001	0.001
	O	67	0.001	0.000

Table B40: Scan and Dose data for Patient 40 in FPOP procedure

Patient ID	Exam Type	Dose Area Product (mGy·cm <sup>2</sup> )	Effective Dose ICRP 60 (mSv)	Effective Dose ICRP 103 (mSv)
LN1	F	282	0.011	0.007
	O	461	0.017	0.011
	O	240	0.005	0.003
	O	220	0.003	0.002
	O	101	0.001	0.001
	O	70	0.001	0.000
	RM	1106	0.019	0.011
	O	331	0.016	0.009
	F	844	0.005	0.003
	F	275	0.002	0.001
	F	275	0.002	0.001
	F	1615	0.010	0.005
	F	269	0.001	0.001

Table B41: Scan and Dose data for Patient 41 in FPOP procedure

Patient ID	Exam Type	Dose Area Product (mGy·cm <sup>2</sup> )	Effective Dose ICRP 60 (mSv)	Effective Dose ICRP 103 (mSv)
LN2	O	642	0.088	0.063
	O	173	0.005	0.003
	O	675	0.016	0.008
	O	117	0.001	0.001
	O	85	0.001	0.001
	F	307	0.004	0.002
	RM	470	0.003	0.002
	F	308	0.002	0.001
	O	69	0.001	0.001
	O	57	0.001	0.000
	F	1571	0.019	0.011
	F	297	0.002	0.001
	F	861	0.059	0.049
	F	313	0.002	0.001
	F	302	0.002	0.001
	F	302	0.007	0.004
	F	1183	0.007	0.001
	F	318	0.002	0.001
	F	333	0.002	0.001
	F	1550	0.010	0.006
F	622	0.004	0.002	
F+				

F+	2580	0.016	0.010
SEL2	380	0.004	0.002
SEL2	500	0.006	0.003

---



**APPENDIX E:**

**Patients Scan and Dose Data for Transarterial Chemoembolization (TACE)**

Table C1: Scan and Dose data for Patient 1 in TACE procedure

Patient ID	Exam Type	Dose Area Product (mGy·cm <sup>2</sup> )	Effective Dose ICRP 60 (mSv)	Effective Dose ICRP 103 (mSv)
PIG	O	21814	2.836	2.596
	O	8017	1.205	1.064
	O	43450	5.059	4.449
	F	22084	2.421	2.118
	F	22280	2.316	2.411
	F	25003	2.405	2.454
	F	22015	2.188	2.206
	O	35219	4.225	3.748
	O	26680	2.787	2.404

Table C2: Scan and Dose data for Patient 2 in TACE procedure

Patient ID	Exam Type	Dose Area Product (mGy·cm <sup>2</sup> )	Effective Dose ICRP 60 (mSv)	Effective Dose ICRP 103 (mSv)
PIG2	O	22527	2.660	2.817
	O	15311	1.657	1.637
	O	20706	2.741	2.082
	O	17681	1.855	1.902
	O	21200	2.808	2.162
	O	25482	3.406	2.625
	O	41289	4.343	3.575
	O	21119	3.111	2.503
	O	25253	3.720	2.993
	F	62613	9.223	7.421

Table C3: Scan and Dose data for Patient 3 in TACE procedure

Patient ID	Exam Type	Dose Area Product (mGy·cm <sup>2</sup> )	Effective Dose ICRP 60 (mSv)	Effective Dose ICRP 103 (mSv)
GIV	F	23735	3.427	2.501
	O	4684	1.062	0.960
	F	23528	4.540	3.751
	O	4943	1.129	0.939
	O	9936	1.815	1.609
	O			

O	12349		
F	24229	2.189	1.910
O	10464	4.281	3.682
		1.931	1.674

Table C4: Scan and Dose data for Patient 4 in TACE procedure

Patient ID	Exam Type	Dose Area Product (mGy·cm <sup>2</sup> )	Effective Dose ICRP 60 (mSv)	Effective Dose ICRP 103 (mSv)
AGG1	O	15032	2.018	1.906
	O	25727	3.955	3.481
	O	21898	3.110	2.643
	O	22494	2.917	2.213
	O	6686	0.709	0.688
	O	15434	1.719	1.738
	O	10940	1.295	1.276
	O	12189	1.724	1.376
	O	15441	1.886	1.361
	F	107363	11.114	10.931
	O	30108	3.705	2.776

Table C5: Scan and Dose data for Patient 5 in TACE procedure

Patient ID	Exam Type	Dose Area Product (mGy·cm <sup>2</sup> )	Effective Dose ICRP 60 (mSv)	Effective Dose ICRP 103 (mSv)
AGG2	O	7446	0.843	0.777
	O	18485	2.901	2.472
	O	14952	1.861	1.391
	O	19746	2.864	2.176
	O	25718	2.969	2.317
	O	9476	1.435	1.251
	F	104393	13.042	9.739

Table C6: Scan and Dose data for Patient 6 in TACE procedure

Patient ID	Exam Type	Dose Area Product (mGy·cm <sup>2</sup> )	Effective Dose ICRP 60 (mSv)	Effective Dose ICRP 103 (mSv)
AGG3	O	21469	2.277	1.940
	O	18468	2.296	1.760
	O	19179	2.148	1.810
	F	29290	3.107	2.647

Table C10: Scan and Dose data for Patient 10 in TACE procedure

Patient ID	Exam Type	Dose Area Product (mGy·cm <sup>2</sup> )	Effective Dose ICRP 60 (mSv)	Effective Dose ICRP 103 (mSv)
KAG	O	7334	1.030	0.986
	O	4822	0.771	0.711
	O	10807	1.680	1.501
	F	20175	2.275	2.067

Table C11: Scan and Dose data for Patient 11 in TACE procedure

Patient ID	Exam Type	Dose Area Product (mGy·cm <sup>2</sup> )	Effective Dose ICRP 60 (mSv)	Effective Dose ICRP 103 (mSv)
PES1	F	14548	1.990	1.733
	F	14478	1.980	1.725
	F	14504	2.167	1.773
	O	10258	2.672	2.310
	O	1935	0.435	0.412
	O	8752	2.187	1.920
	SEL	5824	1.015	0.832
	SEL	3512	0.896	0.765
	SEL	9896	2.211	2.038

Table C12: Scan and Dose data for Patient 12 in TACE procedure

Patient ID	Exam Type	Dose Area Product (mGy·cm <sup>2</sup> )	Effective Dose ICRP 60 (mSv)	Effective Dose ICRP 103 (mSv)
NIK	F	5715	0.898	0.735
	F	5476	0.911	0.754
	O	6742	1.702	1.246
	F	10784	1.708	1.406
	F	5467	1.269	0.875
	O	2954	0.642	0.574
	F	15942	2.483	2.432

Table C13: Scan and Dose data for Patient 13 in TACE procedure

Patient ID	Exam Type	Dose Area Product (mGy·cm <sup>2</sup> )	Effective Dose ICRP 60 (mSv)	Effective Dose ICRP 103 (mSv)
KAE	F	24786	2.078	2.152
	O	8207	1.446	1.293
	O	6986	1.224	1.100
	O	5346	1.104	0.970
	O	7773	1.235	1.103
	F	24803	4.974	3.767
	O	6702	1.046	0.937

Table C14: Scan and Dose data for Patient 14 in TACE procedure

Patient ID	Exam Type	Dose Area Product (mGy·cm <sup>2</sup> )	Effective Dose ICRP 60 (mSv)	Effective Dose ICRP 103 (mSv)
PES2	O	10326	2.071	2.135
	F	34588	5.833	5.073
	O	19193	2.914	2.664
	O	3933	0.965	0.865
	O	8583	1.947	1.757
	F	18532	4.213	3.552
	O	5333	0.940	0.927
	O	16733	2.563	2.267

Table C15: Scan and Dose data for Patient 15 in TACE procedure

Patient ID	Exam Type	Dose Area Product (mGy·cm <sup>2</sup> )	Effective Dose ICRP 60 (mSv)	Effective Dose ICRP 103 (mSv)
KRI	F	26139	2.726	2.500
	O	12279	1.804	1.711
	O	22999	3.547	3.331
	O	21797	2.053	1.895

Table C16: Scan and Dose data for Patient 16 in TACE procedure

Patient ID	Exam Type	Dose Area Product (mGy·cm <sup>2</sup> )	Effective Dose ICRP 60 (mSv)	Effective Dose ICRP 103 (mSv)
KAE			1.212	1.087
	O	7110	6.838	6.076
	F	59270	1.603	1.439
	O	8743	2.133	1.858
	O	13781		

O	14313	2.058	1.805
O	8915	1.419	1.228
O	9538	1.794	1.628

Table C17: Scan and Dose data for Patient 17 in TACE procedure

Patient ID	Exam Type	Dose Area Product (mGy·cm <sup>2</sup> )	Effective Dose ICRP 60 (mSv)	Effective Dose ICRP 103 (mSv)
TEG2	O	14237	3.176	3.262
	O	3973	0.820	0.777
	O	9262	1.719	1.545
	O	9251	1.746	1.572
	S	1173	0.143	0.125
	SEL	8687	1.742	1.578
	SEL	11951	2.219	1.994
	F	45353	5.970	5.273

Table C18: Scan and Dose data for Patient 18 in TACE procedure

Patient ID	Exam Type	Dose Area Product (mGy·cm <sup>2</sup> )	Effective Dose ICRP 60 (mSv)	Effective Dose ICRP 103 (mSv)
VEG	O	6714	1.728	1.474
	O	1989	0.509	0.403
	F	4817	0.804	0.586
	F	19889	2.781	2.173
	O	1862	0.442	0.362
	O	2885	0.693	0.569
	F	4788	0.769	0.601
	O	7790	1.607	1.510

Table C19: Scan and Dose data for Patient 19 in TACE procedure

Patient ID	Exam Type	Dose Area Product (mGy·cm <sup>2</sup> )	Effective Dose ICRP 60 (mSv)	Effective Dose ICRP 103 (mSv)
MIS	O	4762	0.830	0.774
	O	14864	2.389	2.292
	F	37653	4.422	3.798
	O	9741	1.684	1.444
	O	10967	1.390	1.096
	O	8987	1.840	1.577
	O	16741	2.372	1.912

F	37683	6.024	5.564
F	37819	4.717	4.548
F	75720	13.095	12.338

Table C20: Scan and Dose data for Patient 20 in TACE procedure

Patient ID	Exam Type	Dose Area Product (mGy·cm <sup>2</sup> )	Effective Dose ICRP 60 (mSv)	Effective Dose ICRP 103 (mSv)
MIS2	O	9322	1.509	1.450
	F	99942	14.389	12.507
	O	20871	3.338	2.908
	F	49616	6.105	5.293
	O	24928	3.354	2.992
	O	8403	1.379	1.311

Table C21: Scan and Dose data for Patient 21 in TACE procedure

Patient ID	Exam Type	Dose Area Product (mGy·cm <sup>2</sup> )	Effective Dose ICRP 60 (mSv)	Effective Dose ICRP 103 (mSv)
KAI	O	16816	2.273	2.111
	O	18285	2.861	2.636
	O	9994	1.773	1.537
	F	48234	20.033	15.592

Table C22: Scan and Dose data for Patient 22 in TACE procedure

Patient ID	Exam Type	Dose Area Product (mGy·cm <sup>2</sup> )	Effective Dose ICRP 60 (mSv)	Effective Dose ICRP 103 (mSv)
SIE	O	9222	4.747	3.599
	O	10326	1.583	1.326
	O	4610	0.917	0.769
	O	8999	1.505	1.327
	O	8027	1.356	1.213
	F	15529	1.820	1.596

Table C23: Scan and Dose data for Patient 23 in TACE procedure

Patient ID	Exam Type	Dose Area Product (mGy·cm <sup>2</sup> )	Effective Dose ICRP 60 (mSv)	Effective Dose ICRP 103 (mSv)
SFA	O	7343	1.249	1.111
	O	6679	0.988	0.888
	O	7975	1.294	1.165
	O	3298	0.519	0.550
	O	10980	2.044	1.792
	F	14645	2.658	2.185
	O	6284	1.253	1.024
	F	14266	2.567	2.082
	O	5546	1.036	0.861
	O	13723	2.280	2.097

Table C24: Scan and Dose data for Patient 24 in TACE procedure

Patient ID	Exam Type	Dose Area Product (mGy·cm <sup>2</sup> )	Effective Dose ICRP 60 (mSv)	Effective Dose ICRP 103 (mSv)
KOA	O	21638	2.621	2.325
	O	11138	1.294	1.083
	O	6761	0.867	0.718
	F	13064	1.566	1.428
	O	5794	0.981	0.850
	F	20425	2.274	1.937
	S	879	0.091	0.076
	O	16188	2.624	2.230

Table C25: Scan and Dose data for Patient 25 in TACE procedure

Patient ID	Exam Type	Dose Area Product (mGy·cm <sup>2</sup> )	Effective Dose ICRP 60 (mSv)	Effective Dose ICRP 103 (mSv)
FAP	F	1171	0.147	0.127
	O	22184	3.203	2.726
	F	3125	0.575	0.451
	O	14922	2.526	2.198
	O	25281	4.423	3.830
	S	1295	0.166	0.145
	O	17640	2.784	2.594

**APPENDIX F : Patients Bio-data for EVAR procedure**

Patient	Age (years)	Weight (kg)	Total height (m)
VX	58	120	1.75
GC	61	76	1.74
KM	81	57	1.62
VI	78	67	1.65
FN	54	105	1.85
KE	56	104	1.83
SN	73	90	1.76
TA	50	82	1.78
AG	82	72	1.66
ZI	63	128	1.72
VS	78	55	1.62
ZK	64	94	1.70
BT	82	69	1.63
FM	64	61	1.69
PI	78	70	1.65
SA	67	87	1.73
ME	72	62	1.62
KK	66	86	1.82
NA	66	115	1.90
LG	73	55	1.65
KN	68	103	1.90
MM	75	102	1.62
MN	70	70	1.76
TS	69	94	1.75
KA	80	85	1.85
MS	74	80	1.62
CP	83	65	1.67
TG	83	80	1.70
	70	83	1.72
	50	55	1.62
	83	128	1.90

**APPENDIX G: Patients Bio-Data for FPOP Procedure**

Patient	Age (years)	Weight (kg)	Height (cm)
GA	63	73	171
GN	75	47	165
KA	88	100	170
KS	48	110	170
KN	84	57	162
KD	78	80	175
BI	77	85	180
PI	66	70	165
PE	58	70	160
SK	54	63	174
PP	64	89	176
GM	79	85	168
SM	87	70	172
II	73	94	180
TS	78	60	170
VS1	47	84	172
DE	52	94	178
LF	72	60	170
KE	69	81	168
VS2	47	84	172
VA	72	75	170
DG	82	80	165
AD1	59	70	170
MP	83	60	160
FE	69	70	165
CM	91	65	170
ML	74	75	175
SG	58	106	182
VE	77	72	180
FV	78	72	160
CS	52	60	175
KV	74	84	170

SA	70	73	165
FG	59	93	174
MG	75	70	165
AD2	51	78	165
ZS	70	62	170
DA	67	79	168
KC	57	87	171
LN1	82	90	180
<u>LN2</u>	<u>82</u>	<u>90</u>	<u>180</u>



**APPENDIX H: Patients Bio-data for TACE procedure**

Patient	Age (years)	Weight (kg)	Height (cm)
Patient	Age (years)	WEIGHT	HEIGHT
PIG	40	103	184
GIV	53	74	165
AGG	52	93	165
MOM	70	81	170
PIG	70	103	184
KRI	70	91	180
AGG	70	93	165
LEA	70	93	170
KAG	71	85	170
PES	79	65	140
SOM	44	70	172
TEG	44	69	168
NIK	70	55	165
KAE	54	73	160
LEA	79	93	170
AGG	79	93	165
TEG	81	69	168
VEG	81	56	163
MIS	71	78	172
KAI	79	82	174
SIE	79	76	171
KAE	80	70	160
FAP	58	85	172
SFA	58	75	165
KOA	58	86	170
FAP	65	85	172
PRN	59	87	181
STI	72	101	176
VLG	77	100	168
PRN	75	87	181
MIS	77	78	172
FAP	78	85	172
PES	77	65	140

Table C26: Scan and Dose data for Patient 26 in TACE procedure

Patient ID	Exam Type	Dose Area Product (mGy·cm <sup>2</sup> )	Effective Dose ICRP 60 (mSv)	Effective Dose ICRP 103 (mSv)
FAP3	O	690	0.129	0.123
	O	28338	3.374	2.895
	F	70243	8.764	7.778
	SEL	5015	0.614	0.561
	SEL	5782	0.708	0.647
	SEL	20454	2.339	2.016
	SEL	15173	1.953	1.402
	SEL	10454	1.075	0.992

Table C27: Scan and Dose data for Patient 27 in TACE procedure

Patient ID	Exam Type	Dose Area Product (mGy·cm <sup>2</sup> )	Effective Dose ICRP 60 (mSv)	Effective Dose ICRP 103 (mSv)
PRN1	F	28118	2.751	2.512
	O	16492	2.355	2.242
	F	28431	3.221	2.950
	O	16669	2.590	2.474
	O	15288	1.945	1.769
	F	27522	4.413	3.579
	O	13601	1.833	1.576
	O	8860	1.573	1.422
	F	13919	1.631	1.590
	O	23117	2.595	2.193
	O	20551	2.320	1.959

Table C28: Scan and Dose data for Patient 28 in TACE procedure

Patient ID	Exam Type	Dose Area Product (mGy·cm <sup>2</sup> )	Effective Dose ICRP 60 (mSv)	Effective Dose ICRP 103 (mSv)
PRN2	O	12019	1.395	1.210
	O	5153	0.740	0.608
	O	1448	0.215	0.191
	F	53838	5.803	5.761
	O	3853	0.502	0.519

Table C29: Scan and Dose data for Patient 29 in TACE procedure

Patient ID	Exam Type	Dose Area Product (mGy·cm <sup>2</sup> )	Effective Dose ICRP 60 (mSv)	Effective Dose ICRP 103 (mSv)
STI	S	1375	0.123	0.117
	O	12157	1.573	1.448
	O	11924	1.686	1.559
	O	19352	2.938	2.616
	O	15144	2.924	2.242
	O	24225	2.796	2.269
	O	24525	2.787	2.256
	O	41894	4.599	4.064
	O	38230	4.349	3.978
	S	1091	0.122	0.108
	O	25208	3.260	2.876
	F	72003	8.702	7.655

Table C30: Scan and Dose data for Patient 30 in TACE procedure

Patient ID	Exam Type	Dose Area Product (mGy·cm <sup>2</sup> )	Effective Dose ICRP 60 (mSv)	Effective Dose ICRP 103 (mSv)
VLG	O	15243	2.098	1.940
	F	15866	1.850	1.646
	O	18624	2.257	2.088
	O	35086	3.684	3.119
	O	28801	2.733	2.277
	F	15660	2.375	1.892
	O	15377	2.560	2.063
	F	31171	4.623	3.742
	F	30814	4.861	3.943
	F	15496	2.466	2.135
	O	29836	4.178	3.477
	F	15543	2.080	1.972
	F	66751	9.912	9.263
	O	18200	2.674	2.225
	S	1419	0.141	0.119
	O	9540	1.448	1.254